Modeling and Assessment of the Wisconsin Institutes for Discovery Ground-Coupled Heat Pump

by

Christian Herrera

A thesis submitted in partial fulfillment of the requirements for the degree of

Master of Science

(Mechanical Engineering)

at the

UNIVERSITY OF WISCONSIN-MADISON

2016

Approved by

Acknowledgements

First and foremost, I would like to thank my advisors, Gregory Nellis, Douglas Reindl, and Sanford Klein. Their guidance kept me on the right track and their constructive criticism made me a more effective engineer. They pushed me to take on and overcome challenges that I had thought were beyond my abilities. Meeting with me on a weekly basis and showing sincere interest in the development of my research really meant a lot to me. Special thanks to Doug for helping extensively with the fieldwork portion of this research.

I would also like to thank Kelly Burton and the Graduate Engineering Research Scholars (GERS) fellowship program not only for funding my research for a year, but more importantly, for providing a support network of other underrepresented students. Through GERS I became a member of a diverse community of UW-Madison engineering graduate students, faculty, and staff that continue to offer professional development opportunities after graduation; I hope to pay it forward someday.

A big thank you to the Wisconsin Alumni Research Foundation (WARF) for also funding my research especially the extensive fieldwork that was completed. Special thanks for helping with the fieldwork portion of my research goes to Adam McDaniel of the UW Geological Engineering Dept., John Nelson, Todd Kiley, James Tinjum, David Hart, Eric Smithback, Erin Badger, and many others.

Many, many thanks to my friends and peers at the Solar Energy Lab for their advice, help, and for making my experience there fun. I particularly appreciate the friendship and mentoring of Luis Fonseca; my time helping him as an undergrad is what motivated me to enter graduate school.

Finally, I would like to thank my family. They raised me to be respectful, humble and instilled in me the work ethic necessary to become a successful man. Thank you for the mental, spiritual, financial, and emotional support. I hope to pay back one day what you've sacrificed for me. Sinceramente gracias.

Table of Contents

List of Figures

List of Tables

Chapter 1. The Ground-Coupled Heating System

1.1 Ground-Coupled Heat Pump (GCHP) Design

A Ground Source Heat Pump (GCHP) is a heating and/or cooling system that uses the earth as a heat source or sink Figure 1-1. The GCHP system takes advantage of relatively stable temperatures of the ground below a few meters in order to maintain high operating efficiently over a wide range of ambient temperature conditions. The system, in its most basic configuration, consists of a heat pump with either the condenser (cooling mode) or evaporator (heating mode) linked with the underground heat exchanger using a secondary fluid.

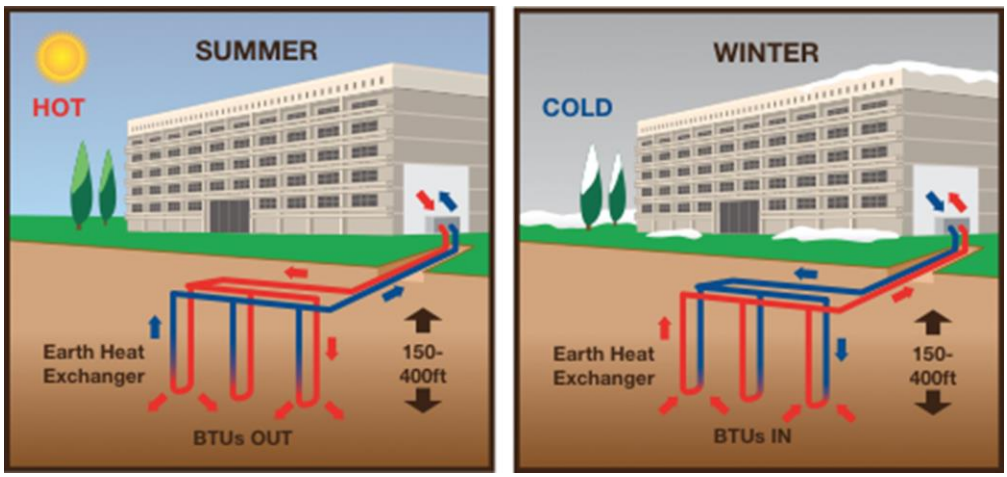

Figure 1-1: General layout of a geofield in the vertical configuration showing heating and cooling modes. (EnLink Geoenergy Services, Inc, 2010)

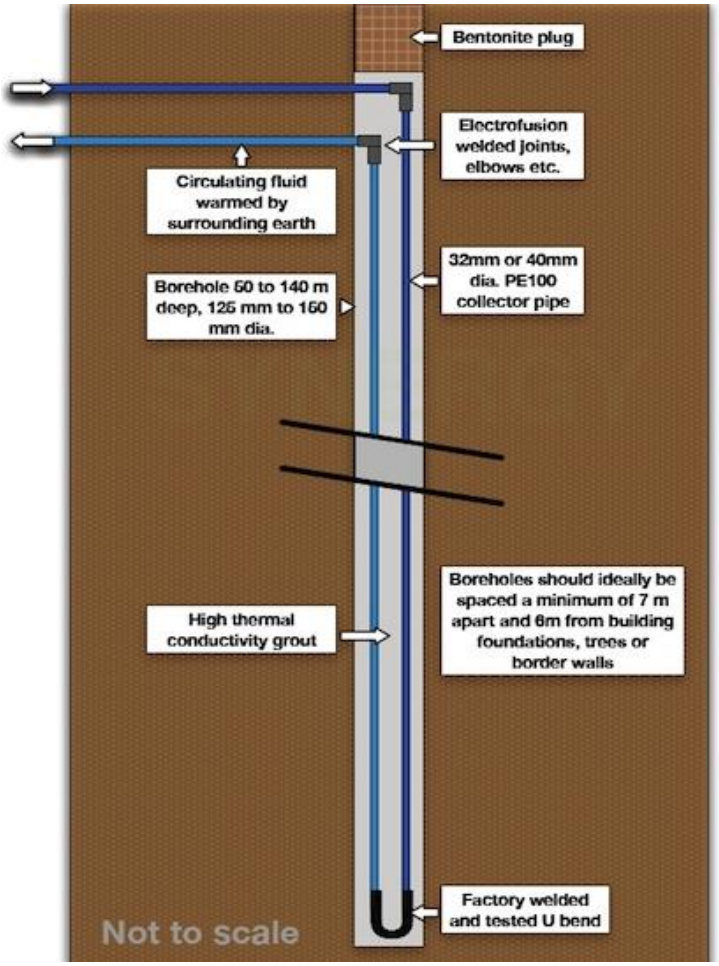

Figure 1-2: Layout of an individual bore showing the grout used to fill the space between the u-tube and the ground. (Synergy Boreholes and Systems ltd., 2016)

Increasingly common are ground heat exchangers in a vertical bore configuration that consist of single U-tubes grouted into 6-inch holes drilled to 100-500 ft. in depth with the typical layout shown in Figure 1-2. To obtain a sufficiently sized heat exchange area, a given GCHP system will require several vertical bores with U-tubes piped in parallel to comprise a "geofield." Although GCHP systems are now relatively widespread and well-established, research on designs that can be optimized to improve their performance continues. In fact,

the larger the system the more there is to gain from a proper characterization of the heat transfer to the ground (Gehlin, 2002), which is one of the research objectives of this thesis.

1.2 The Thermal Response Test

To adequately size the geofield for larger Geoexchange systems, it is necessary to accurately determine the ground thermal properties. The most common approach to infer ground properties is to drill a "test bore" at the installation site and perform a Thermal Response Test or "TRT". Accurately estimating soil thermal properties enables designers to determine ground heat exchanger parameters for the single bore to accurately simulate system performance when scaled up to include an entire geofield over both shorter-term and longer-term intervals. During a TRT, a circulating fluid, usually water, is heated (or cooled) and then circulated through the U-tube within an exemplar bore (i.e. the "test bore"). In its most common configuration, the TRT is performed using a test rig that contains the following elements: a circulating pump, flow meter, heating element, and temperature sensors at the inlet and outlet tubing of the rig as in Figure 1-3 below. Data measured include the fluid flow rate and the temperature difference of the fluid between the inlet and outlet as a function of time (usually a minimum period of 48-hours is required). Data collected during the test are input to either an analytical model such as the line-source model (Mogensen, 1983) or a numerical parameter estimation technique, such as those created by Hellström (Hellström, 1982) and Shonder and Beck (Shonder & Beck, 1999).

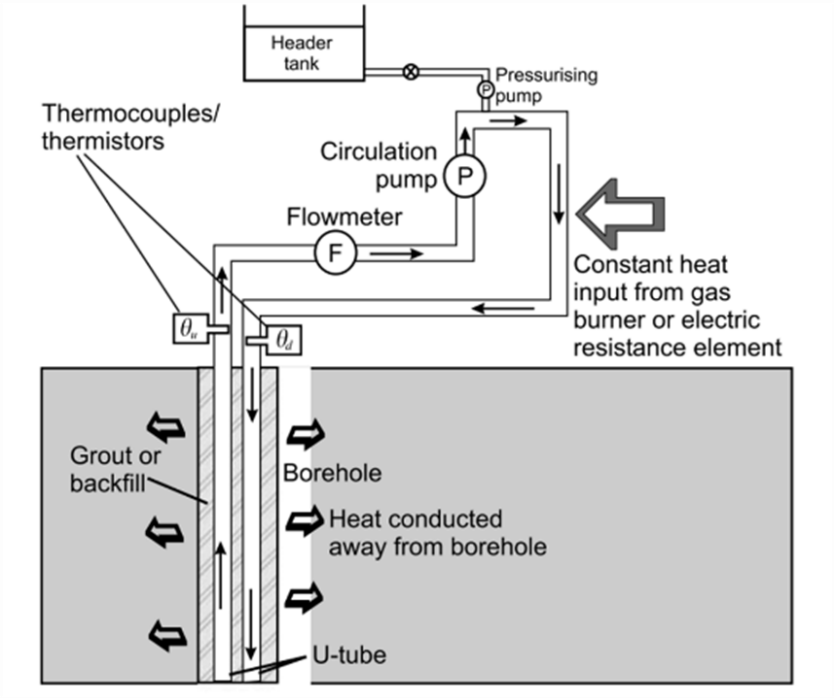

Figure 1-3: TRT rig general layout. (Banks, 2008)

The result of post-data collection analysis is an "effective ground conductivity" that represents an average thermal conductivity of the ground along the entire length of vertical bore. The test provides no information relative to the actual varying conductivity as a function of bore depth which reflect the distinct soil layers present in the ground. A TRT test that provides information about the thermal properties of the ground resolved across the different geological layers would allow improved models for GCHP design.

1.3 The Wisconsin Institutes for Discovery

The Wisconsin Institutes for Discovery or WID, Figure 1-4, was designed with an emphasis on reducing environmental impact. Per the original Basis of Design (BOD), a large contributor to the planned energy cost savings for space conditioning at the facility is the

Ground Coupled Heat Pump (GCHP) system (BOD , 2011). This system was designed to reject and absorb heat from the ground via a geofield as needed to meet the building's reheat and chilled water loads. The exchange of thermal energy in the geofield is accomplished through the use of HDPE pipes in each of the individual bores using water as the circulating fluid. Due to plumbing issues discovered after start-up, the system was permanently converted to a cooling-only configuration where only the cooling load of the building would be addressed by the GCHP. Therefore, energy would only ever be put into the ground and never extracted from the ground. The original operating modes are described in Table 1-1 and the reduced capability is indicated by the modes that are crossed out.

Modes of Operation	*Description*
Mode 1 – Cooling Mode with recovered reheat	HP unit evaporator produces chilled water for building cooling load. Hot water from unit condenser is recovered for use in building reheat system while additional heat is rejected to the geo field.
Mode 1a – Cooling Mode with heat rejection to geoexchange.	HP unit evaporator produces chilled water for building cooling load while condenser waste heat is rejected to the geo field.
Mode 2 – Heating Mode with heat absorption from geoexchange.	HP unit evaporator produces hot water for building reheat. Cold condenser water is circulated through the geo field to absorb heat from the Earth.
Mode 2a – Heating Mode with recovered chilled water	HP unit evaporator produces hot water for building reheat. Cold condenser water is recovered for building cooling load with additional heat rejection to geo field.
Mode 3 – Geoexchange Test Mode	HP unit evaporator and condenser are disabled. Water is circulated through geo field to measure field temperatures

Table 1-1: WID GCHP reduced functionality

It was thought that since the building has a year-round cooling load, this change would not adversely impact overall operation (Knudson, 2013). However, it was not understood what the long-term impact of this change on the geofield would be. Since the ground is not perfectly insulated, heat should dissipate to the surroundings over time. Therefore, in theory a GCHP system should be able to operate at near its design capacity, albeit a very low capacity, when the heat input to the geofield and thermal decay are balanced. In practice though the heat dissipation is so low that it is not worth the effort of building a system that will only operate in cooling mode.

Figure 1-4: Wisconsin Institutes for Discovery Building. (Wisconsin Institutes for Discovery, 2016)

The WID's reheat water system was intended to primarily use the hot water coming from the GCHP condenser to serve the reheat coils for facility air conditioning. The secondary source for this system would be the steam from the campus district system. Approximately one third of the WID's reheat coils have a design supply temperature of 105 °F and the other two thirds are sized for 130°F. The GCHP system is not capable of providing condenser water at 130°F and its performance is inversely proportional to the entering condenser water temperature. Due to the inability of the GCHP to provide hot enough condenser water to the coils, the reheat system is not used (Knudson, 2013).

After operating the WID GCHP system solely in cooling mode for an extended period of time, the circulating fluid temperatures within the geofield have risen far higher than anticipated. Previous research (Knudson, 2013),attributed the elevated geofield temperatures to one or more of the following: the actual ground conductivity is lower than the value estimated from the test bore TRT, geofield heat exchanger fouling, and gaps in the grout for individual bores in the geofield. Following the completion of this initial work, other hypotheses have also been proposed including the presence of perched ground water enveloping the geofield bores and low grout conductivity.

1.3.1 WID GCHP System Basis of Design: Cooling Loads

The design cooling loads for WID include 1830 tons (building ventilation), 365 tons (process chilled water), and 200 tons (vivarium). The process chilled water load includes the data center and any cooling load that is not related to human comfort except for the "chilled beams" which are used to cool lab spaces. The estimated peak cooling load for the facility is 2,395 tons. A large data center within the building is always on and must be cooled at all

times. The data center comprises 48 racks at 9 kW per rack which results in a base cooling load of 123 tons. The data center cooling load is included in the process chilled water load (BOD , 2011).

1.3.2 WID GCHP System Basis of Design: The Geofield

The geofield is composed of 82 bore holes[1] with an estimated capacity of 4 tons per bore which leads to a design cooling capacity of 300 tons. The bore holes are each 300 ft deep with the test bore, which was eventually incorporated into the geofield, that drilled to 400 ft deep. In each bore, a U-tube made of HDPE is inserted to carry the circulating heat transfer fluid which is water. These U-tubes are connected in parallel and are split into four branches piped in a reverse-return configuration to maintain equal flow rates through all bores (Figure 1-5). The bores are distributed along the perimeter of the building as in Figure 1-6.

[1]The original BOD specified 75 bore holes but in reality there are 82.

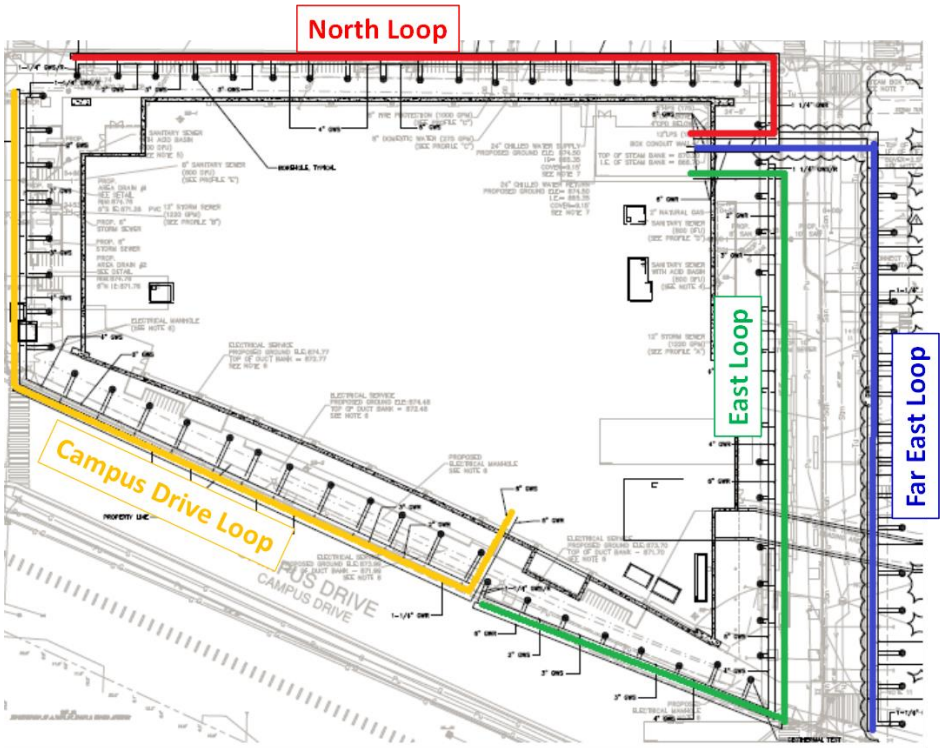

Figure 1-5: WID geofield branch circuits.

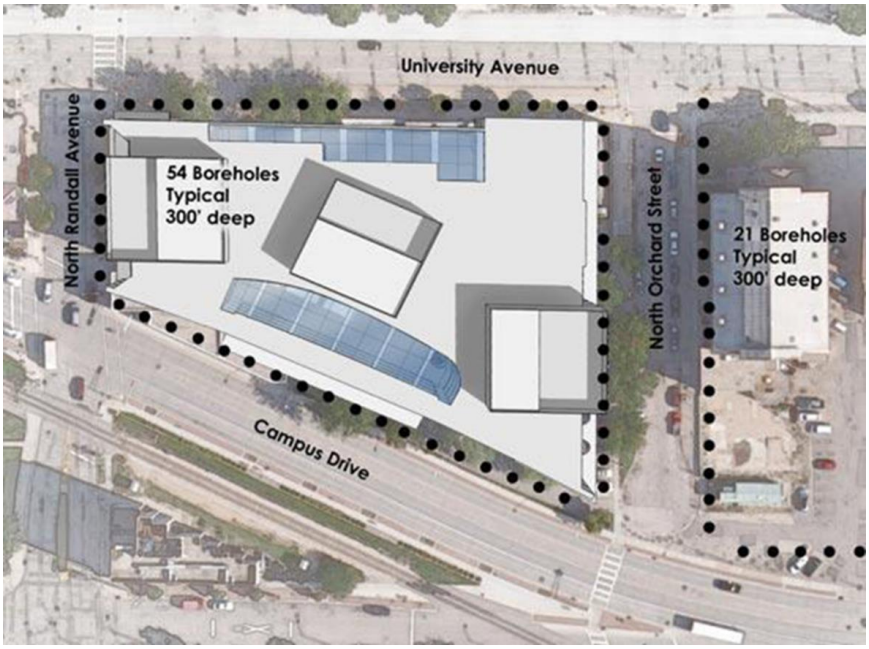

Figure 1-6: WID geofield bore arrangement. (Kelly, 2009)

1.3.3 WID GCHP System Basis of Design: Heat Pumps

The WID's GCHP was designed to be the first stage of the building chilled and reheat water; the rest of the cooling load would be provided by the campus district chilled water system. The GCHP system consists of six water-cooled Multistack, modular heat pumps and each module contains two separate refrigeration systems. Therefore, there is a total of twelve compressors. The heat pumps use R-410A as the refrigerant. The compressors are all scroll-type and loads are met by cycling the individual modules on or off. Table 1-2 displays the manufacturer performance data at nominal conditions for the Multistack heat pumps.

GENERAL INFORMATION

Chiller I.D. (6) MS70X6H2R

Dimensions (inches): (dimensions do not include junction boxes)

Length: 194
Width: 78 1/4
Height: 64

Load Flow - 0% Glycol:
Source Flow - 0% Glycol:

Cooling Mode Performance - EER = 13.5

Load water:	*700 GPM @ 13.3 Feet Pressure Drop*		
Entering Temp.	57.2 °F	**Leaving Temp.**	44.0 °F
Source water:	*578.2 GPM @ 7.2 Feet Pressure Drop*		
Entering Temp.	85.0 °F	**Leaving Temp.**	105.0 °F
Cooling Capacity:	385.1 Tons	THR:	5785.4 MBH

Heating Mode Performance - COP = 3.3

Load water:	*700 GPM @ 13.3 Feet Pressure Drop*		
Entering Temp.	115.5 °F	**Leaving Temp.**	130.0 °F
Source water:	*977 GPM @ 19.3 Feet Pressure Drop*		
Entering Temp.	50.0 °F	**Leaving Temp.**	42.7 °F
Heating Capacity:	5075.3 MBH	Heat Extracted:	3526.7 MBH

Table 1-2: WID Multistack heat pump manufacturer performance data at nominal conditions.

1.4 GCHP in Madison

The WID GCHP is not the first large-scale system of its kind in Madison, WI. There are several commercially sized GCHP systems in operation that have also been studied to varying degrees. The hydro-geological characteristics of Madison have previously produced unanticipated GCHP geofield behavior that has warranted research into underlying causes. Pertzborn investigated the performance of the GCHP system of the Tobacco Lofts apartments in downtown Madison (Pertzborn et al., 2011). The Tobacco Lofts geofield had bores drilled to the same depth as those of the WID (300 ft). The investigation involved the validation of a heat transfer model, the Duct Storage (DST) (Hellström, 1982) model that is used to simulate the behavior of the geofield. The results of the validation showed that the model tended to over-predict the performance of the geofield. This implies that the geofield is underperforming when compared to the thermal properties inferred as a result of the TRT conducted before the system was built. In this case, the effective thermal conductivity was calculated from the TRT at 3.5 W/m-K. During the model sensitivity testing, it was found that reducing the TRT-inferred thermal conductivity by 50% would create much better agreement between the modeled and as-measured temperature change across the inlet and outlet to the bore. This can be seen in Figure 1-7; the top left plot shows modeled versus actual temperature when the parameters obtained from the TRT are used in the model. Going clockwise after the top left plot the parameters are altered: the capacitance of the ground is halved providing a slight change which provides neither better nor worse agreement, in the next plot the undisturbed ground temperature is halved causing an offset that causes worse agreement, and in the last plot the thermal conductivity of the ground is halved which provides the best fit.

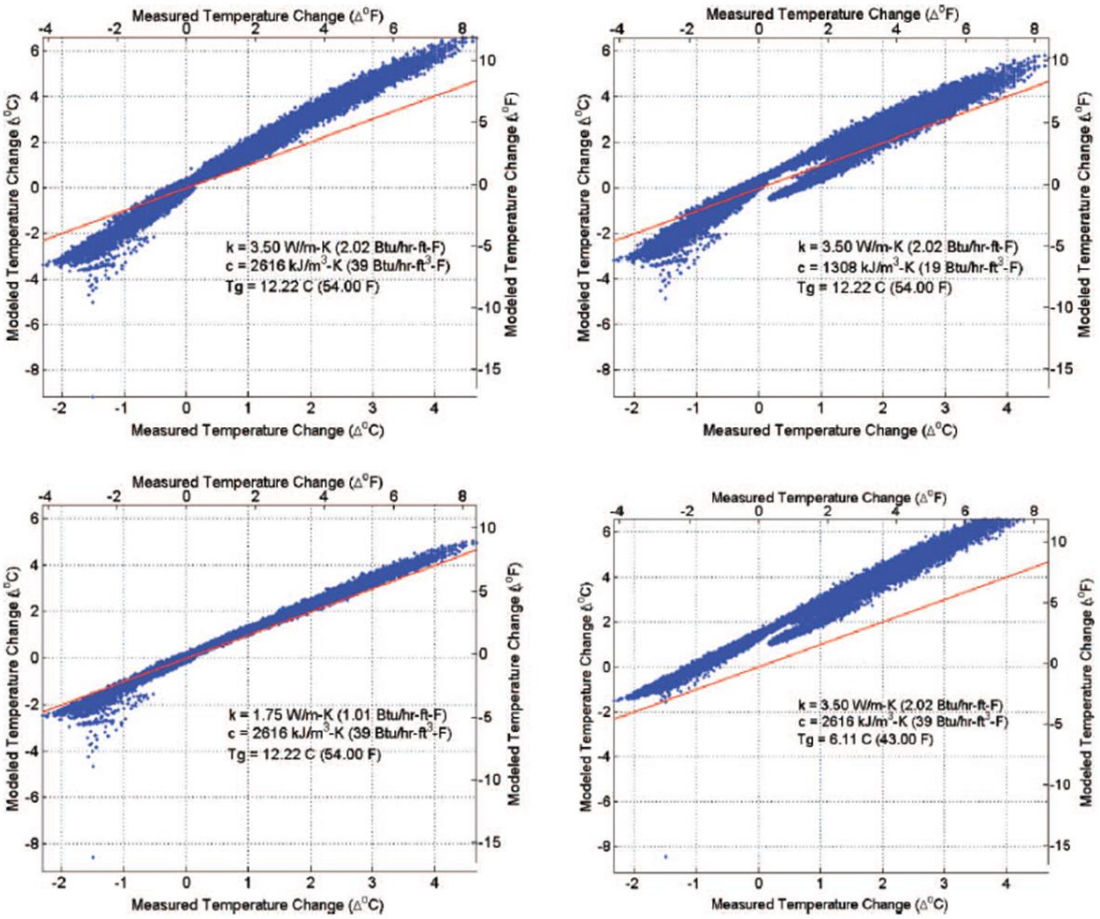

Figure 1-7: Effect of ground thermal properties on the accuracy of the DST model results. (Pertzborn, et al. 2011)

Epic Systems, a healthcare software company, uses a GCHP system to meet the heating and cooling demands of their large headquarters campus. Their geofield is made up of 6172 bores, at depths that vary from 300 to 500 feet, and is still currently expanding. The Epic campus is heavily cooling dominated, which has translated into problems with high geofield temperatures not unlike the WID's. An investigation into that system's behavior is currently underway and initial heat dissipation models suggest persistent elevated temperatures when used in a cooling dominated application, but this effect is reduced with

higher groundwater movement as shown in Figure 1-8 (Özdoğan-Dölçek, 2015). This plot shows the temperature at the center of the geofield over time under continuous (solid lines) and intermittent (dotted lines) operation where intermittent operation means the field is idled for 1 year after every 4 years of operation making it a 5-year cycle. Groundwater flow was active for the red lines and inactive for the black lines in both the continuous and intermittent modes. The velocity of the ground water flow is labeled by *v adv* in the plot which means *velocity, advection* in units of *m/d* or meters per day. In all instances, Figure 1-8 shows constantly increasing overall temperatures where the heat put in to the field during a cooling season is not dissipated; even during intermittent operation the field does not recover to its original temperature. The plot does show that groundwater flow has a significant impact on the heat dissipation of the geofield although still not enough to reset the field temperatures.

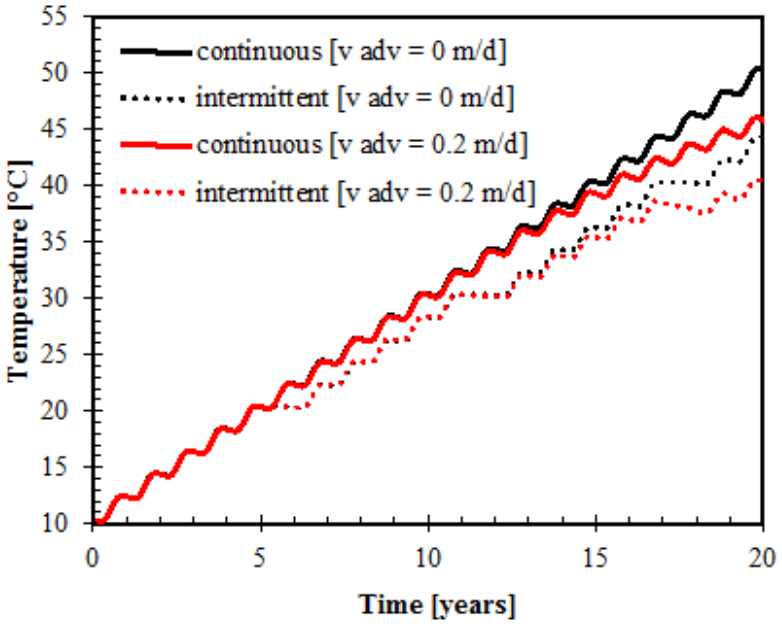

Figure 1-8: Ground temperature response at the center of the geofield under intermittent (idled for 1 out of every 5 years of operation) and continuous operation. Also with and without groundwater flow. (Özdoğan-Dölçek, 2015)

1.5 Research Objectives

In May 2013, the WID geothermal heat pump system ran at a high capacity in cooling-only mode over a period of several days. The concentrated heat addition to the geofield resulted in a substantial rise in entering condenser water temperature (in excess of 121°F); thereby, necessitating the shutdown of the heat pumps with the leaving condenser water temperature in excess of 130°F.

Knudson (2013) had previously completed an evaluation of the energy and thermal performance of the WID heat pump system, but this abnormal operating event occurred at the conclusion of his project. Nonetheless, Knudson had noted aberrations in his monitoring and analysis of the heat pump system's geofield during the course of his research and recommended that follow-on work be pursued to assess potential factors that may be responsible for the geofield's thermal performance.

From the outset of this project, several specific diagnostics aimed at testing hypotheses conceived to explain the geofield's behavior were identified, with the overarching goal of developing a better understanding of the performance characteristics of the WID geofield that caused the condenser operating temperatures to rapidly rise and persist after extended operation. This research effort aims to perform a battery of tests to eliminate or confirm possible causes of reduced capability. In addition, a new type of TRT that incorporates a fiber optic Distributed Temperature Sensing (DTS) system was executed to validate previous TRT testing and to refine our understanding of the test bore, including ground properties as a function of depth. The goal of this method is to allow more accurate ground heat exchanger models to be developed in the future. The scope of this research also

includes the modeling and simulation of the entire system to determine what factors contribute to the performance of the WID GCHP system and GCHP systems in general. This information was then used to optimize and plan the operation for the WID's GCHP with tools like performance maps to sustainably meet the needs of the WID.

Chapter 2. Thermal Response Test model

2.1 Introduction

Prior to the construction of WID, a thermal response test was performed in order to determine the ground thermal conductivity at the building's location. The original thermal response test (TRT) was performed by Geothermal Resource Technologies, Inc (GRTI) on February 5, 2008 (GRTI, Inc., 2008). The TRT was a traditional type as-discussed in section 1.2. GRTI analyzed the collected data using the line source method (LSM) which assumes an infinitely thin source of heat in a continuous medium and is therefore not valid for early test times because sufficient time must pass to ensure non-homogeneities associated with the bore such as grout do not meaningfully influence the resulting ground conductivity estimate (Mogensen, 1983). The simplified LSM equation, rearranged to solve for the thermal conductivity, is shown below as equation (2.1). In this equation, the average heat input during steady heat flux phase of the TRT is used for $\dot{Q}_{avg}$, the length of the U-tube is L, and S represents the slope of a linear regression between the average fluid temperature and the natural log of time.

$$\lambda_{effective} = \frac{\dot{Q}_{avg}}{4\pi LS} \qquad (2.1)$$

GRTI's test lasted 47 hours and they reported an effective ground thermal conductivity of 4.03 W/m-K (2.33 Btu/hr-ft-°F) which is high when compared to the thermal

conductivity for sandstone, 2.91 W/m-K (1.68 Btu/hr-ft-°F), which makes up most of the bedrock in the south-central Wisconsin region. As part of the TRT, a drill log was produced and the bedrock composition on the drill log did match the known geology of Madison. One big difference between the test bore and the other bores subsequently drilled for the WID geofield is the bore depth. The bore drilled for the thermal response test was 122 meters while the other bores for WIDs geofield are 91.4 meters deep.

Since the GCHP system was designed based on the ground thermal properties determined by the GRTI TRT, it was hypothesized that an inaccurate TRT could be to blame for the poor behavior of the geofield. There were several red flags identified with the GRTI TRT that warranted further investigation. One was the potential for extremely cold ambient conditions that could have contributed excessive heat losses from the TRT test rig to the ambient environment and not to the ground. This was particularly concerning since the TRT was conducted during February of an unusually cold winter. Also, there was no measurement of the undisturbed ground temperature that preceded heat input to the bore as part of the thermal response test; an estimate based on the geographic area was used for analysis purposes.

Before there was any fieldwork or experiments done in-situ as part of the present research, the data from the GRTI TRT were reanalyzed using the same LSM method to confirm their analysis. Then a new parameter estimation method was utilized to analyze the original raw TRT test bore data. The new method is called the *Crossed Contours Method* (Leyde, 2016) and this method relies on a different ground heat exchanger model called the

Duct Storage Model. The goal of this "re-analysis" effort was to confirm or deny the accuracy of the GRTI TRT results.

2.2 TRNSYS and the DST model

The single bore model used to analyze data from a TRT was created using TRNSYS. TRNSYS is an extremely flexible graphically based software environment used to simulate the behavior of transient systems. A simulation time step suitable for the analysis is selected and key model variables can be output as the program marches through each simulation time step. The single borehole is modeled within TRNSYS using component Type 557a "Vertical U-Tube Ground Heat Exchanger". At the heart of TRNSYS Type 557a is the DST model developed by Hellström (Hellström, 1982). The DST model is a complex model that superimposes three different solutions to calculate the ground temperature: a global, local, and steady-flux solution. Type557a uses the DST model to calculate the temperatures within a specified volume of earth surrounding the bores called the "storage volume" as shown in Figure 2-1. Any volume outside of the "storage volume" is considered the undisturbed ground. The individual bores are made up of the u-tubes and grout. The DST model also assumes the bores are laid out in the "storage volume" in a hexagonal configuration; however, this geometric arrangement is not consistent with the WID's geofield where they are in a rectangular arrangement. According to Hellström (Hellström, 1982), rectangular arrangements have similar heat transfer characteristics.

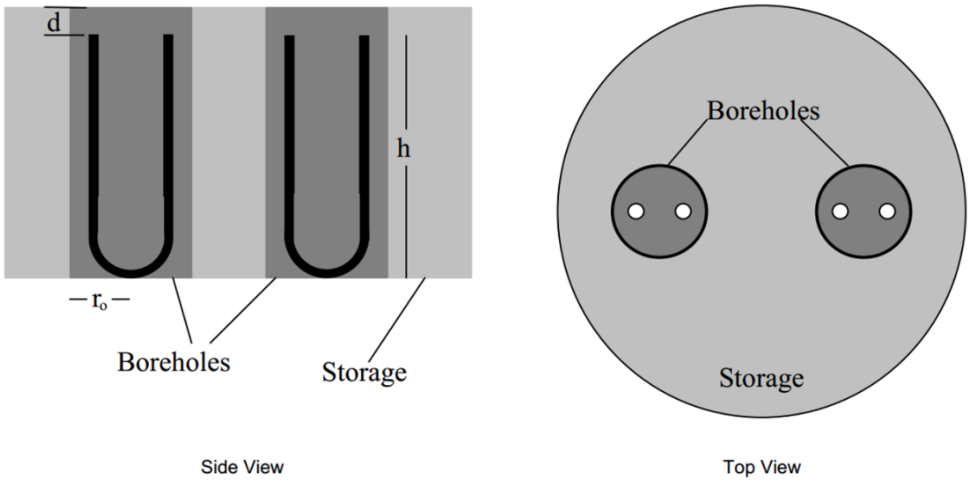

Figure 2-1: Diagram of the DST model simulation regions.

The Type 557a TRNSYS component has many parameter fields that are used to specify the various properties that govern the heat transfer in a u-tube ground heat exchanger. These parameters are set within the program and are summarized in Table 2-1.

Parameter name	Value	Units
Storage Volume	3558.4	m^3
Borehole Depth	121.919999	m
Header Depth	2.1336	m
Number of Boreholes	1	-
Borehole Radius	0.062	m
Number of Boreholes in Series	1	-
Number of Radial Regions	1	-
Number of Vertical Regions	50	-
Storage Thermal Conductivity	2.33	BTU/hr.ft.F
Storage Heat Capacity	2878	kJ/m^3/K
Negative of U-Tubes/Bore	-1	-
Outer Radius of U-Tube Pipe	0.021	m
Inner Radius of U-Tube Pipe	0.01725	m
Center-to-Center Half Distance	0.026543	m
Fill Thermal Conductivity	1	BTU/hr.ft.F
Pipe Thermal Conductivity	0.277	BTU/hr.ft.F
Gap Thermal Conductivity	5.04	kJ/hr.m.K
Gap Thickness	0	m
Reference Borehole Flowrate	1245	kg/hr
Reference Temperature	11.666688	C
Pipe-to-Pipe Heat Transfer	0	-
Fluid Specific Heat	4.183	kJ/kg.K
Fluid Density	997	kg/m^3
Insulation Indicator	0	-
Insulation Height Fraction	0.5	-
Insulation Thickness	0.0254	m
Insulation Thermal Conductivity	1	kJ/hr.m.K
Number of Simulation Years	1	-
Maximum Storage Temperature	500	F
Initial Surface Temperature of Storage Volume	53	F
Initial Thermal Gradient of Storage Volume	0	any

Table 2-1: TRNSYS type 557a parameters for model of original GRTI TRT.

A model consistent with the WID test bore was created in the simulation studio environment of TRNSYS where the Type 557a component is coupled to an interpolator that takes experimental data files as input and creates a set of temperatures according to the time step that are transferred to the Type 577a. The model takes these experimental temperature

data as input and predicts the fluid output temperatures for comparison with the experimental outlet fluid temperature data. There is also a printer component that creates a text file that contains the simulation results for each time step. These results are used in the Crossed Contours parameter estimation analysis.

2.3 Crossed Contours Parameter Estimation Method

The function of the TRNSYS simulation model is to output simulated temperatures, based on previously known, user specified parameters; it does not provide a method to estimate unknown parameters based on experimental data. An obvious solution would be to perform a single variable optimization on the storage thermal conductivity that would provide the best fit between the modeled and simulated data vis a vis trial and error. Unfortunately, it has been shown by (Pertzborn et al, 2011) and (Leyde, 2016) that there are multiple combinations of parameters, in this case ground thermal conductivity, borehole radius, and grout thermal conductivity, that can produce temperature profiles that match experimental data. Furthermore, the transient nature of the heat transfer occurring in the borehole means the optimized parameters might change with time. A parameter estimation method that provides multiple-variable optimization for all time during a TRT along with a way to automate the process using software that interfaces with TRNSYS was developed to analyze the TRT data.

The Crossed Contour (CC) method (Leyde, 2016) is an optimization technique used to fit borehole physical and ground thermal transport properties to temperature data during a TRT test. The CC method finds the optimum values for, in this case, the ground thermal conductivity and borehole radius for a set of discreet time windows. The Crossed Contours

Method requires a set of experimental data taken from the field which will be compared to data produced by an appropriate model of the experimental test. A suitable metric must be chosen to compare the two sets of data; in the case of a borehole, the inlet and resultant outlet temperatures are used. The delta slope error characterization shown in equations 2.2 and 2.3, using a least squares linear regression is applied to the data.

$$slope_{model} = regress\left(T_{out,model}, time\right)$$
$$slope_{real} = regress(T_{out,real}, time) \quad (2.2)$$

$$Error = \Delta slope = slope_{model} - slope_{real} \quad (2.3)$$

The error will be minimized as in any other optimization; however, the Crossed Counters method is unique in that this error is minimized for each time window analyzed not for all time. The size of the time windows can be used as a parameter in the analysis by the engineer. For each time window the optimization between the storage thermal conductivity and borehole radius creates a three-dimensional error surface or contour when plotted (Figure 2-2).

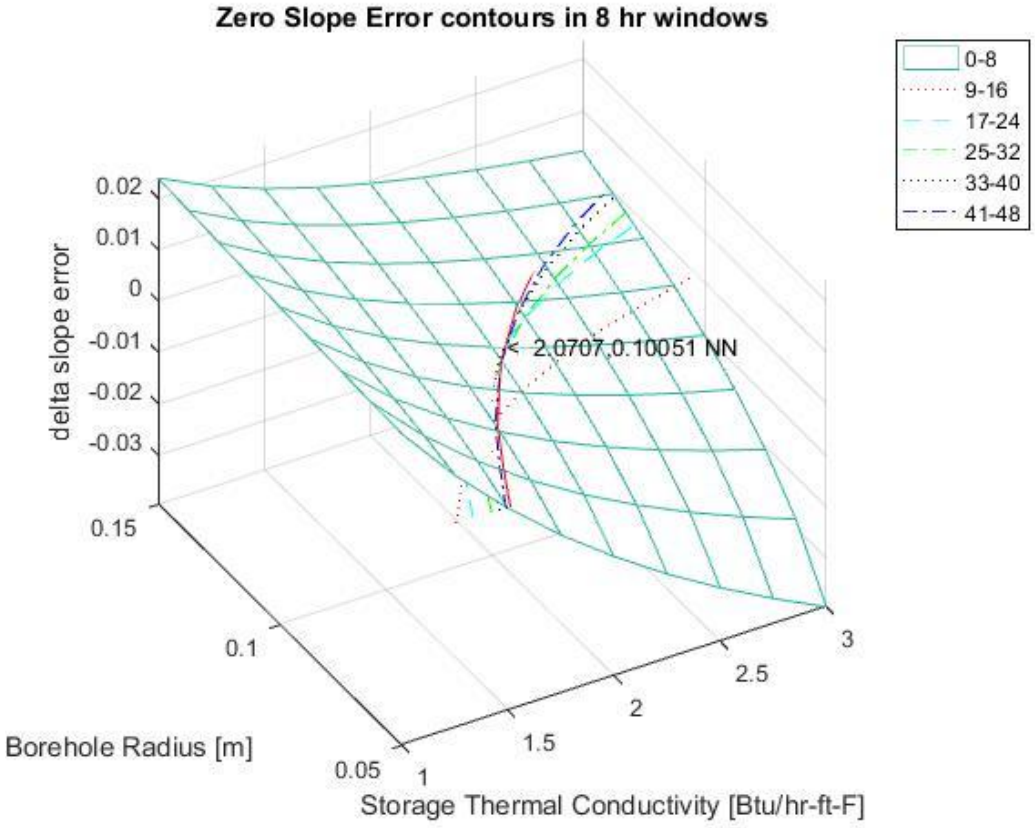

Figure 2-2: CC method output showing the minimized error lines for each time window along with the entire error contour for a single window to demonstrate how the line where the contour intersects the zero-error surface forms a line.

The points where these error contours are minimized form a continuous line that is different for each time window. The lines from all the time windows are overlaid onto one 2-dimensional plot of storage thermal conductivity versus borehole radius so that it can be determined where they intersect (Figure 2-3). This intersection point represents the single set of parameters that provide the best fit between the modeled and experimental data over all time windows.

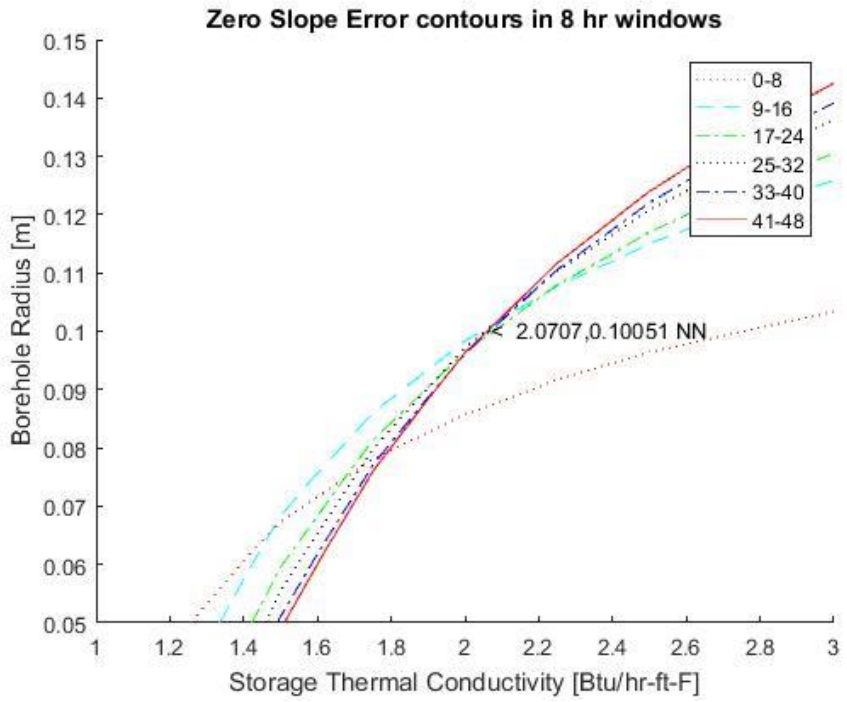

Figure 2-3: CC method, zero error intersect lines for all time windows overlaid on a single 2-D plot with the best intersection point shown.

In practice, manually trying different permutations of storage thermal conductivity and borehole radius in TRNSYS is very time consuming and tedious. For this reason, MATLAB, a numerical computing environment/language, is used to implement algorithms that automate this process. The automated method must (1) systematically generate a set of parameters to implement and then write them into the .dck file that TRNSYS executes from, (2) run the actual simulation in TRNSYS (which can be the most time intensive step), (3) calculate the error between the real and simulated results, (4) after all the permutations have been carried out, plot the zero error contour for each time window on one plot, and finally (5) find the best intersection point for all the contours. This process is illustrated in the diagram in Figure 2-4.

The intersection point of all the minimized error contours can be difficult to find because it may not exist at all; some contours might intersect at a point while others might not. It is necessary to find the single point that is closest to the largest number of contours. A nearest-neighbor-type algorithm was developed that involves initially building a grid of reference points with x and y coordinates ranging from 0 to 1 at a specified resolution, this is the reference grid. The x/y coordinates of the points that make up the minimized error contour lines on the 2-D plot of storage thermal conductivity versus borehole radius are normalized so that the smallest distance between one of the points from the reference grid and one of the contour lines can be calculated. This is done for all the contour lines so that these distances can be summed up for each reference grid point. The grid point with the minimum sum of the distances to all the contour lines represents the best intersection.

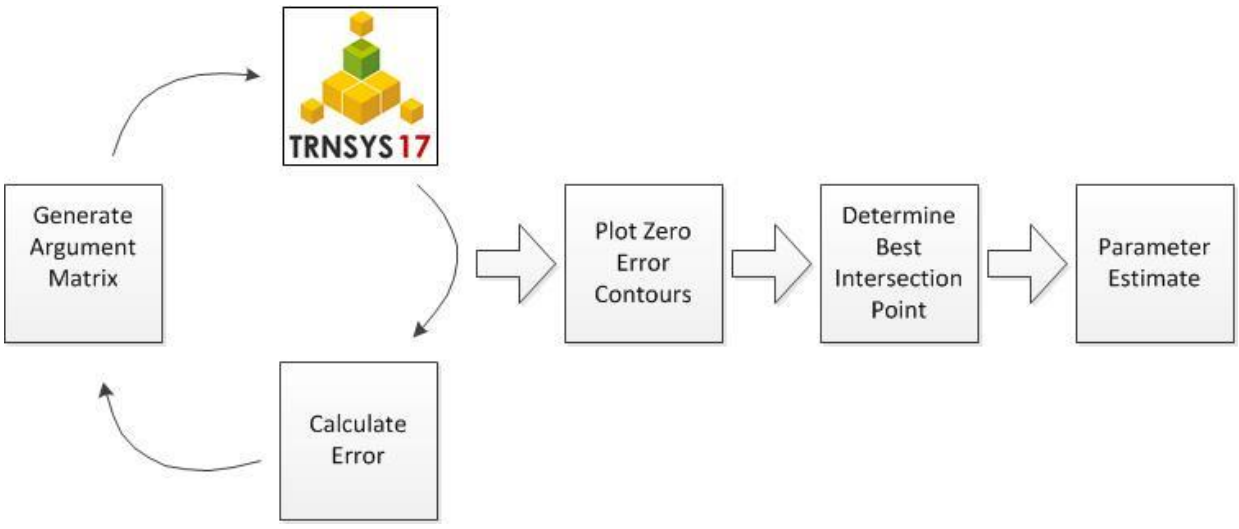

Figure 2-4: Parameter estimation process

2.4 Crossed Contours Method Validation

In order to verify the accuracy and validity of the CC method analysis a test was implemented in which artificial data is fed into the program and results compared to the inputs (see Figure 2-5). The test procedure requires that artificial data be generated by an artificial borehole model whose parameters are well specified and known. A specified cooling load is applied to the fluid input to the artificial borehole and the resulting artificial temperature inlet/outlet data is printed to a file. This artificial borehole data file is then used as the "experimental" temperature data that is fed to the borehole that the CC method is being applied to. This "real" borehole has the exact same parameters as the artificial borehole except the ground conductivity and the borehole radius or whichever two parameters will be varied in the analysis. The artificial experimental inlet temperature data is fed to the real borehole which then outputs an outlet temperature. The CC method analysis uses the real and artificial outlet temperature data to find the combination of parameters that will make these two data sets equal. If the whole process is done correctly and if the CC method is valid the intersection point of the contours should be equal to the values of the parameters specified in the artificial borehole model.

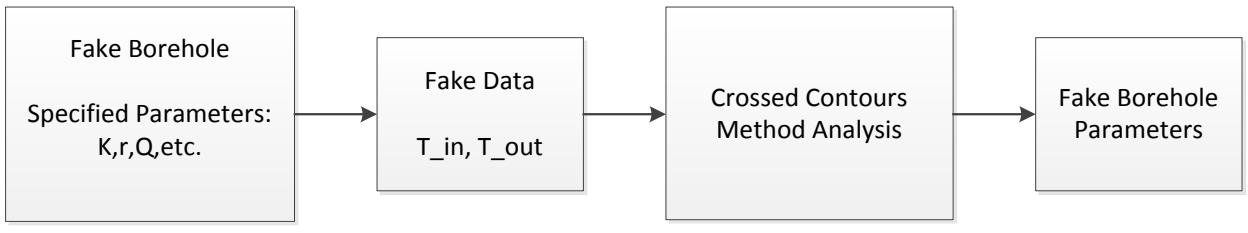

Figure 2-5: CC method verification process flow.

When this procedure was implemented with the fake bore thermal conductivity and bore radius arbitrarily set at 2 Btu/hr-ft-°F and 0.08 meters respectively, Figure 2-6 shows that the CC method results were within 0.5% of the fake bore values.

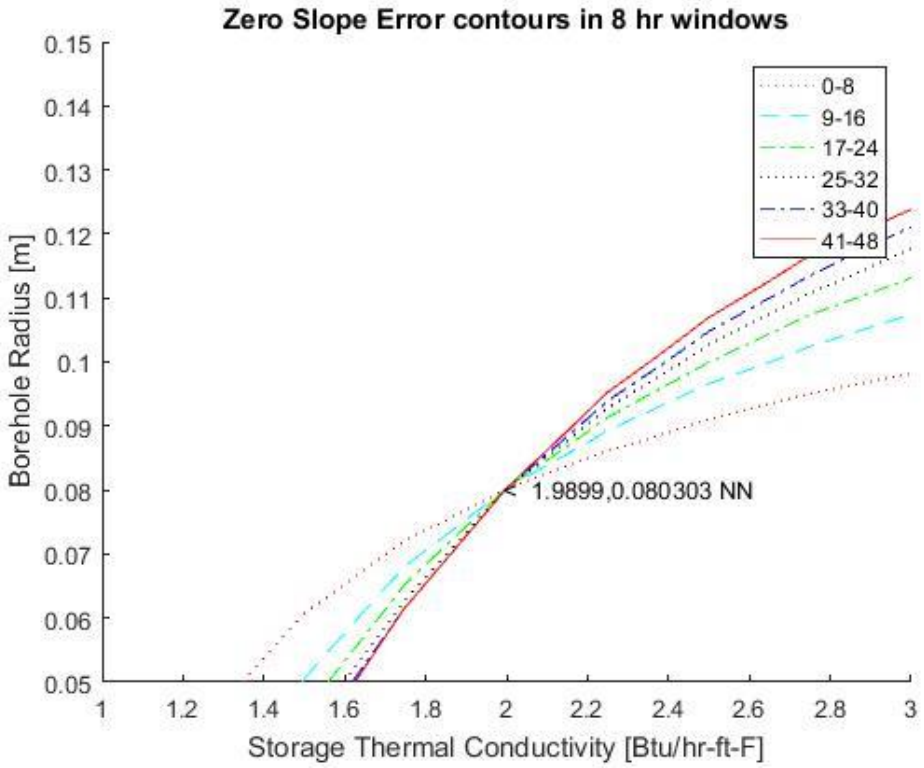

Figure 2-6: CC method analysis results given fake bore data.

2.5 Results

The temperature data from the GRTI TRT was reanalyzed by doing a linear regression on temperature versus the natural log of time to get a slope and using the other quantities specified in the GRTI report with the simplified LSM equation. The resultant thermal conductivity of 4.1 W/m-K (2.37 Btu/hr-ft-°F) is similar to the reported value of 4.03 W/m-K (2.33 Btu/hr-ft-°F).

For the Crossed Contours analysis, the thermal conductivity and borehole radius were taken as the set of optimization parameters. To avoid the influence of start-up transient effects associated with the TRT, the first 8 hours of the test were ignored which is consistent with the recommendations provided in the GRTI report. As a result, the first time-window was excluded from the CC analysis when finding the best intersection point on the contour plot as seen below in Figure 2-7.

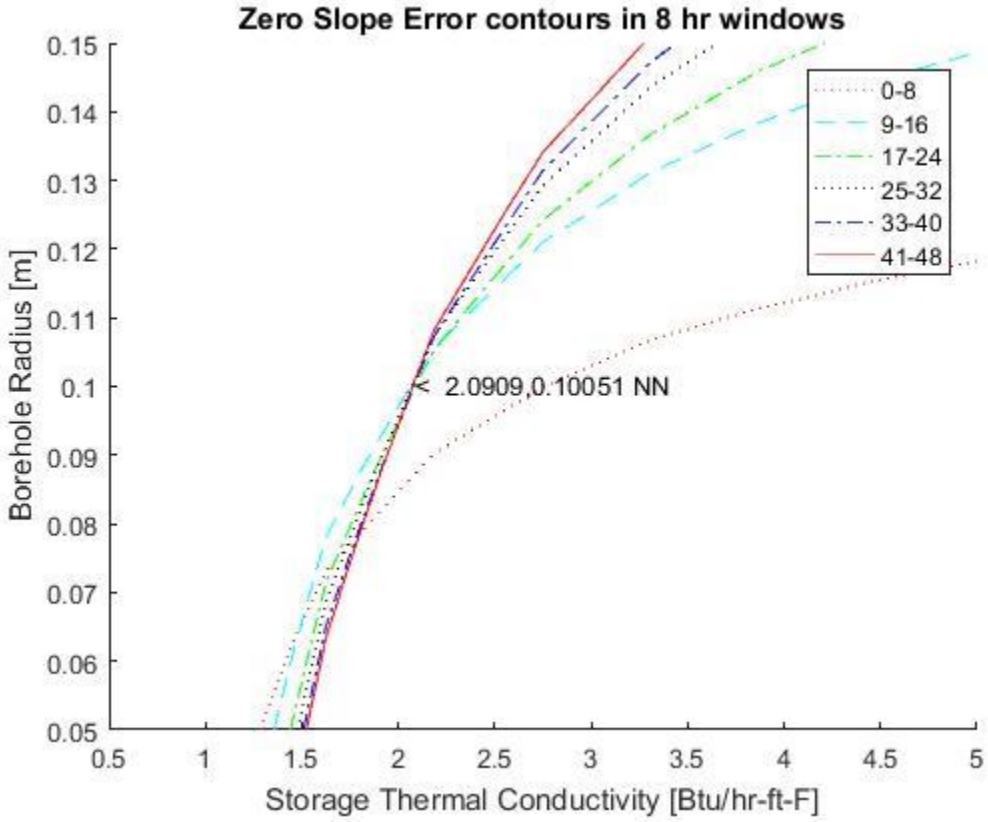

Figure 2-7: GRTI TRT, Crossed Contours Method optimization.

The best intersection point indicated an estimated thermal conductivity of 3.62 W/m-K (2.09 Btu/hr-ft-°F) and a borehole radius of 0.10 meters. The thermal conductivity by the

CC method is 10% lower than the original GRTI TRT predicted, which is greater than the measurement uncertainty given by GRTI of ±5% but within the uncertainty of ±10% recommended by Witte et al. for field testing the ground conductivity (Witte, et al. 2002). This means that the reevaluation of the GRTI TRT is inconclusive since it neither concretely proves nor disproves that the ground thermal conductivity established during the design phase of the system was accurate. Nonetheless, the WID geofield has clearly underperformed since its original installation so other hypotheses had to be considered to explain the underlying causes to the underperformance. A series of hypotheses were developed and tested during the fieldwork which began Fall of 2015.

Chapter 3. Geofield Assessments/Diagnostics

3.1 Motivation

In May 2013, the WID geothermal heat pump system ran at a high capacity in cooling-only mode over a period of several days. The concentrated heat addition to the geofield resulted in a substantial rise in water temperature returning from the geofield (to more than 121°F); thereby, resulting in the heat pumps shutting down on high head pressure because the leaving condenser water temperature was in excess of 130°F. After the heat pumps were shut down, the geofield pumps were periodically operated to monitor the geofield return water temperature. After a period of nine days, the average temperature of the geofield had rapidly dropped to approximately 75°F. However, the apparent geofield ground temperature remained persistently high for several months – never re-approaching the expected undisturbed ground temperature for Madison of 53°F, see Figure 3-1.

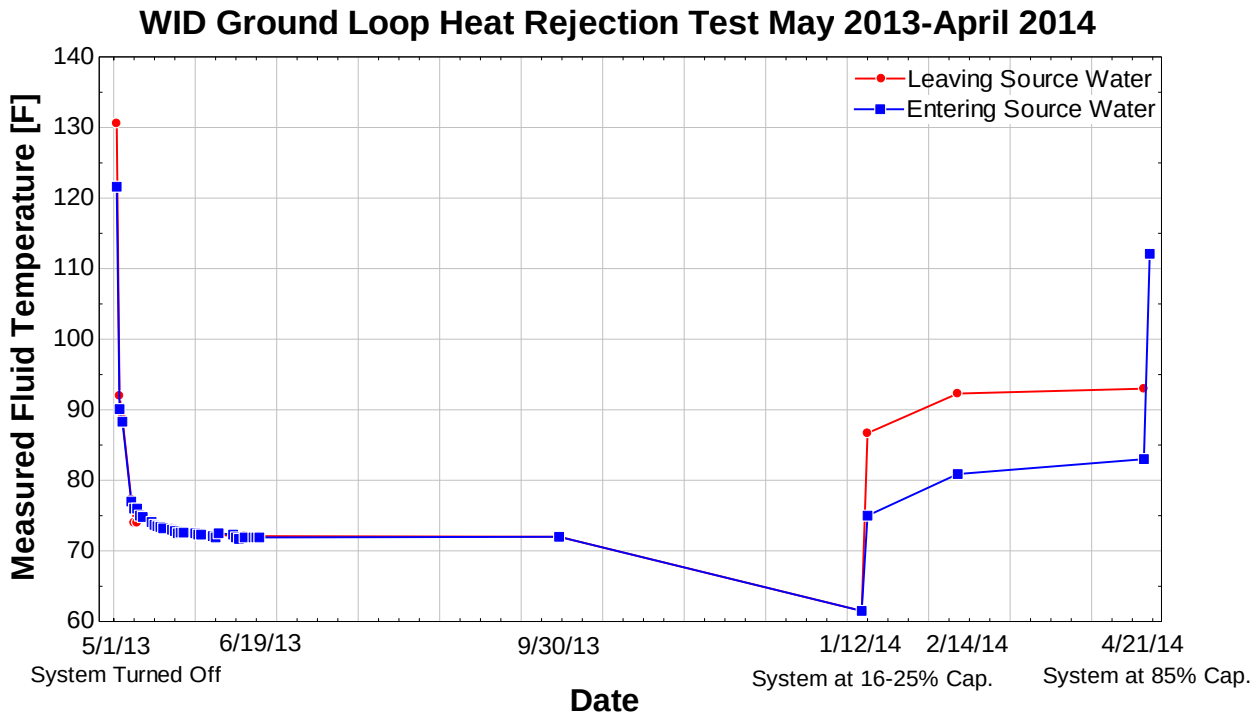

Figure 3-1: High ground temperatures observed at the WID by periodically operating the geofield pumps to observe the fluid return temperature.

In the fall of 2014 with the geofield being idled for over a year, a team comprised of UW faculty, graduate students and outside engineers brainstormed hypotheses with a battery of corresponding diagnostics that could be pursued to better understand the factors contributing to its under-performance. The initial set of hypotheses identified included (1) inaccurate initial thermal conductivity estimates from the original test bore results, (2) water flow imbalance in geofield, and (3) high in-situ bore thermal resistance. Because the geofield had experienced iron bacteria contamination, it was unknown if biofouling from the contamination was responsible for high thermal resistance between the condenser water and the u-tube. Poor ground coupling could also be the result of low grout thermal conductivity which was suspected due to inconsistencies between the original grout specification and drill

logs. WARF funded a work plan to collect data to better understand the thermal performance of the geofield. The centerpiece of the planned work was to excavate to expose the heads of two bores in the geofield so further inspection and in situ experiments could be performed on the geofield.

The actual fieldwork at WID took place the following year during the Fall of 2015 which began by excavated two of the WID's geofield bores to expose the wellheads and make them available for the tests. This fieldwork also included the installation of Permanent Wellhead Monitoring Stations on the two bore holes. These stations were designed to allow easy access to the wellheads into the future and their presence enabled a new TRT to be conducted during the summer of 2016. The initial observations, corresponding hypothesis and diagnostic tests, and results are summarized in Table 3-5.

3.2 Scope

The fieldwork consisted of two main objectives: the preparation and installation of permanent access stations at two boreholes to monitor the geofield and various in-situ diagnostic tests planned in order to provide data that would otherwise not be possible without excavation and exposure of one or more of the geofield's bores. Future access to a portion of the geofield is expected to not only help support operational decisions for WID's heat pump system but also support further research in geothermal systems.

As discussed previously there are various hypotheses that have been proposed to explain the behavior of WID's geofield and the planned tests discussed herein have provided information and data to test these hypotheses. During past operation of the WID heat pump

system, the geofield exhibited a rapid increase in ground loop fluid operating temperature. The observed high fluid temperature may be due to one or more of the following factors: (1) higher than anticipated thermal resistance of the ground, (2) pipe fouling, (3) and/or hydronic imbalances in the geofield. Also observed was anomalous behavior associated with the slow rate of thermal decay of the geofield following a rapid initial rate after the heat pump system was shut down for an extended period. Such behavior could be attributable to high thermal capacity of the grout/ground or the presence of stagnant subsurface groundwater.

The battery of tests conducted during the fieldwork were designed to provide data to test these hypotheses.

3.3 Excavation and Exposure

Ground was broken the morning of September 28, 2015 with Daniels Construction as the contractor performing the excavation work to expose the two selected wellheads. The selected wellheads were on the "Far East" branch of the WID geofield with the two exposed bores designated as the '"North Bore" and "South Bore" based on their compass positions relative to each other. There was, initially, some difficulty associated with finding the wellheads as they were not found in the physical location shown on the as-built drawings for the geofield. After some exploratory digging, the supply, return, and homerun headers were found very near to the service building; more than 12 ft east of their location as-indicated on the as-built drawings. On the second day, after pumping out rainwater that had accumulated overnight, the north and south wellheads were found.

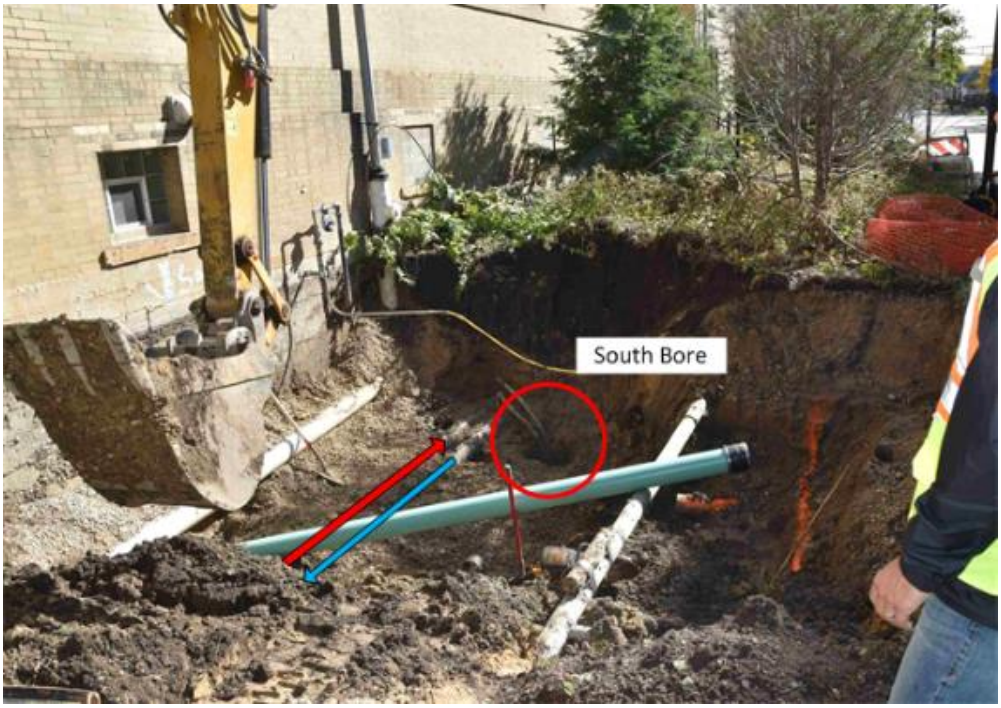

Figure 3-2: South Bore excavation with supply (red) and return (blue) headers visible.

Figure 3-3: North Bore

While exposing the South Bore's wellhead, the research team speculated the grout would also be revealed since it was poured through the entire depth of the bore. Not having experience with excavating vertical bores have been in service for several years, the research team was expecting the grout to be solid with a consistency like gypsum concrete. Both assumptions proved false. By hand digging around the well head and removing layers of clay, a bore-shaped hollow cavity surrounding the supply and return tubes was revealed (Figure 3-4). Although this circular cavity did not extend more than a few feet (verified by probing with a steel rod) it initially provided some reason for concern because it made retrieving an uncontaminated grout sample impossible without more extensive excavation. Additionally, since the research team expected the grout to be solid, it gave the appearance of only more clay apparent at the top of the bore due to the ability to readily penetrate the bore with the steel rod used to check the depth. At the suggestion of team members from the Geology department, a soil sampling tool was used to extract the apparent grout material from the bottom of the cavity surrounding the bore's supply/return lines. The actual material extracted was grey colored with a consistency analogous to peanut butter. After consulting with the grout manufacturer, it was concluded that the material the team was examining was indeed the grout. The gap that existed at the top of the bore (Figure 3-4) is now believed to be due to grout settling after the original installation. The team also understands that some drillers will pack the top of the bore with clay chips to "seal" the hole. These two factors made the plans for in situ grout thermal conductivity testing infeasible. Therefore, planned work for both in-situ and laboratory thermal conductivity testing of the grout was abandoned as discussed further in Section 3.5.

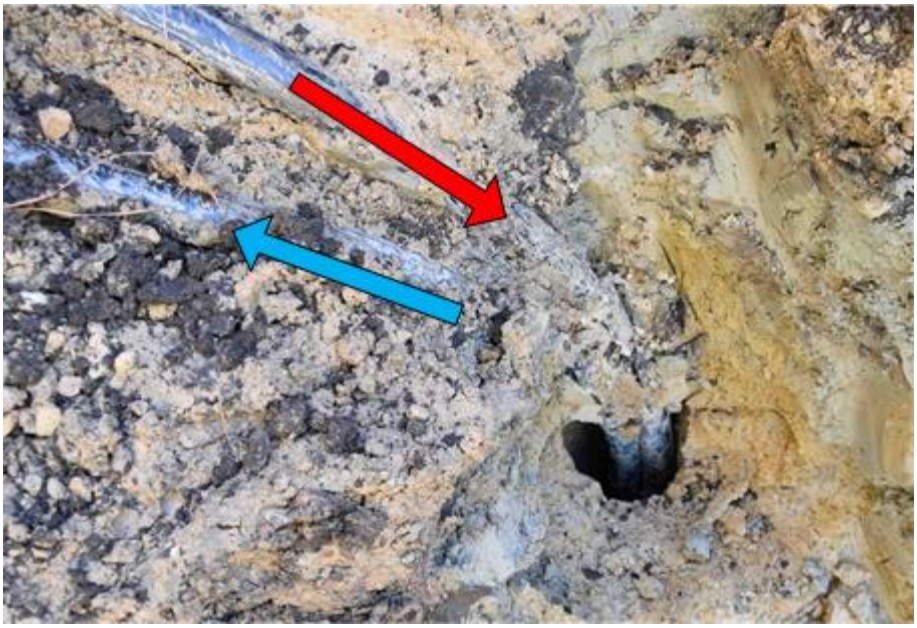

Figure 3-4: South Bore exposed showing gap created by settling grout.

To gain access to each u-tube individually, the supply and return lines for each bore were severed and three-way ball valves installed in each along with risers (Figure 3-5). The three-way valves allow the wells to be isolated from the rest of the geofield so that they may be exercised and tested without interrupting the normal operation of the GCHP system. Circuit setters were also installed on the supply/return lines of each bore to enable accurate measurements of water flow in the supply/return for each u-tube (Figure 3-6: South Bore). These components, minus the circuit setters, were eventually incorporated into the Permanent Wellhead Monitoring Stations.

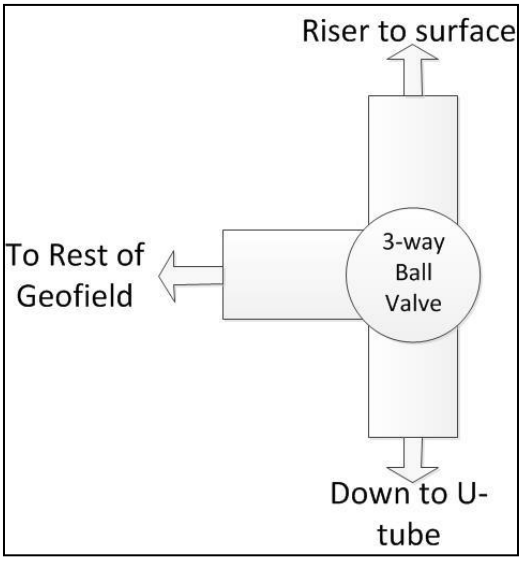

Figure 3-5: Schematic of the 3-way ball valve.

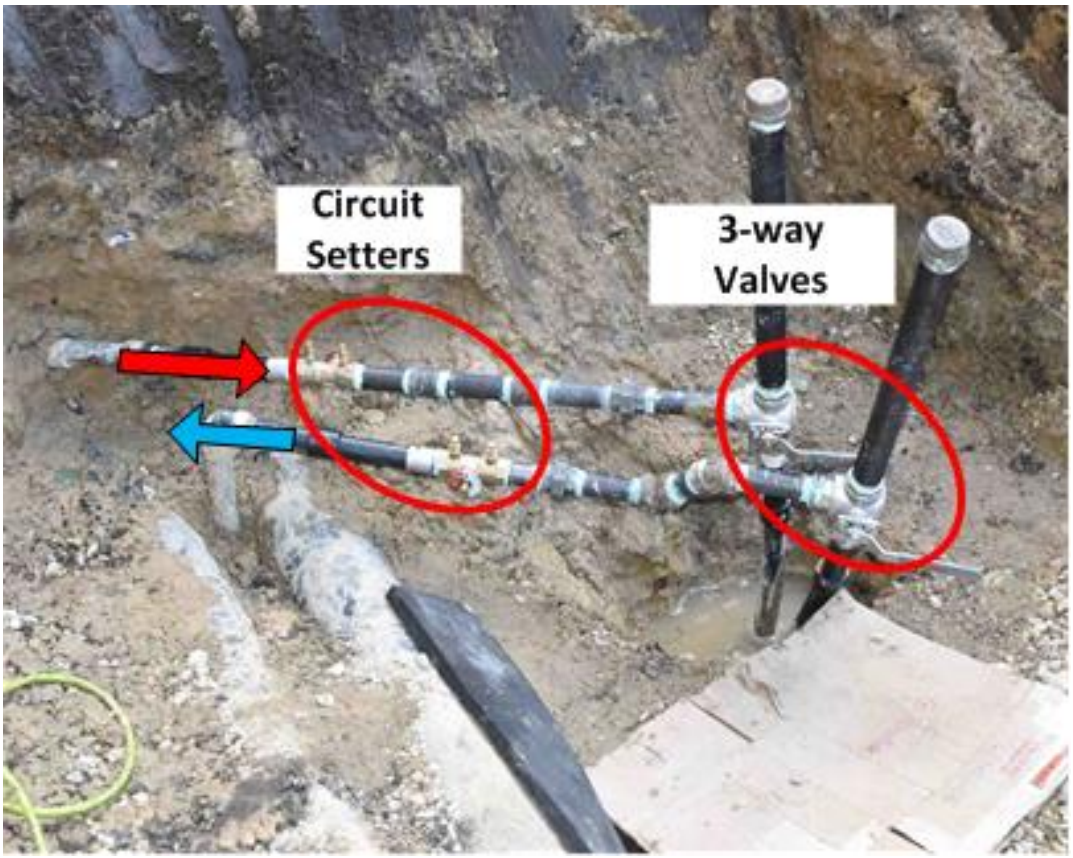

Figure 3-6: South Bore

3.4 Pipe Fouling

Previously, the entire water-side of the geofield experienced biological infiltration and amplification of iron bacteria. Although the entire condenser water circuit was treated and filtered, it was postulated that there could be residual deposition biofouling in the HDPE u-tube piping. Biofouling, if present, could have a negative adverse effect on the hydrodynamic performance of the geofield due to increased pressure drop, which would reduce water flow rate due to the flat head flow curve associated with the pump that is used

for the condenser water system. Biofouling would also reduce the thermal performance of individual bore u-tubes. To ascertain the extent of biofouling, three tests were planned: condenser water sampling, visual examination using a borescope, and pipe section sampling.

When the contractor (General Heating) initially cut into each the north bore and south bore, two water samples were collected for laboratory testing. Two sections of the pipe itself were also harvested and bagged. For the borescope inspection, a commercial unit was initially used but found to produce poor image quality as the onboard cameras lights could not provide sufficient illumination. A custom self-contained bore scope was made by waterproofing a DVR camera and adding supplemental LED lights and a battery for powering the lights as shown in Figure 3-7. This package was secured to a fishing line along with lead weights for ballast.

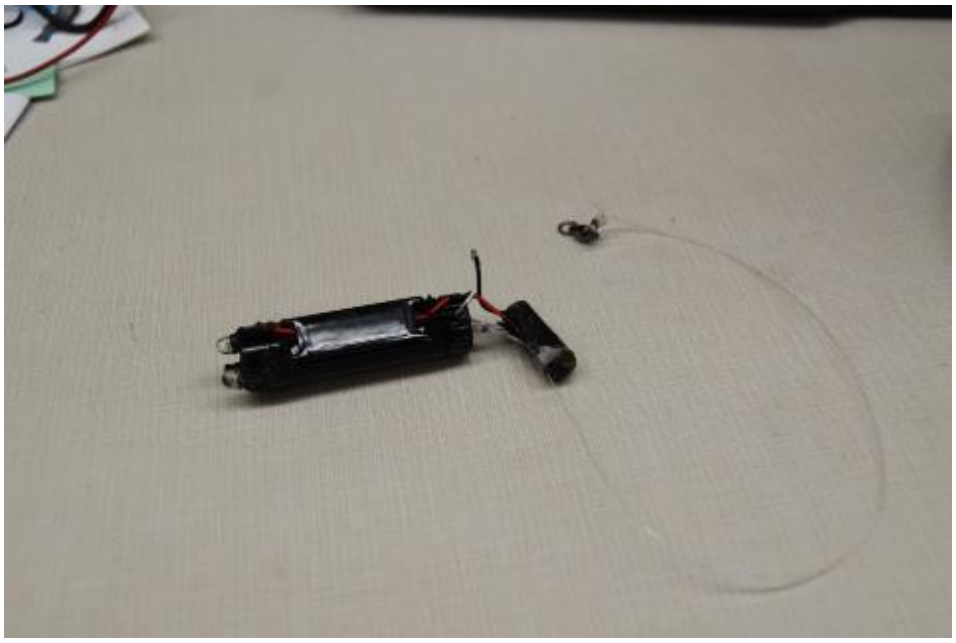

Figure 3-7: Custom made self-contained borescope.

Before using the borescope for the u-tube visual inspection, the water in the u-tubes was flushed because the hydrostatic pressure associated with water present in the u-tube would have exceeded the camera's underwater pressure rating. The water within the u-tubes was cleared by running a line from a compressed air cylinder to one end of the u-tube and attaching a discharge hose to the other end then slowly increasing the pressure on one side to push the water out of the other as shown in Figure 3-8.

Figure 3-8: Compressed air used to flush the water out of the u-tube.

3.4.1 Water Sample Test

As noted previously, two water samples were gathered for evaluation when the contractor initially cut into each the north bore and south bore hydronic loop. The samples were sent to U.S. Water Services for further testing of biologicals and other contaminants. In

actuality, U.S. Water Services did not test the samples; rather, Facilities Planning and Management (FPM) staff conducted a Biological Activity Reaction Test (BART) locally. The test showed the presence of iron-reducing bacteria (IRB). The team relied on the subsequent visual inspection of the piping and thermal testing to assess whether the IRB may be responsible for degraded field performance.

3.4.2 Pipe Sample

A visual examination of the segments of u-tubes cut out of the system showed a slight accumulation of a thin reddish film on the inside of the tubes, but the extent of the accumulation was minor (see Figure 3-9). The team concluded that this level of film was not abnormal and not expected to have an adverse effect on performance.

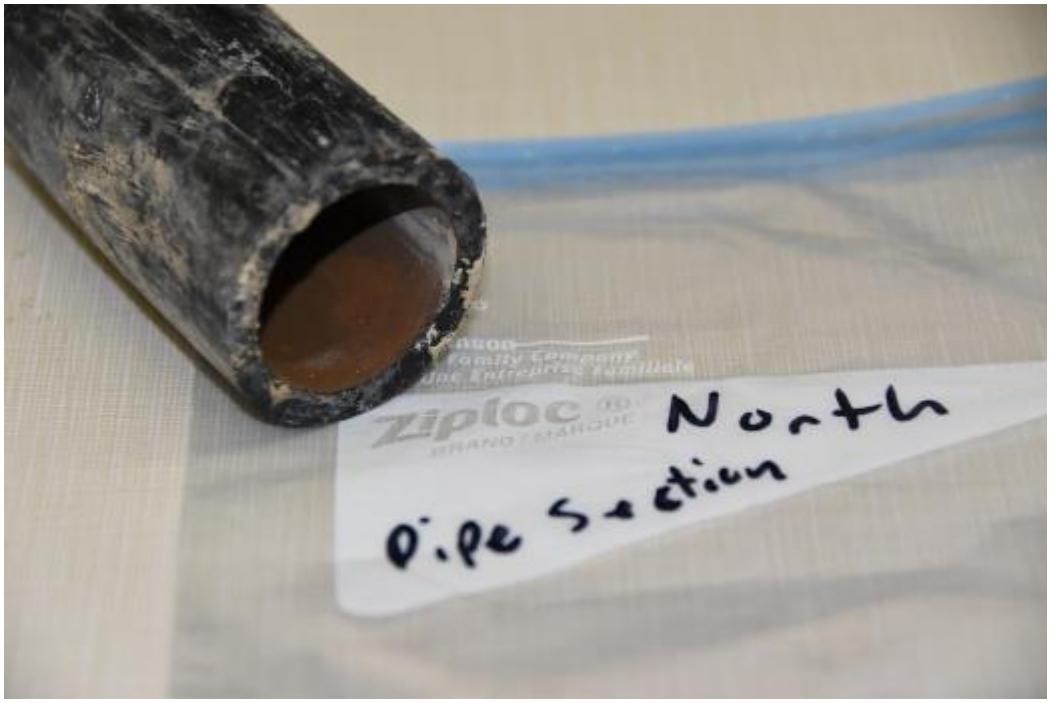

Figure 3-9: Pipe section showing slight build-up.

3.4.3 Borescope Inspection

A commercially-available borescope capable of meeting the strict requirements necessary to visually reach the bottom of the bore at 300 ft. and fit in the 1.5-inch diameter pipe could not be sourced. The closest commercial product found had a line limit of 40 meters (131 ft). This ½" scope included two 30 meter extensions to reach the 300 ft mark. This borescope had poor image quality and the built-in LED lights were not bright enough to effectively illuminate the u-tube; therefore it was abandoned.

An alternative option that consisted of a small self-contained high-definition camera with external LED lights for illumination was used as described above in Section 3.4. This rig had much better image quality and the LED lights were bright enough to see the tube walls but, since it was self-contained, the unit was not capable of providing a "live video feed" – only a video recording. Getting the camera to descend to the bottom of the bore also proved to be difficult. Even with lead weights attached to the camera unit, it was only able to reach a maximum depth of about 70 feet. The inability of the camera unit to descend further was due to the frictional resistance of the fishing line against the walls of the u-tube. This was exacerbated by the fact that the u-tubes were not plumb. Even though the camera did not make it to the bottom of the u-tube, recorded images of the internal surfaces of the u-tube revealed fouling slightly greater than but substantially similar to that seen in the pipe section taken at the top (see Figure 3-10 and Figure 3-11).

Figure 3-10: South Bore scope inspection not showing much fouling.

Figure 3-11: North Bore, tracks left by camera scraping side walls can be seen here.

During the process of flushing water out of the bores before the scope inspection, a catch bucket was placed at the end of the discharge hose. The contents of this bucket did reveal some sediment had accumulated at the bottom of the u-tubes. On its own, the presence of sediment at the bottom of the u-tube is not believed to have a significant effect on the heat transfer properties. It would, however, influence the hydronic flow characteristics of the u-tube which in turn can affect the heat transfer properties. This would be further assessed during the planned hydronics testing in section 3.6.

Based on (1) the difficulties in getting the camera to descend past 70 ft, (2) the absence of any significant fouling in the portions of u-tubes that were visually inspected, and (3) the clarity of water being expelled after flushing out the u-tubes, it was decided that further bore borescoping of the u-tubes was unnecessary.

Figure 3-12: Sediment from the bottom of u-tube collected in catch-bucket. Subsequent flushing produced drastically less sediment.

3.5 Grout Testing

The geofield diagnostic plans originally called for both an in-situ grout conductivity test and a laboratory analysis of grout samples extracted from the excavated bores. These plans were developed while assuming the grout itself would be a hard, concrete-like consistency so that the top could be exposed, drilled into, and probed to determine thermal conductivity in-situ. Furthermore, the team envisioned "chipping" samples of the grout from the bore to allow laboratory tests. Since the actual grout was a semi-solid with a consistency like peanut butter slurry and because settling of the grout occurred, in-situ probing for conductivity testing was not possible. In addition, the team was not able to harvest grout samples without suspected contamination from clay chips; therefore, laboratory testing of the thermal conductivity of field-harvested grout samples was also abandoned.

3.5.1 Sampling

After the initial confusion about expectations of the bore grout appearance and where it should be was resolved, the grout sampling test evolved from drilling and cutting, to digging and scooping. Since the grout has the consistency of peanut butter, a post-hole digger and a hand auger were used in attempts to harvest unadulterated samples of the bore grout. Figure 3-13 shows one of the samples where there is evidence of stray traces of clay (brown in color) that has contaminated the grout (slate gray in color).

Figure 3-13: Sample of grout from North bore.

It was difficult to obtain a highly pure sample from the top of the well head. Therefore, the post-hole digger was used to excavate more of the "surface clay" before using a hand auger (see Figure 3-14) to reach deep between the supply and return lines – a location which appeared to offer the best grout samples.

Figure 3-14: Hand auger used to harvest grout samples.

3.5.2 Grout Composition

Each of the grout samples collected were tested for composition by drying them and putting them through a series of finer and finer sieves to separate the different sized grains. These grains are then weighed and the percent composition of fines is determined. Since the bentonite is made of very fine particles (<300 µm) that are meant to clump together, the team expected that grains under this size represent the actual bentonite. The grout material information specifies 30 - 66% solids, with the WID installation having 66%. The samples

were found to have 71 - 74% solids. It is expected that water content will change once in the ground, and a change of 5-8% is reasonable. The percent of the solids finer than 300µm (consistent with the grain size of bentonite) is estimated at about 55% - which is more than enough to account for the 1 to 5 grout/sand bag ratios which the GeoPro Thermal Grout Lite 100 (GeoPro, Inc., 2016) calls for.

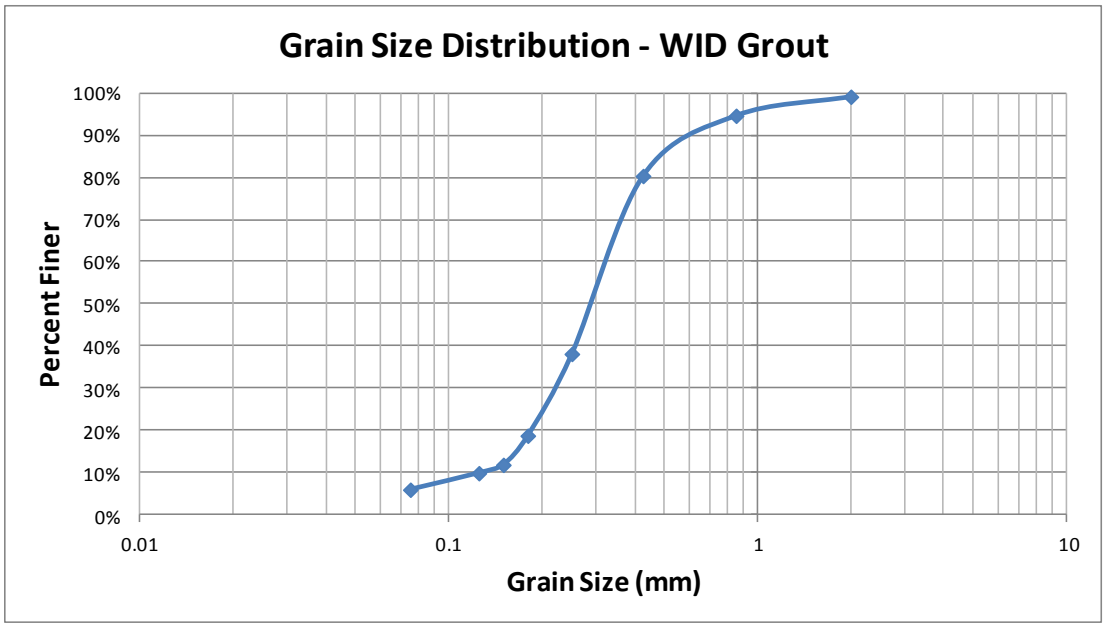

Figure 3-15: GeoPro TG Lite 100 composition analysis.

It was concluded that the grout composition was consistent with the specifications for the grout that was installed. This means that the thermal properties reported as-tested by the manufacturer can be assumed to apply to the grout in the bore.

3.5.3 Grout Thermal Property Assessment

The original objective of testing the grout was to determine whether the thermal properties of the actual grout used in the WID geofield installation were consistent with the grout manufacturer-listed specifications. The project specification called for "GeoPro TG-Lite 100" grout to be used on the installation and the geofield installer (Webster and Sons) indicated that the TG-Lite 100 was the actual grout used in the installation. In reviewing documentation on-file, a discrepancy arose that seemed to raise a question about the grout material installed. Specifically, a different grout material was noted on two well construction logs (well logs for UK126 and UK169 indicated a grout material called "BLACK HILLS 20 LITE" was used as-noted under the heading "Grout and other sealing material", see Appendix A). Later correspondence with Brad Webster reported that "The product used on this project is the TG-Lite grout. That is what was specified, submittals approved for and installed on the WID building project."(Brad Webster, personal communication, August 26, 2014). The team needed another approach to reconcile conflicting information so we would have a higher level of confidence on the material used in grouting the WID bores.

In reviewing the grout installation guidance, the team noted that the grout manufacturer, GeoPro, recommended that installers submit samples for testing to ensure the field mix for the grout was achieving the appropriate thermal properties. The research team contacted the grout manufacturer to determine (1) whether such samples were submitted as part of the original installation of the WID geofield and (2) whether the test results showed the grout conductivity consistent with the grout specification if samples were submitted. GeoPro did have records of this project on-file and confirmed that the driller, Webster &

Sons, in fact had submitted six samples of the grout mixed on site during the original WID geofield installation process (see Appendix A for test results obtained from GeoPro). The first three grout samples submitted by Webster & Sons had a thermal conductivity just below the target of 1.73 W/m-K (1.0 Btu/hr-ft-F) and the remaining three samples were just over. Because it is common for the installer to adjust the grout blend to achieve the desired mix properties based on feedback from lab testing, the evidence appears to indicate that the grout conductivity was at the target for those bores installed subsequent to the first three being installed.

3.6 Geofield Hydronics

Excavating two of the geofield bores created a unique opportunity to collect flow measurement data directly at each of the exposed bore u-tubes. In addition, pressure taps available at each of the WID geofield branches allowed measurement of the dynamic pressure for the four branches with the goal of evaluating whether there were possible flow balance/imbalance issues that may be impacting the field's ability to reject heat from the geothermal heat pumps.

Appendix B includes a table that summarizes the hydronic tests conducted prior to and after severing the u-tubes of the two bores exposed following their excavation. In addition, the operating procedure followed during the tests is included. All official flow data of record were collected by a certified test, adjust, and balance (TAB) contractor – T&B Services, Ltd. In addition, the research team did make some independent measurements of u-tube flow using a non-invasive ultrasonic flow meter. The plan view drawing of the geofield

(figure 4-16) shows a break-out detail of the two bores excavated as part of this diagnostic effort including equipment implemented for flow measurement.

The hydronic measurements were intended to:

1. evaluate the flow balance and other characteristics in the far-east geofield heat exchanger;
2. determine the branch flow in the two exposed bores;
3. take data sufficient to determine overall system characteristics such as pump impeller size;
4. determine the flow vs. pressure drop for the u-tubes in the two bores exposed; and
5. enable other measurements as may be appropriate to understand the root cause of the conditions enumerated below.

These data are intended to help assess whether there is one or more of the following conditions:

a. flow imbalance (due to fouling, over pressurization, installation defect)
b. low u-tube flow (due to fouling, installation defect)
c. low overall system flow (larger hydronic – side pressure drop combined with flat pump curve characteristic)

During the field work, a number of measurements were made to determine if there was probable cause for hydronic system anomalies that may be contributing to the field's apparent underperformance. Figure 3-16 shows a plan view of WID and its geofield with highlights to distinguish the four separate loops comprising the facility's' heat pump geofield. Each loop branch is piped in a reverse-return arrangement intended to facilitate self-balancing flow to each loop. Also, each loop is equipped with isolation valves on both the supply and return to enable valving out one or more of the loops if-required.

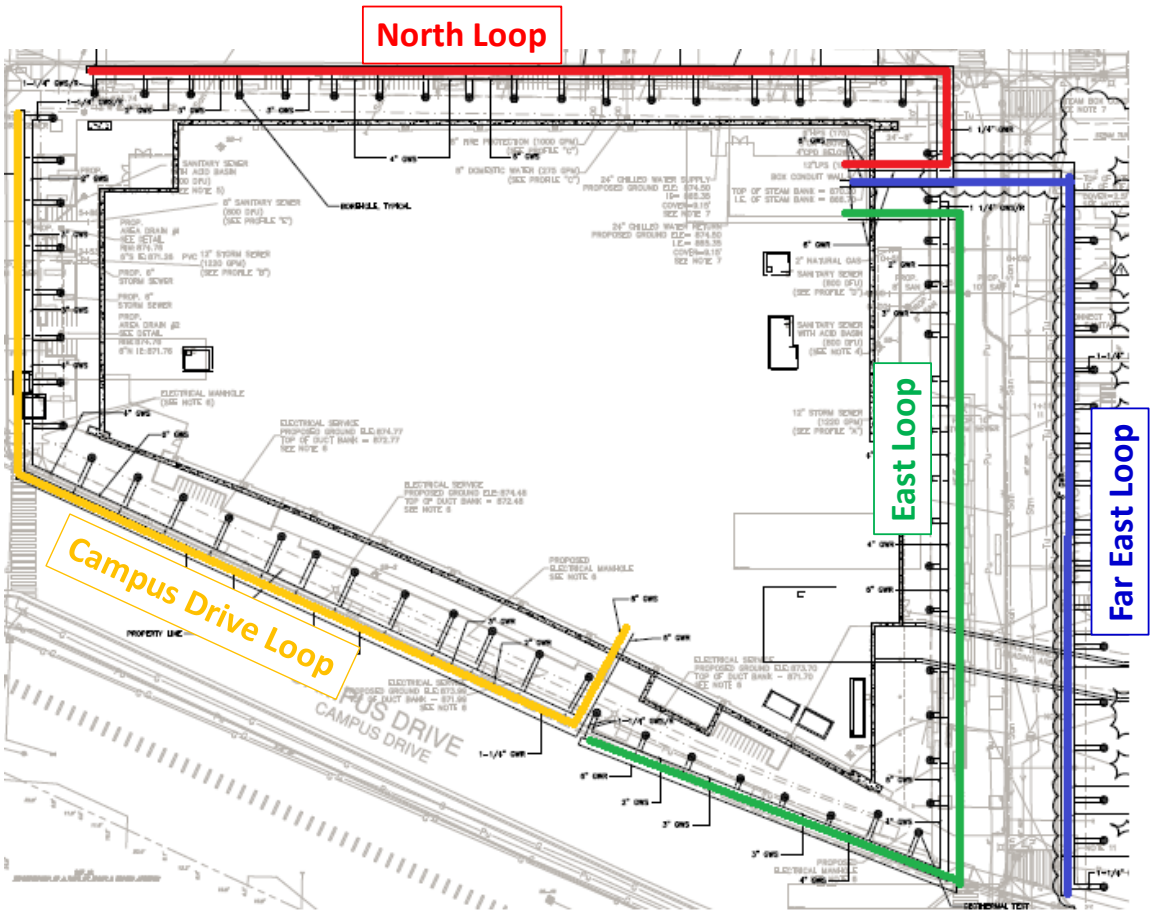

Figure 3-16: Plan view of the WID geofield.

In addition to using the pressure taps that work like a pitot tube to infer flow for each of the four geofield branch loops, Bell and Gossett Circuit Setters (model: CB 1-1/4) were installed in the supply and return for each of the u-tubes exposed in the course of this diagnostic effort, as shown in the illustration and photos below. The CB 1-1/4 Circuit Setters have a flow coefficient of C_V = 12.5 and work like orifice flow meters that have an adjustable opening with a known flow coefficient for the different settings. Equation 3.1 is used to infer the flow rate where A is the orifice area, ρ is density, and P_1/P_2 are the inlet/outlet pressures.

$$\dot{m} = C_V A\sqrt{2\rho(P_1 - P_2)} \qquad (3.1)$$

The use of Circuit Setters on the supply and return of each u-tube enabled accurate measurements of water flow for each of the two u-tubes exposed during excavation as shown in schematic and subsequent photos in Figure 3-17, Figure 3-18, and Figure 3-19.

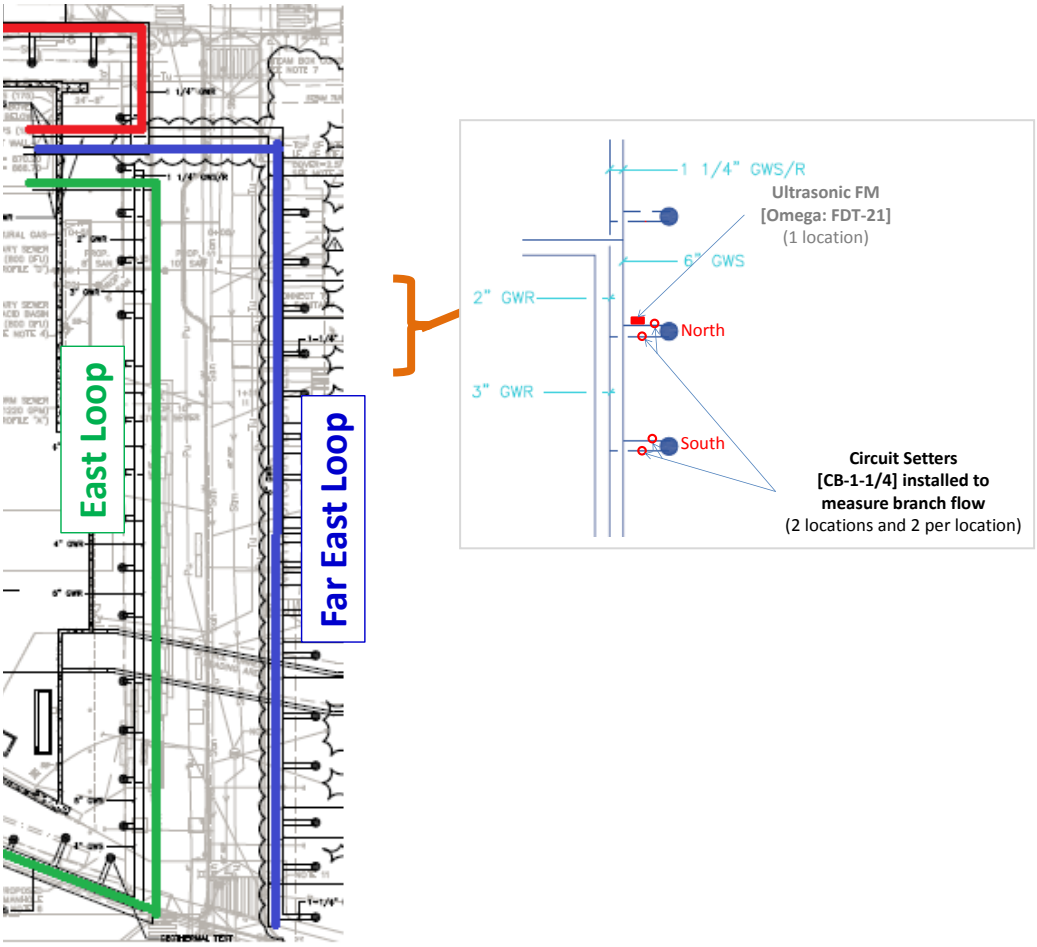

Figure 3-17: Portion of the Far East loop that the research port installation and u-tube flow measurements.

Figure 3-18: Field installation of the ultrasonic flow meter (Ultrasonic Flow Meter -Omega: FDT-21; upstream and downstream transducers - S2H).

Figure 3-19: Field installation of B&G Circuit Setters (CB 1-1/4) on the supply and return of each u-tube (left) and differential pressure measurements being made during testing (right).

A series of flow measurements were made for each of the u-tubes exposed (North bore and South bore) while (1) operating a single circulating pump and (2) operating both circulating pumps. Table 3-1 below shows the measured flow at each of the u-tubes exposed as-measured using the Circuit Setters. With two pumps operating at 60 hz, the average flow for the two bores is 13 gpm compared to the design flow rate for each of the u-tubes is 12 gpm. Assuming 82 bores in the field and their operation at 13 gpm, the total flow would be 1,070 gpm which is close to the design flow for two pumps operating in parallel.

Pump Speed (hz)	Pumps Operating	North Bore Flow (gpm)	South Bore Flow (gpm)
70	2	16.1	14.1
60		13.8	12.3
40		9.0	8.1
20		3.7	2.8
60	1	12.7	11.7
40		8.2	7.2
20		2.8	2.7

Table 3-1: Flow data for the two u-tubes exposed by excavation (all four zones of the geofield in operation).

A particular emphasis was placed on determining the flow vs. pressure drop for each of the excavated u-tubes (North and South bores). The pressure drop across a given u-tube is expected to follow a quadratic relationship and, as shown in the plot that follows, the

measured characteristic obeys this principle. Interestingly, the pressure drop in the South bore is systematically higher than the pressure drop in the North bore. This greater pressure drop causes the observed flow rate for the South bore to be lower.

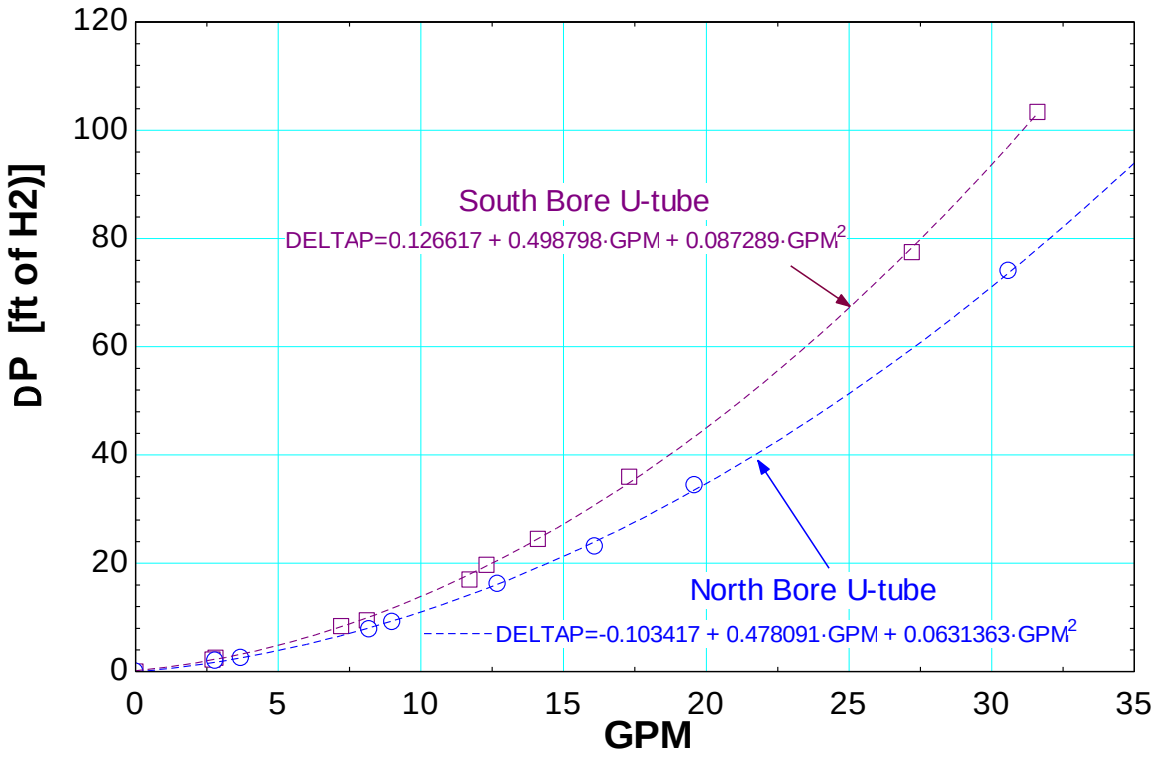

Figure 3-20: Measured and curve fit pressure drop vs. flow for the u-tubes in the South and North bores.

The team also ran a "stress test" on the Far East loop while taking flow measurements in the North and South bore u-tubes. The goal of this set of measurements was to determine the flow rate in the u-tubes and the corresponding velocity. The operating condition had both geofield pumps running (P-11 and P-12) while only the Far East loop was operating (all other zone isolation valves closed). The u-tube flow rates and corresponding tube velocities for this run are shown in Table 3-2.

Pump speed (hz)	North Bore (gpm)	Velocity (ft/s)	South Bore (gpm)	Velocity (ft/s)
70	35.9	8.0	31.6	7.0
60	30.6	6.8	27.2	6.1
40	19.6	4.4	17.3	3.9

Table 3-2: Flow data for the two u-tubes exposed by excavation (all zones except the Far East loop in the geofield isolated with both geofield pumps operating).

Originally, the WID geofield circulating pumps selected were two Bell & Gossett 1510 3AC series pumps arranged in parallel (see Figure 3-21); however, the 3AC pumps were not available so 4AC pumps were selected. Pump curves for both the 3AC and 4AC are shown below in Figure 3-22 with two pumps operating in parallel. One significant difference between the 4AC and the 3AC series selection is the design operating point on the parallel pump curves. The 3AC shows a more favorable design operating point that is "down on the curve" whereas the 4AC design operating point is "back on the curve." By selecting the circulating pump back on the curve, small changes in head translate in to substantial changes in flow.

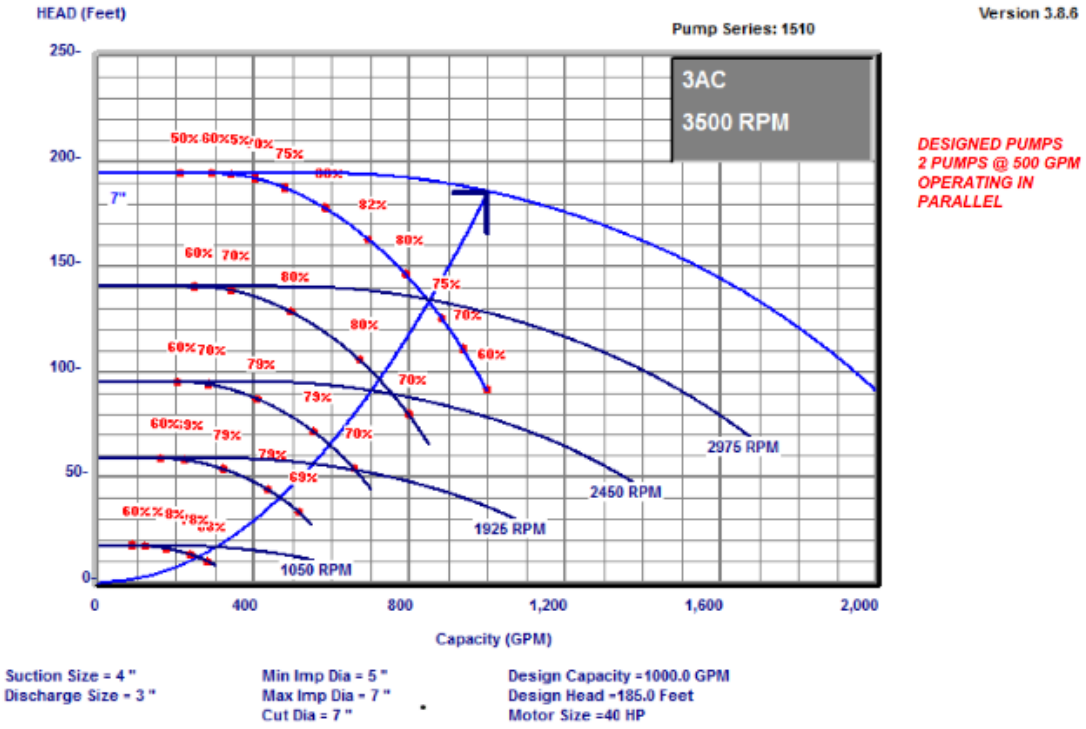

Figure 3-21: Pump curves for the two B&G 1510 3AC series WID geofield circulating pumps operating in parallel selected but not installed. Operating point marked by inverted L bracket.

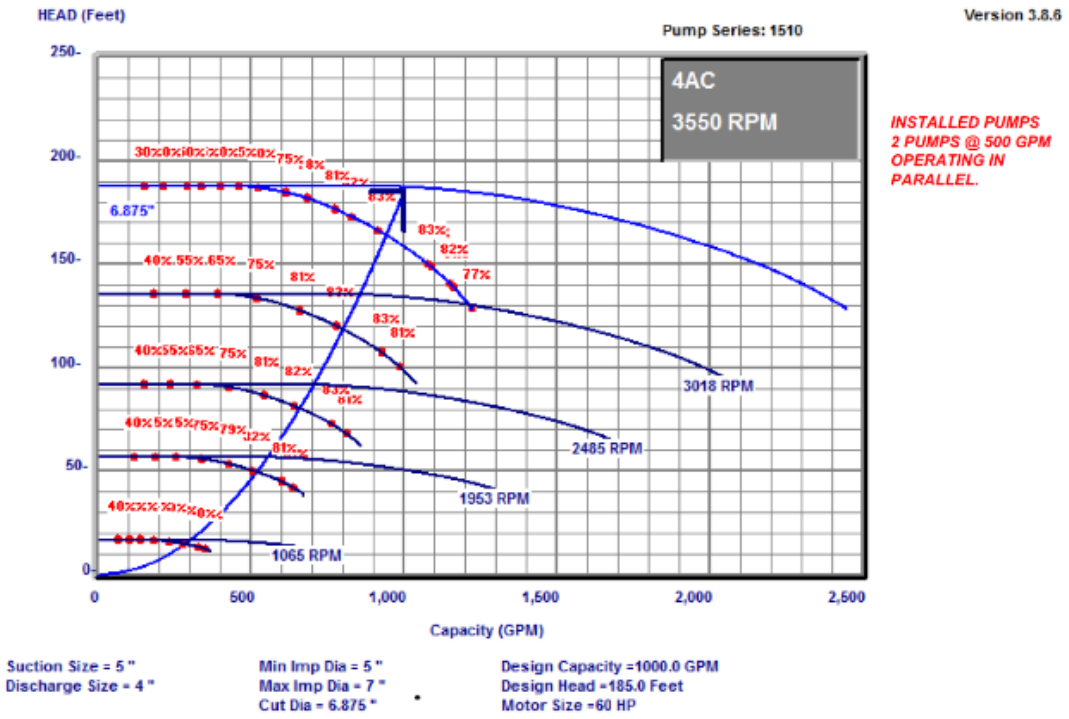

Figure 3-22: Pump curves for the two B&G 1510 4AC series WID geofield circulating pumps operating in parallel actually installed. Operating point marked by inverted L bracket.

In addition to u-tube flow measurements for the North and South bores, the branch flow to each of the four loops comprising the total WID geofield were determined by measuring the water's dynamic pressure via pressure taps installed in each of the branch lines. Because the geofield was known to have had iron bacteria, the pressure taps for each branch of the geofield were bled prior to data collection. Upon initial opening of the taps, the water being bled was highly discolored as shown in Figure 3-23. The discoloration and odor of the fluid was indicative of amplification of iron bacteria in the deadleg created by each pressure tap. Enough water was bled through the tap until the flow of water became clear in appearance.

Figure 3-23: Pressure taps being bled in preparation for branch flow measurements (left) and appearance of fluid initially bled from branch line pressure tap (right)

Table 3-3 below shows the design flow rates for each of the geofield branches compared to the indicated flow rate by differential pressure measurements using the Presso pressure taps with two pumps running at 60 hz. With all geofield branches open, the sum of the branch flows to each of the zones totaled 685 gpm (based on velocity pressure measured by the Presso taps) vs. a total flow developed by the geofield pumps of 1,050 gpm[2] based on the head developed by the pumps and their corresponding pump curves. Further, the average u-tube flow as-measured with two pumps operating in parallel at 60 hz was 13 gpm. For all 82 bores, the total flow rate would be 1,066 gpm which agrees closely with the inferred pump flow data. The estimate of the total flow from the pump curves is within 3% of the total flow of the two pumps measured during WID startup[3]; however, this total flow is 53% greater than

[2] The geofield pumps (P-11 & P-12) are Bell & Gossett 1510 series 4AC pumps.

[3] The WID original balance report dated 10/9/10 showed pump P-11 developing 475 gpm at 192.8 ft of head (60 hz) while P-12 developed 550 gpm at 192.3 ft of head (60 hz) for a total of 1,025 gpm.

the sum of the branch flows (685 gpm) as-shown in the table below. A corrected flow coefficient (Cv) for each branch was calculated based on the indicated differential pressure for the respective branch vs. branch flow rate corrected such that the total flow for all four branches matched the total pump flow rate of 1,050 gpm.

Branch	# of bores	Flow rate (gpm)		% diff	Corrected Cv
		Design	Presso Indicated		
North	19	228	180	-21	241
Far East	21	252	155	-38	238
East	22	264	170	-36	238
Campus Dr.	20	240	180	-25	241
Total	82	984	685	-30	240

Table 3-3: Flow data for each of the WID geofield branch loops comparing design flow with indicated flow using velocity pressure measured at the Presso taps for each branch of the geofield loop.

Next, a series of branch flow measurements were made by closing all zone isolation valves except each successive branch loop while ramping the twin parallel pumps down in speed. Table 3-4 shows the estimated branch flow using the Presso taps available at each

branch connection. As noted above, the reliability of the flow data being inferred from the Presso taps is not high. Thus, the data below are of limited utility. With that being said, the average flow at the 60 hz pump operation for each loop is 555 gpm.

Geofield Loop Isolation Valve Position				Flow Measurements
North	East	Far East	Campus Dr.	
Closed	Closed	Open	Closed	Far East loop flow rate – 530 gpm @ 60 hz 350 gpm @ 40 hz 110 gpm @ 20 hz
Closed	Open	Closed	Closed	East loop flow rate – 590 gpm @ 60 hz 400 gpm @ 40 hz 205 gpm @ 20 hz
Open	Closed	Closed	Closed	North flow rate – 570 gpm @ 60 hz 370 gpm @ 40 hz 170 gpm @ 20 hz
Closed	Closed	Closed	Open	Campus Drive flow rate 530 gpm @ 60 hz 295 gpm @ 40 hz -[4] @ 20 hz

Table 3-4:Individual geofield loop flow measurements (using the branch Presso taps).

[4] When the pump flow was reduced, the differential pressure on the Presso pressure taps decreased below a threshold that would allow estimates of flow.

In summary, the hydronic system data collected were intended to assess whether there is one or more of the following conditions:

a. flow imbalance (due to fouling, over pressurization, installation defect)

b. low u-tube flow (due to fouling, installation defect)

c. low overall system flow (larger hydronic – side pressure drop combined with flat pump curve characteristic)

Based on the data collected and the visual observations of the u-tubes bore scoped, **there does not appear to be any water-side fouling that is appreciably impacting the hydrodynamic performance of the geofield**. The average u-tube flow rate with two circulating pumps operating at 60 hz was found to be 13 gpm which is 8% higher than the expected design flow rate of 12 gpm per bore. **There did not appear to be any significant flow imbalance between the four geofield loop segments; however, high uncertainty in the inferred branch flow rates somewhat clouds this conclusion.** Independent estimates for the overall system flow rate for all four branch loops included (1) 1,050 gpm based on pump curves and (2) 1,070 assuming 82 bores operated at the same average flow per bore (13 gpm) as the measured flow rate for the two exposed bores. These flow rates were within 9% of the expected design flow rate of 984 gpm. Consequently, there does not appear to be any appreciable flow anomalies; however, the flat head vs. flow characteristic of the 4AC series pumps makes the geofield susceptible to significant decreases in system flow should water-side fouling occur in the future.

3.7 Temperature Profiles

The goal of this test was to obtain an experimentally-measured temperature profile of the water within the u-tube of each bore exposed post-excavation. Prior to conducting this test, the geofield pumps were turned off for at least 8 hours to ensure water within the individual u-tubes will be in equilibrium with the surrounding ground.

Measured temperatures in the u-tube(s) for each bore greater than "typical" geothermal gradients for the Madison-area are suggestive of abnormally slow bore thermal decay. Measured temperatures establish a known "starting point" that can serve as a reference for a subsequent thermal response test. The shape of the temperature profile will provide insight into the vertical distribution of heat transfer properties throughout the geological layers surrounding the bore. These results could support a better understanding of enhancement or degradation of heat transfer mechanisms at various elevations throughout a given bore, such as ground water flow and stratigraphic unit layers having varying thermal properties.

To measure the static temperature profile throughout the vertical bore, a custom fishing pole-like rig was used to lower a temperature/pressure data logger down the entire 300 ft. depth of bore. The "levelogger" shown below in Figure 3-24 is capable of measuring the temperature of whatever fluid it is immersed in; be it water or air. It also has the ability to measure static pressure which can be used to determine its depth. The logger was lowered incrementally and allowed to thermally equilibrate for 5 minutes with the surrounding fluid as shown in Figure3-25.

Solinst Levelogger (Model 3001) LT F300/M100

- Logger dimensions: 7/8" x 6.25" (22 mm x 159 mm)
- Weight: 4.6 oz. (129 grams)
- Temp. Sensor Accuracy: ± 0.05°C

Figure 3-24: Levelogger

Figure3-25: Fishing the levelogger down the u-tube in order to obtain a temperature profile of the bore.

3.7.1 Fiber Optic Distributed Sensing Temperature Profile

A fiber-optic cable provides the capability of obtaining a temperature profile of the entire depth of the borehole in real time (as opposed to the levelogger which only measures temperature one point at a time). In this project, the fiber-optic cable was used to compare the equilibrium temperature profiles of each bore obtained by both techniques. Later, it was used in conjunction with the thermal response test (TRT) to provide temporal and spatial information about the temperature in the bore.

For this test, lead weights were attached to the fiber-optic cable and the other end was plugged into the "interrogator." The "interrogator" is a device that contains a powerful laser that produces a signal in the cable that is then interpreted and converted into a temperature reading. In this case the cable was only deployed in one end of the south bore u-tube (Figure 3-26).

Figure 3-26: Fiber optic distributed sensing system being used on the south bore.

3.7.2 Levelogger and Fiber

One of the working hypotheses to explain the apparently higher than expected formation thermal conductivity obtained during the initial TRT but diminished field performance once the bore was thermally challenged is the presence of a large subsurface aquifer that the geofield is tapping into which has a higher heat capacity than the dry ground but would retain heat once it is thermally charged. This type of structure would experience a slow thermal decay of ground temperatures. A temperature profile along the entire depth of the bore provides insight into regions of high or low thermal conductivity and heat capacity.

The undisturbed ground temperature is expected to be a constant below 50 feet and, for Madison Wisconsin, the temperature should be approximately 53°F (see Figure 3-27 below). The highest temperatures observed in the water returning from the WID's geofield

were in excess of 120°F when running at full load (Knudson, 2013). This occurred following a sequence of operation of the heat pump system over a period of approximately three days resulting in a thermal overload to the geofield. On May 1, 2013, the heat pumps were shut down and the field temperature subsequently monitored over a period of several months as shown in Figure 3-28. Initially, the average temperature of the geofield rapidly dropped to approximately 75°F within nine days after idling the heat pumps. However, the temperature remained persistently high for several months – never re-approaching the expected undisturbed ground temperature lending further support to the hypothesis of a large pool of perched subsurface ground water that became warmed by the short period of intense thermal input from heat pump operation. With a large volume to surface ratio, high heat capacity due to the water, and low thermal conductivity, such as perched ground water would exhibit very low heat dissipation to the surrounding formation at the undisturbed ground temperature. The geofield temperature rise in January 2014 coincided with the start-up of the heat pumps at a reduced capacity followed by another spike in temperature when the system's capacity increased resulting in a greater heat load being imposed on the geofield.

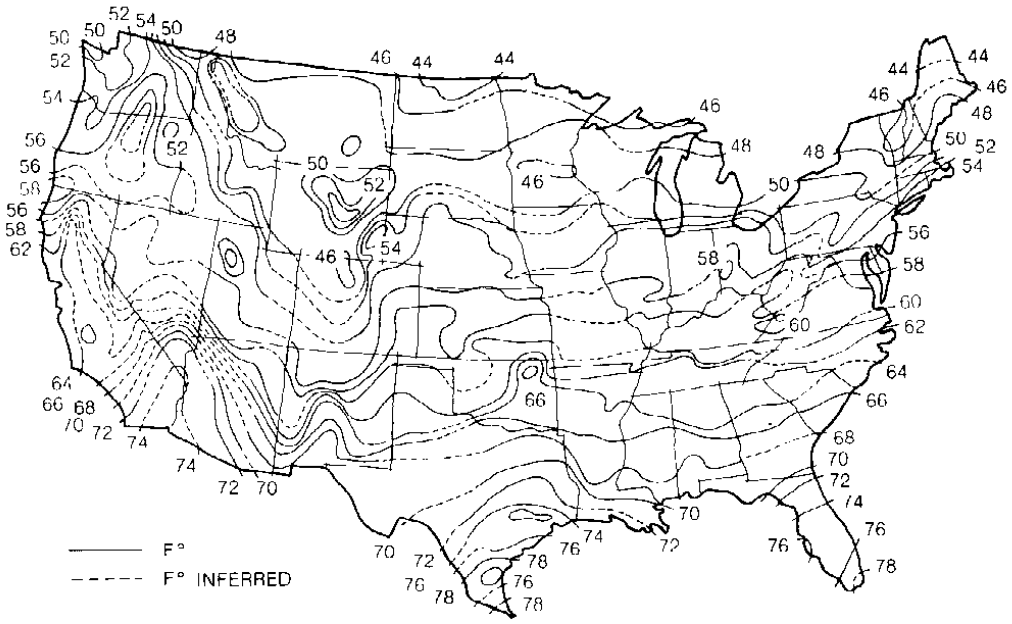

Ground water temperatures. Map courtesy of National Water Well Association.

Figure 3-27: Contour map of undisturbed ground temperatures. http://mb-soft.com/public3/water502.html

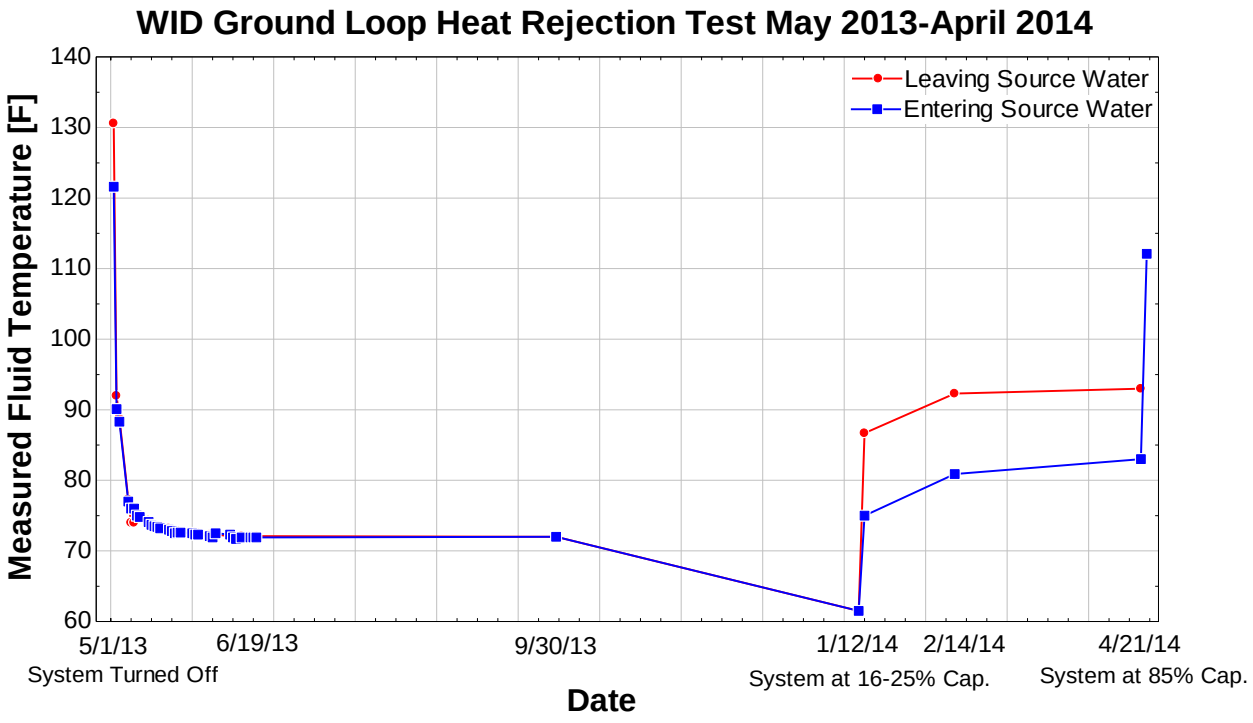

Figure 3-28: WID geofield average water temperature during a decay period following a thermal overload to the field.

Given enough time without any thermal heat input to the geofield, one would reasonably expect the field to return to the undisturbed ground temperature of 53°F. At the time the present diagnostic field work began (September 28, 2015), the heat pumps had not been operated since February 2015 which amounts to a 7-month period with no heat addition to the field (except for a very small amount of heat attributable to operation of the circulating pumps which were used to periodically circulate the fluid in the geofield for water treatment and filtration). Seven months of recovery time, it was thought, should be enough to restore undisturbed conditions because the ground can still dissipate heat albeit at a slow pace. A typical temperature profile should begin at a temperature close to ambient and quickly

approach the undisturbed ground temperature no matter the season of the year as shown below in Figure 3-29.

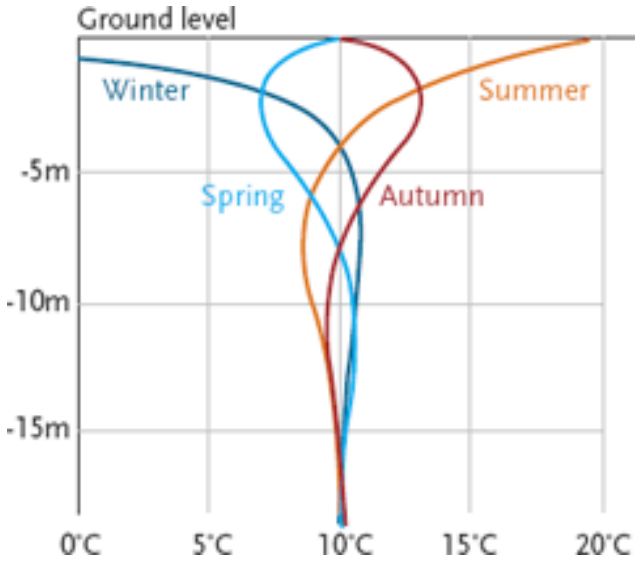

Figure 3-29: Typical temperature profiles. http://www.cibsejournal.com/cpd/modules/2010-04/

Figure 3-30 and Figure 3-31 show initial equilibrium temperature profiles of the north and south bores obtained using the levelogger and the fiber-optic distributed sensing system[5], respectively. Each independently displays the same basic profile shape although there is an offset of 2 degrees between the fiber and the levelogger profiles due to fiber not being fully calibrated at the time this data was collected.

Upon observing the temperature profiles, it is immediately apparent that temperature readings are substantially higher than the undisturbed ground temperature of 53°F. While traversing the depth of the bore, the temperature quickly rises to an average of 78°F which

[5] The profile taken with the fiber optic DTS system is different from the rest due to an offset error in the calibration during this case which was fixed in later measurements.

suggests, that even after an extended period of no load the geofield, it is only about 60% restored to an undisturbed initial condition. Traversing further down the bore, the temperatures begin to drop to a minimum of about 64°F; closer to the undisturbed ground temperature.

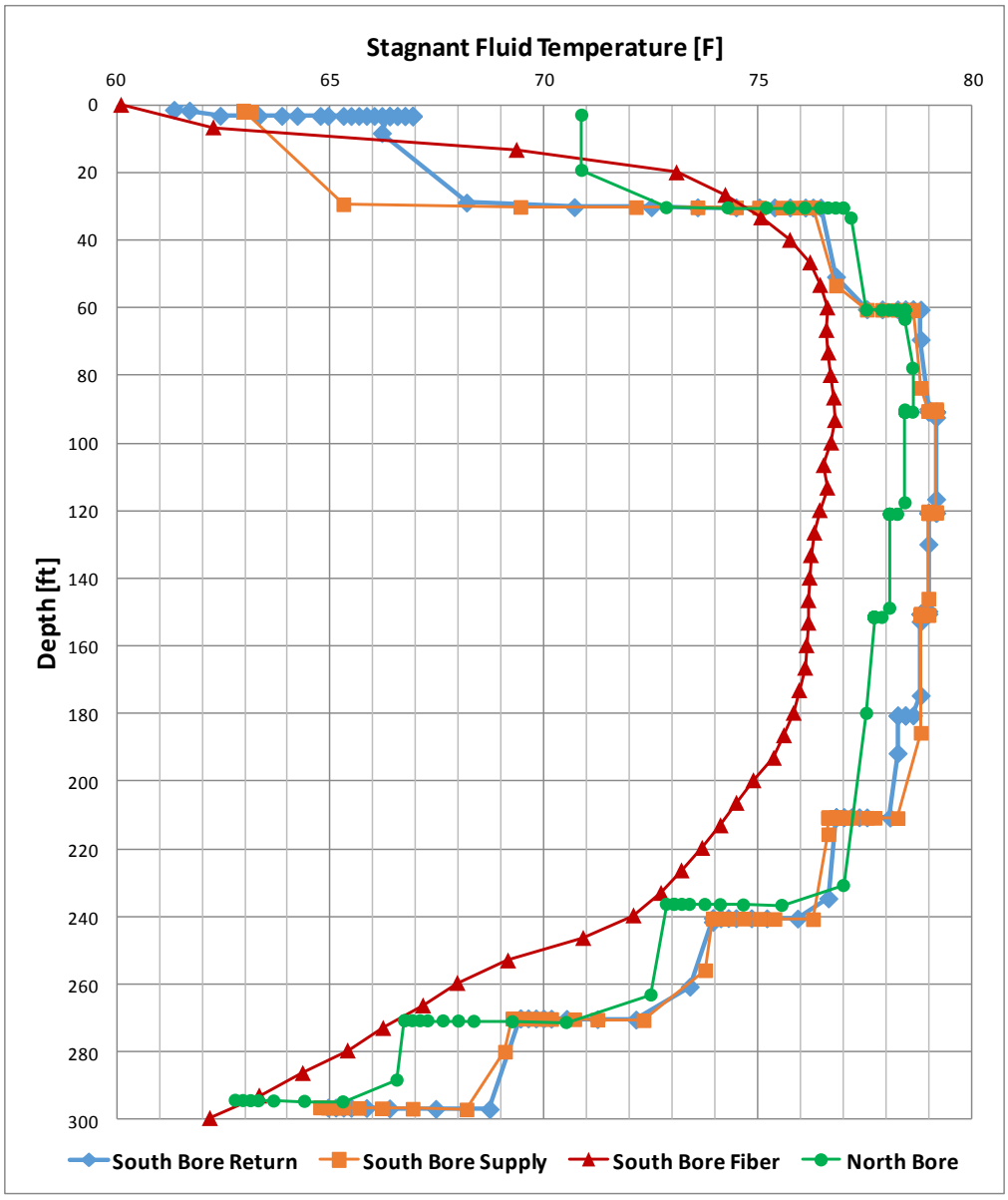

Figure 3-30: Temperature profiles taken with the levelogger unless otherwise labeled.

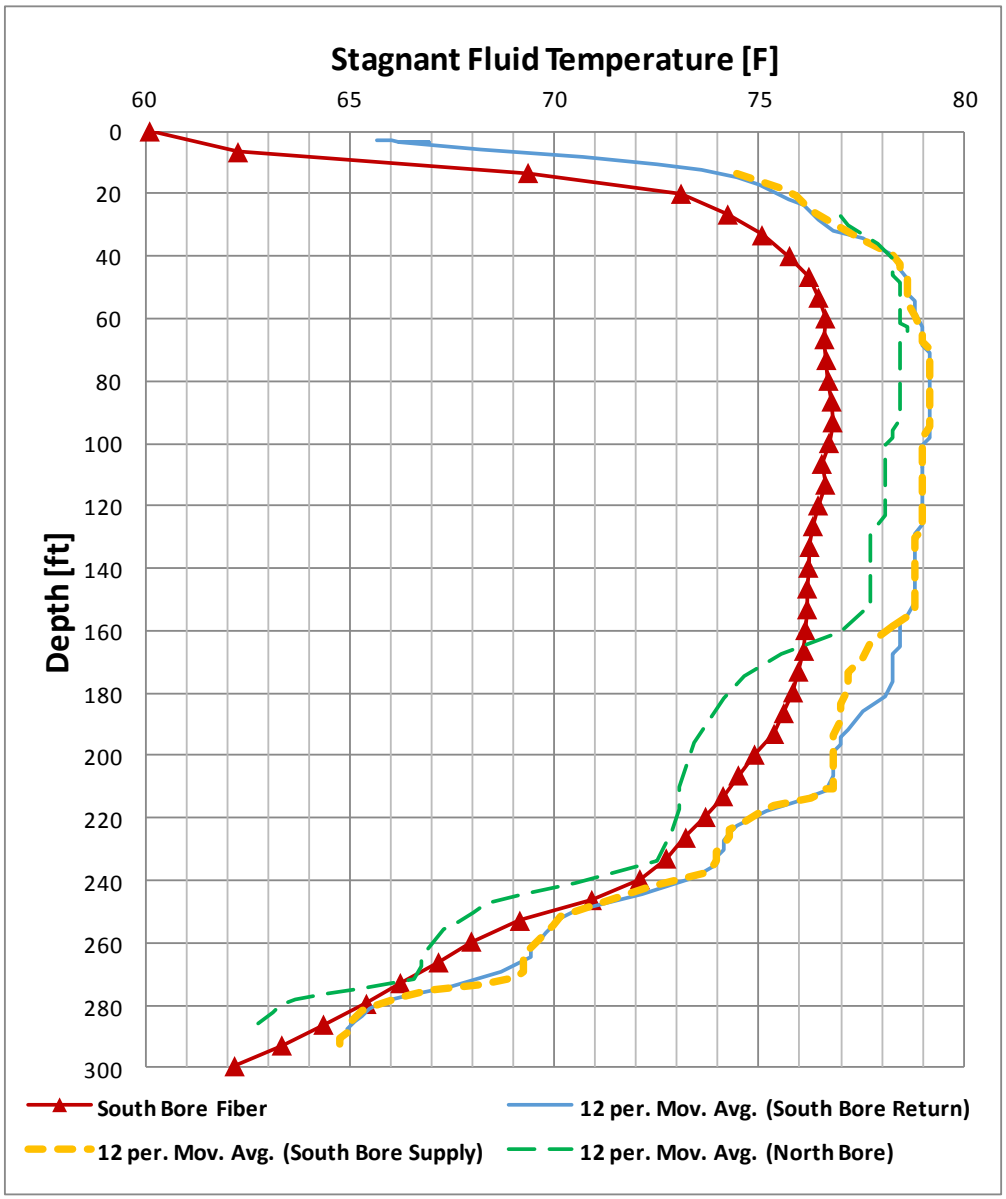

Figure 3-31: Averaged temperature profiles.

The shape of the temperature profiles suggests a stratified geological formation composed of layers with different thermal conductivities. A higher conductivity towards the bottom of the bore would explain the sudden drop in temperatures observed after the plateau seen near the top. Coupling a plot containing the slope of the bore temperature with respect

to depth, with a table of the different geological formations below Madison makes it easy to see if the changes in temperature coincide with the stratification of the ground. Areas with a zero slope represent homogenous layers of ground, while a slope that deviates from zero means change in the properties of the ground; the higher the absolute value of the slope the more drastic the change.

Figure 3-32 shows both the temperature and slope of temperature change side-by-side with a graphic representation of the different geological formations typical of the Madison area. On the figure, the temperature profile follows the pattern of stratification of the ground. During the initial 40 ft of sand and clay drift, the ground temperature is somewhat affected by the ambient; beyond this threshold is the Tunnel City sandstone formation which extends for about 50 ft followed by the Wonewoc sandstone which ends at about 210 ft below surface. The observed ground temperature profile for this region plateaus and remains constant. The ground temperature starts changing again at after the Wonewoc formation at the Eau Claire shale layer. This formation is made of rock that is composed of a much finer grain than the sandstone; therefore, it serves as an aquitard preventing water from diffusing across it. Under the Eau Claire shale is a large, important aquifer which serves the Madison area and is composed of porous, Mt. Simon sandstone. Since this volume of water is used to meet Madison's water demands there is a considerable amount of ground water movement which would explain the dip in temperatures seen from the 200 ft to the bottom of the bore at 300 ft.

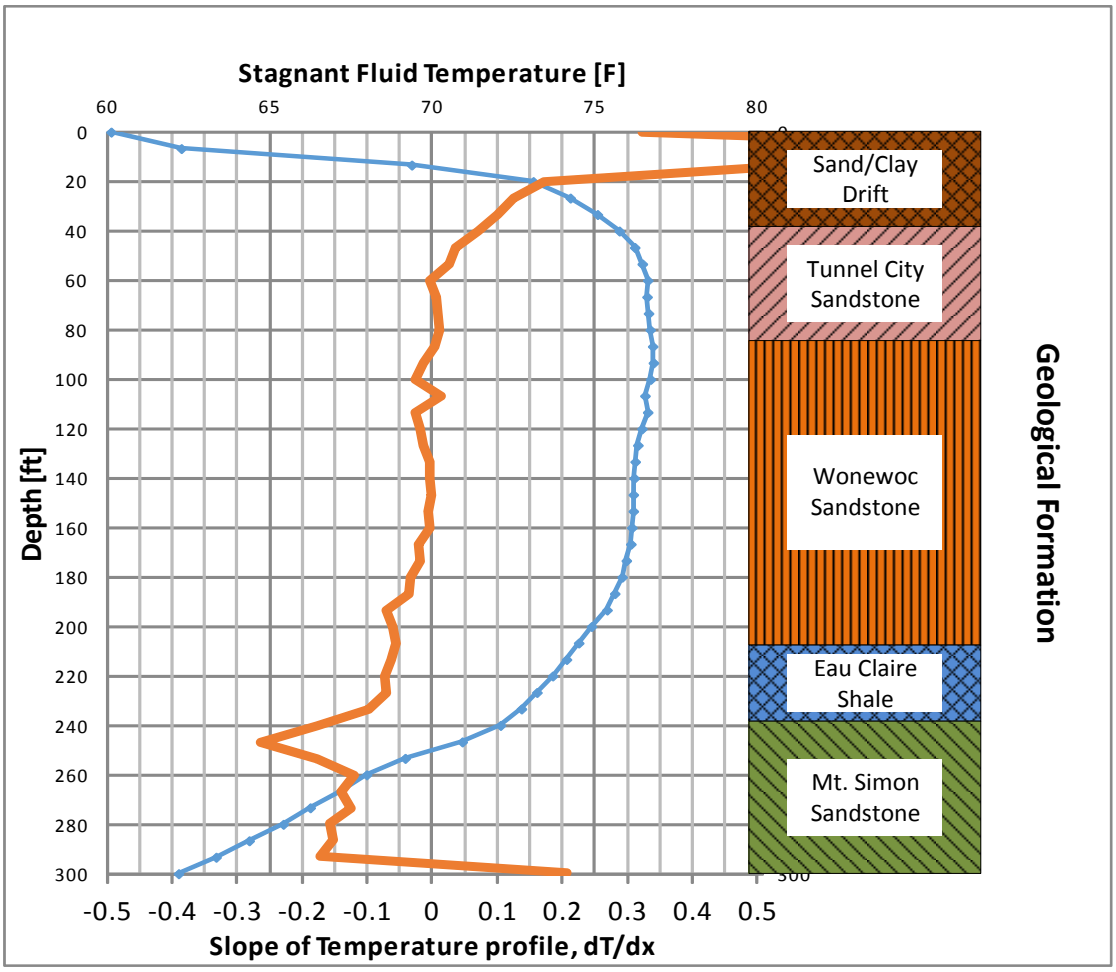

Figure 3-32: Temperature (blue) and slope of temperature change (orange) compared to the different geological strata of Madison. Temperature profile obtained October 2015 during initial excavation using the fiber optic distributed sensing system.

Remarkably, the observed bore temperatures from a depth of 40 ft to 200 ft are abnormally high. It is not until reaching depths of near 300 ft does the bore temperature begin to decrease toward the undisturbed ground temperature.

3.7.3 Thermal Decay

During various periods of time throughout the operational history of the WID's GCHP system, the heat pumps have been turned off while the circulating pumps were left on so that the thermal decay of the geofield temperatures could be observed. One such period was from January 18th to January 22nd 2013 after the Martin Luther King Jr. holiday; we will call it MLK weekend. Entering condenser water temperatures were recorded every 10 minutes through those four days.

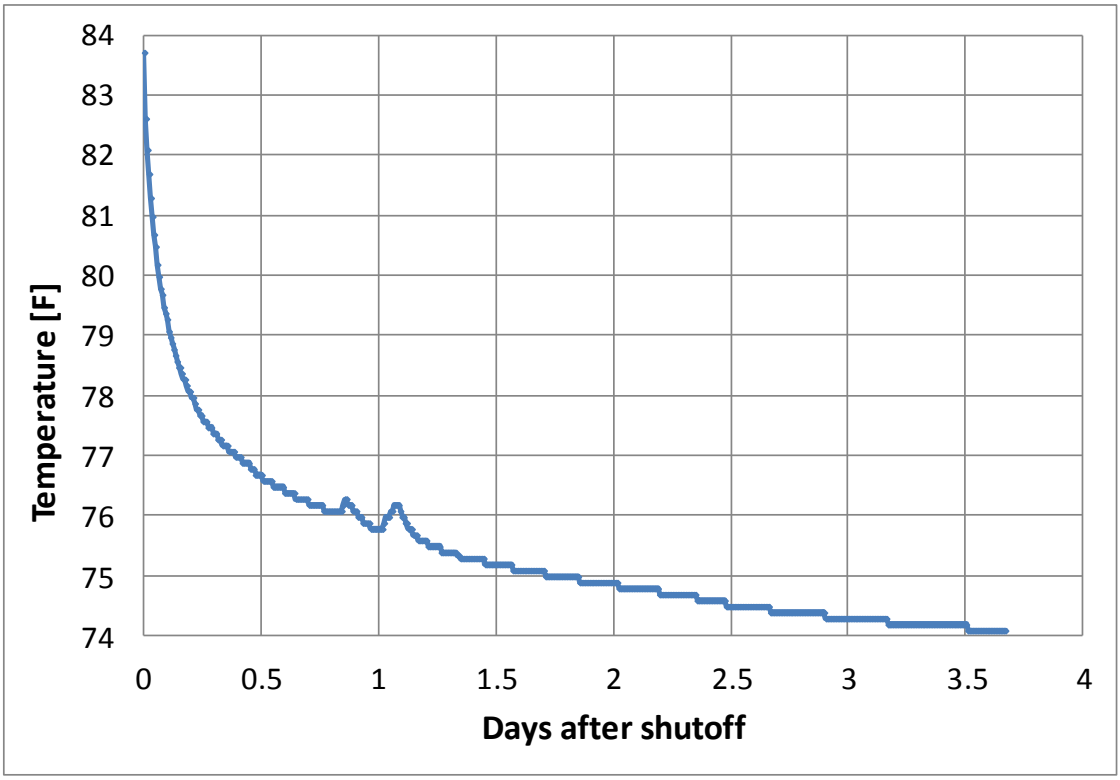

Figure 3-33: Heat pumps shut off from 1/18/13 to 1/22/13 showing a rapid initial decay.

The resulting plot shown in Figure 3-33 exhibits an exponential decay on the short time scale which looks like it will settle to a temperature of about 74°F - well above the

undisturbed ground temperature for this geographical area (53°F). Another shut-off period took place during the entire months of May and June of 2013 which provided a longer window of time to examine the thermal decay of the geofield. The circulating pumps were activated for 1 hour and the resulting temperature data were averaged and recorded by hand for every measurement point plotted in Figure 3-34.

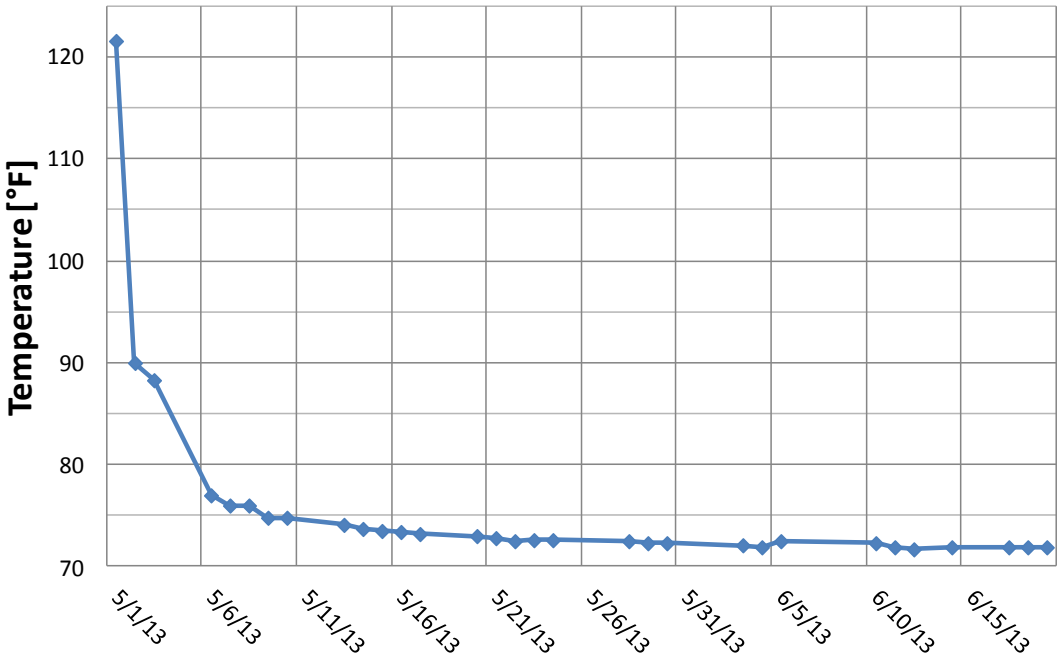

Figure 3-34: Hand logged data for shut off period between May and June 2013.

Figure 3-34 shows the same rapid, exponential decay shown on Figure 3-33 but with a higher temperature. Both decay plots show this characteristically fast initial temperature decrease before settling into what looks like a very slow thermal decay occurring at about 75°F. If we assume that the ground is an infinite heat sink, the observed temperature of the ground should stay at close to the undisturbed ground temperature but the data shows

otherwise. The average temperature of the ground has risen and persists at this elevated temperature. The cause of this rise in average temperature is believed to be, principally, attributable to the unbalanced heat input into the geofield by the building's GCHP system due to it running in cooling-only mode. The bore high temperatures persist because the soil is dissipating heat through conduction to the surrounding earth at a very slow rate. Even though it is reasonable to approximate the surrounding earth as an infinite heat sink, it does not exhibit that behavior at the time scales that are of interest in this application.

As to the initial exponential decay, the behavior makes sense when this problem is looked at from a transient heat conduction standpoint. The reason we see these two distinct patterns of thermal decay, one fast and one slow, is because of the timescale used for observation. One component of the system is heating up and cooling down rapidly when compared to the other and these heat transfer properties are dictated by heat capacity, conductivity, and diffusivity. Thermal diffusivity (α) measures the ability of a material to conduct thermal energy relative to its ability to store thermal energy. A useful concept in this scenario is the diffusive time constant (τ_{diff}) which characterizes, approximately, how long it takes for a thermal wave to penetrate a given distance. For a distance of 10 meters through sandstone it takes about 150 days or 4.5 months for a temperature change to be felt.

$$\alpha = \frac{k}{\rho c}\tau_{diff} \approx \frac{L^2}{4\alpha} \qquad ((1)$$

Over a long enough timescale, the ground will return to the undisturbed ground temperature; however, the ground has a large capacitance (enhanced by slow moving ground water present in the region between 40 ft to 210 ft depth) and low conductivity which correspond to a low diffusivity. The volume of working fluid, in this case circulating condenser water, is low so its thermal capacitance is very small compared to the surrounding earth.

3.8 Conclusion

The results of the preliminary field work completed on the GCHP system proved inconclusive. While there was no single definitive cause found that might explain the unusual behavior of the system, various working hypotheses were proven false. This has narrowed the focus and given new information to use for developing a more accurate model of the GCHP. Table 3-5 provides a summary of the effects, hypothesis, diagnostics, and results.

At the termination of the field work, the two exposed bores were modified to provide permanent access after the site was returned to its original state. This was done in preparation for the new TRT to be performed the following year after a custom rig was built to accommodate the unique fiber optic DTS system; the details of which are covered in the proceeding chapters.

Observation	Hypothesis	Field test	Field Findings
Rapid increase in circulating geofield fluid temperature	Improper grout mixture	Grout sample extraction	Evidence suggests proper grout was used.
		Grout probing	
	High bore hole thermal resistance	Thermal response test (TRT)	TRT (under varied operating conditions) coupled with fiber-optic distributed sensing system provided thermal data to calculate effective ground conductivity.
	Pipe Fouling	Water sample test	Geofield water tested **positive for iron-reducing bacteria** (IRB) via. BART test. Further evidence of activity acquired by visual observations of fluid bled at Presso port locations and as-evidenced by dark colored water purged from the u-tubes. Borescoping u-tubes and sections of tubing harvested showed **minimal biofouling. No evidence that the present biofouling is impacting hydrodynamic performance of the geofield.**
		~~Pipe swab sample~~	
		Borescope (u-tube)	
	Hydronic Anomalies	Ultrasonic flowmeter measurements	The measured **gross flow for the entire field was within 9% of the design flow** (984 gpm actual vs. 1,050 gpm based on pump curves and 1,070 gpm based on 13 gpm/bore for 82 bores). **Design flow rate for each bore is 12 gpm which was close to the measured u-tube flow rates**of 13.8 gpm (north bore) and 12.3 gpm (south bore).
		System Curve: Branch and Header	
		Flow Balance Testing: Branch and Header	
Slow thermal decay	High thermal capacity/low diffusivity of ground/grout	Grout sample extraction	As noted above, evidence suggests grout mix was adjusted to achieve target thermal properties and the appropriate grout was used. Observations of thermal decay during tests were unremarkable on a short time interval basis (e.g. days) but on a longer time interval (weeks/months) the thermal decay is quite slow.
		Grout probing	
	Presence of groundwater	Temperature probe	Reduced temperature confirms ground water flow for bottom 30 meters of bore.

Table 3-5: Geofield Diagnostics

Chapter 4. New Thermal Response Test

4.1 Introduction

Since the previous geofield assessment indicated that there was nothing obviously wrong with the system components, it seemed likely that the anomalous behavior of the WID geofield is caused by the geological properties of the ground. During the diagnostics testing interesting temperature profiles were measured that showed drastically lower ground temperatures present in the bottom 20 meters of the bore. This stratification of ground temperatures implies significant variance in the thermal properties of the ground with depth; this could never have been observed using the traditional TRT conducted by GRTI where homogenous ground is assumed and only inlet and outlet temperatures are measured. The result of the GRTI TRT post-data collection analysis is a single "effective ground conductivity" that represents an average thermal conductivity of the ground along the entire length of vertical bore as opposed to spatially varying conductivity corresponding to the layers of the ground. If the thermal properties of the ground could be distinguished across the different geological layers, then improved models for GCHP design could be realized which would improve the ability to understand and forecast geofield performance.

The results of the TRT conducted during the design phase of the system suggested a thermal conductivity of 2.33 BTU/ft-hr-°F using the traditional experimental setup and the line source model. The TRT discussed in this chapter uses a Fiber Optic Distributed Temperature Sensing (DTS) technology that can measure temperature along the length of the fiber optic cable at discrete distances. A TRT using fiber optic DTS has only been performed

once before, see (Acuña, Mogensen, & Björn, 2009), but that study revealed a relatively homogenous ground which does not appear to be the case in Madison, WI. The goal of this new TRT is to use the relatively new fiber optic DTS measuring device to relate the temperature profiles along the depth of the bore to the geological formations unique to Madison that influence the behavior of the bore field at the Wisconsin Institutes for Discovery.

4.2 TRT Rig Design

The in-situ TRT was conducted during the summer of 2016. It was performed using a custom made thermal response test rig shown in Figure 4-1.

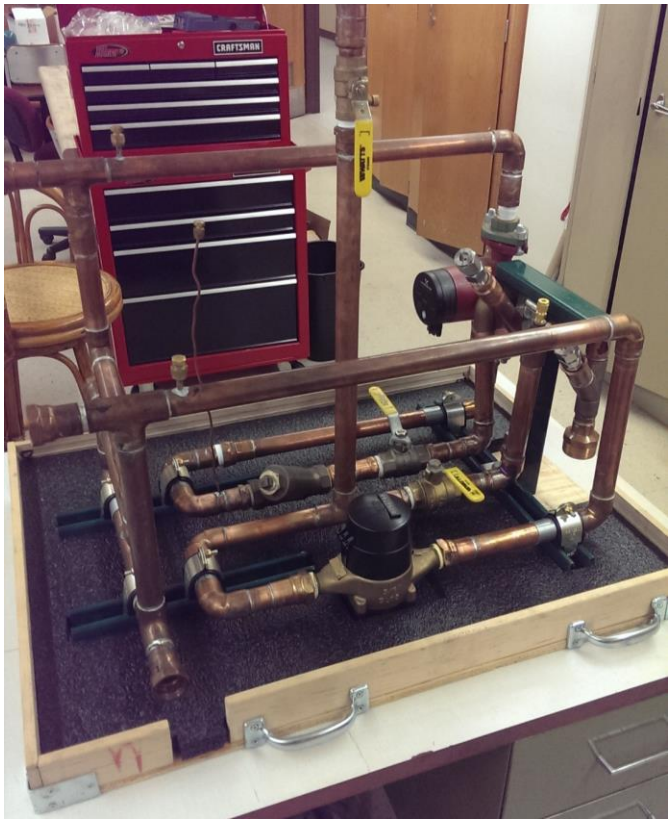

Figure 4-1: Custom TRT rig under construction.

The TRT rig contains the heating elements, circulating pump, flow meter, thermostats, data logger, and SPRT's (thermistors). These components are all contained within the locked plywood body of the rig with ports for the fluid inlet/outlet, power cords, and data access cable. The as-measured total power output is 8400 W. Power is provided to the TRT rig from the 240v electrical outlets of the adjacent physical plant building. Power is routed to a weatherproof portable breaker box that provides surge and short circuit protection. All the powered components are connected to the breaker box seen in Figure 4-2.

Figure 4-2: Yellow breaker box being connected to the TRT rig.

The circulating pump has adjustable flow settings; the highest speed was chosen which resulted in an average flowrate of 6 gpm throughout the test period. Temperature measurements at the inlet and outlet of the TRT rig are made using two Hart Scientific

standard platinum resistance thermometers (SPRT). A four-wire configuration is used to accurately measure the real resistance of the sensor by eliminating the voltage drop contributed by the leads of the current source. A small, 10 μA drive current is provided for measurement to reduce self-heating. Temperature readings are taken every second and 1-minute time-averaged values are stored. A Campbell Scientific CR3000 data logger is used for the SPRT data collection and storage. The data logger also serves as the current source and resistance measuring device.

The distributed fiber-optic temperature sensing system requires three calibration baths to provide accurate temperature data. For this purpose, two baths one hot and one cold with electronic temperature controls, are used. The third bath is an insulated container at ambient temperature. For further details of the dynamic calibration that was done on the fiber optic DTS refer to (McDaniel, et al., 2016). The fiber-optic cable is protected by a polymer conduit running from the calibration baths to the TRT rig. The end of the fiber is weighted with lead fishing weights to overcome the buoyancy of the sheathed fiber-optic cable itself; thereby, ensuring that the cable reaches the bottom of the U-tube. Temperature readings are taken and stored by the interrogator and 4-minute time-averaged values are stored. A summary of the component's specification is displayed in Table 4-1.

	Characteristics	Manufacturer	Capacity	Uncertainty
Heating Elements	Resistance type	Richmond	2x2000W@120v 1x1440W@120v 1x4500W@240v	
Pump	Centrifugal	Grundfos	15 gpm	
Flow Meter	Positive Displacement	Master Meter	20 gpm	~100% Accuracy
SPRT (thermistors)	Standard Platinum Resistance Thermometer	Hart Scientific	–200°C to 480°C	±0.001°C
Data Logger	CR3000	Campbell Scientific	±5Vdc	Resistance: ±2.85μΩ
Fiber Optic DTS Interrogator	Halo-DTS	Sensornet		±0.15°C

Table 4-1: TRT rig component specification

The TRT rig is coupled to the u-tube via a pair of flexible, stainless steel hoses with rubber gaskets that seal against the u-tube risers and the threaded inlet/outlet on the TRT rig, as shown in Figure 4-3. Since these hoses are exposed to the environment and are made of a relatively thermally conductive material it was necessary to insulate them with fiberglass insulation and plastic sheeting to guard against heat loss/gain from the ambient.

Figure 4-3: Stainless steel connecting hoses seen running from inlet/outlet of the finished TRT rig to the risers.

4.3 Accessing the geo field bore

As discussed in Chapter 3, after the diagnostic testing was completed, permanent access stations were installed on the two bores that were exposed. They are composed of three-way ball valves at the wellheads and corresponding risers that reach from the wellheads to surface boxes. The ball valves, which are located approximately 7 feet below grade at the head of the U-tube, provide the ability to redirect the circulating water flow from the rest of the geofield to the newly installed risers which lead to the surface. The ball valves are actuated via hand wheels located in the surface boxes that are connected through a remote operator (see Figure 4-5). See the Appendix C for the standard operating procedure and different operation modes of the permanent access valves.

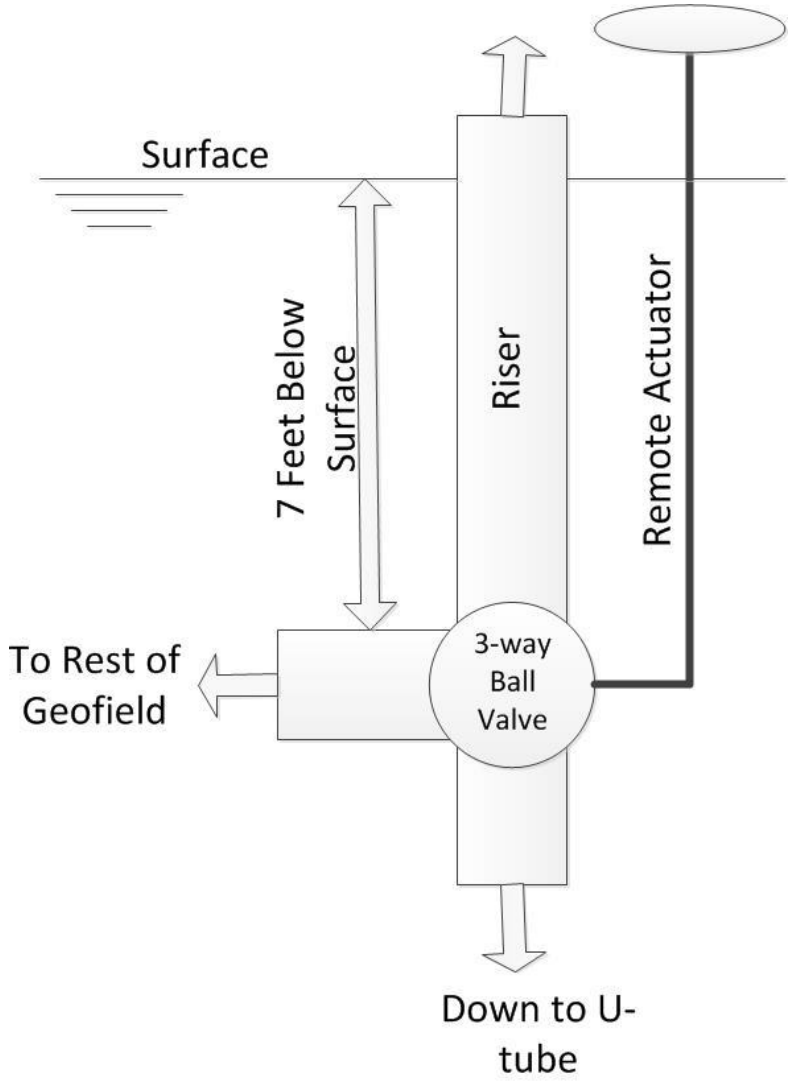

Figure 4-4: Permanent access schematic.

Figure 4-5: North bore permanent access box.

4.4 Test Methods

The testing period consisted of three measurement phases: undisturbed condition, heat injection, and thermal decay or heat dissipation. The first phase focuses on the undisturbed ground condition, which in this case is not truly undisturbed since there has been heat injection in the past, albeit 1.5 years ago, due to regular system operation. Regardless, it is important to get a baseline state of the ground before heat injection. For this purpose, there are periods of no circulation so that the fiber optic DTS system can pick up the stratification of the fluid temperatures within the bore as well as short periods of circulation during which the SPRT sensors can measure the average temperatures between the inlet and outlet of the TRT rig. The second phase consists of the heat injection to the bore. In this case, there was a low and then a high heat injection rate. The data from this period are used to calculate

quantitative ground properties. The final, third phase is characterized by the heat dissipation or thermal decay of the elevated temperatures caused by the second phase heat injection. During this entire period the circulating pump is shut off and the heat loss though the length of the bore is observed using the fiber optic DTS.

4.5 Results

4.5.1 Levelogger Temperature Profile

Once the valves were opened (July 2016), a levelogger was lowered into the bores to obtain pseudo-undisturbed temperature profiles plotted in Figure 4-6. These profiles do not represent a true undisturbed condition for two reasons; the GCHP system has been used in the past (regardless of how long ago that was) and, more significantly, it became known that there was a heat injection period at the end of May 2016. According to maintenance personnel, the system was used at full capacity for approximately two days in May to cover the cooling loads of the WID because of a campus chilled water system failure.

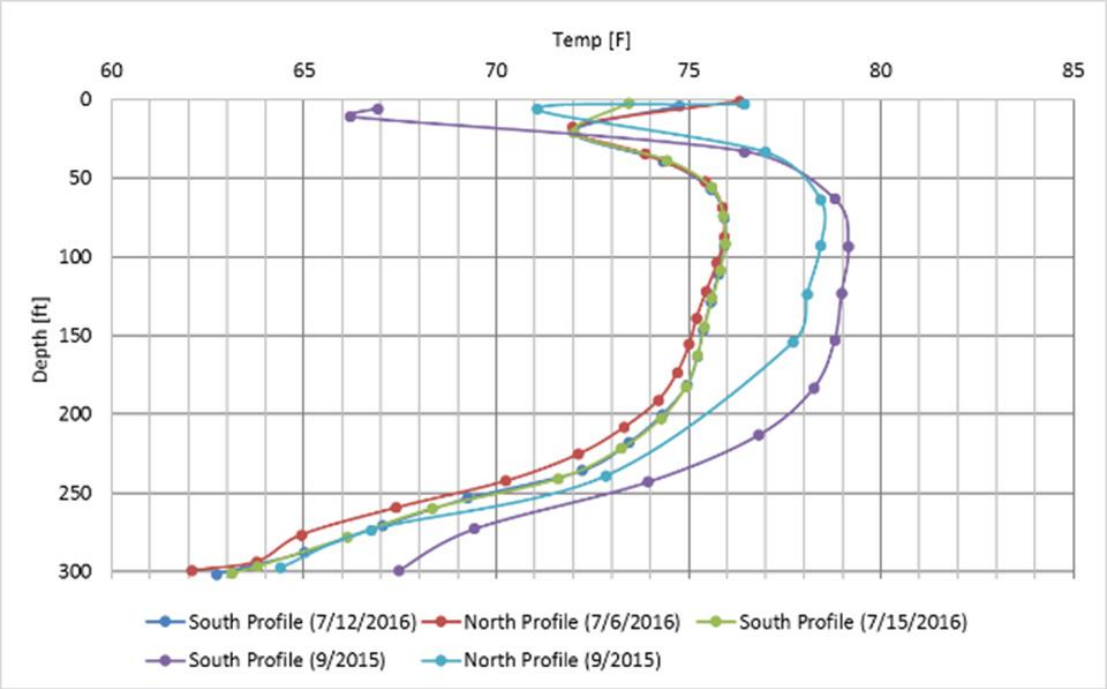

Figure 4-6: Levelogger Temperature Profiles. This figure includes the profiles taken Fall 2015 during excavation in addition to the profiles taken July 2016 just before the TRT.

4.5.2 Undisturbed Ground Temperature

Prior to initiating heat input for the thermal response test, the pseudo-undisturbed ground temperature was measured in two ways because there are two different temperature sensors being used; the SPRT thermistors at the inlet/outlet of the rig and the fiber optic DTS running the depth of the U-tube[6]. The fiber-optic probe was able to capture the stratification of the static water within the U-tube, shown in Figure 4-7. The fiber-optic probe continued to provide temperature data that was logged throughout the entire test so it also captured the temperature of the water once it became mixed after the circulation pump was turned on for short periods of time, which can be seen as the discontinuities in Figure 4-7. The SPRT data

[6] All the fiber-optic data shown in the plots are taken from the return side of the u-tube because the supply-side fiber-optic probe showed data "noise" due to an issue with the fiber splicing.

shows the temperature oscillating as the individual slugs of stratified, unmixed fluid pass by the SPRT sensors and eventually converge after the fluid becomes well mixed during one of the short, 1 hour periods where the circulating pump was active (Figure 4-8). It is important to remember that the temperatures taken with the circulating pump active represent an average of the ground temperature surrounding the bore and that there are regions that are at a higher or lower temperature than this, as shown by the fiber optic DTS.

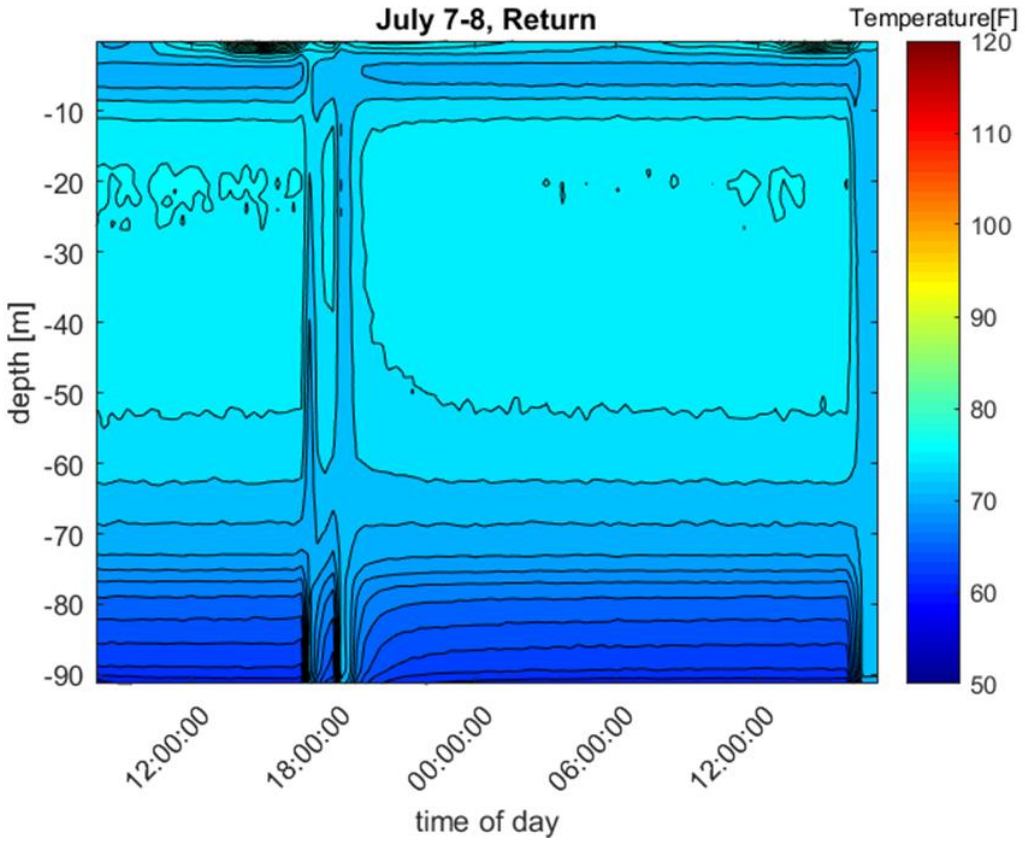

Figure 4-7: Fiber optic temperature profile before, during, and after circulation pump start-up and 1st pseudo-undisturbed ground temperature reading. Most of the plot shows the stratification present when the pump is off and the contours at approximately the 18-hour mark show the mixing during the pseudo-undisturbed ground temperature measurement.

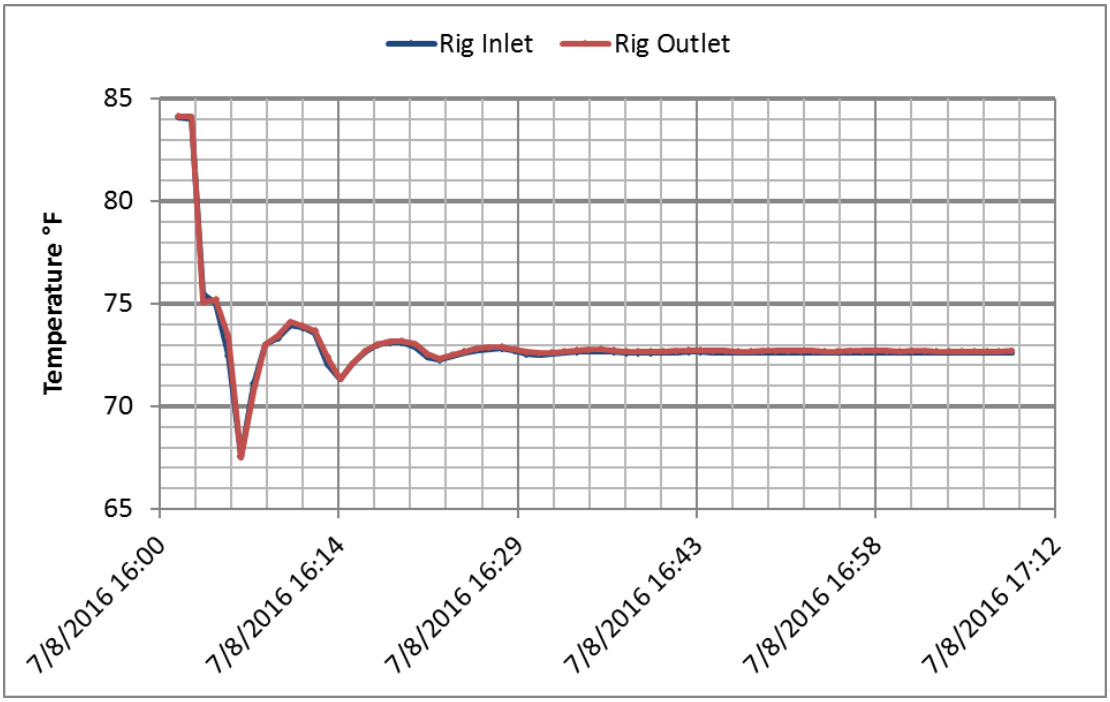

Figure 4-8: SPRT, 1st Psuedo-undisturbed ground temperature reading.

4.5.3 1st Heat Injection

The first heat injection began once the heaters were plugged into the power source. The first heat injection occurred from 7/8/2016 17:15 to 7/10/16 19:10. The water temperature increase caused by the first heat injection looks like a typical TRT except that the change in temperature of 4°F (Figure 4-9) is smaller than expected given the rated heat input of the cartridge heaters of approximately 10 kW. A calculation of the actual heat being input using the average flow rate and the temperature change showed a heat input rate of 3.45 kW, which was less than what the heaters are rated at. Nonetheless the test was not interrupted at this point but the decision was made to continue running for 50 hours at this level of heat input. Afterwards, a multimeter was used to check if all the heating elements were working and it was found that only the 4500 W rated heater was powered and only at a

partial rate, corresponding to the 3.45 kW input that was calculated using the fluid stream. The thermostats were then checked for continuity and it was found that three out of the four were not passing a current. The wiring to the thermostats was then corrected.

The temperature profiles produced by the fiber optic DTS show the hottest fluid at the bottom of the bore (Figure 4-10) because the fiber optic cable hanging in the return side of the U-tube is the source of the measurements.

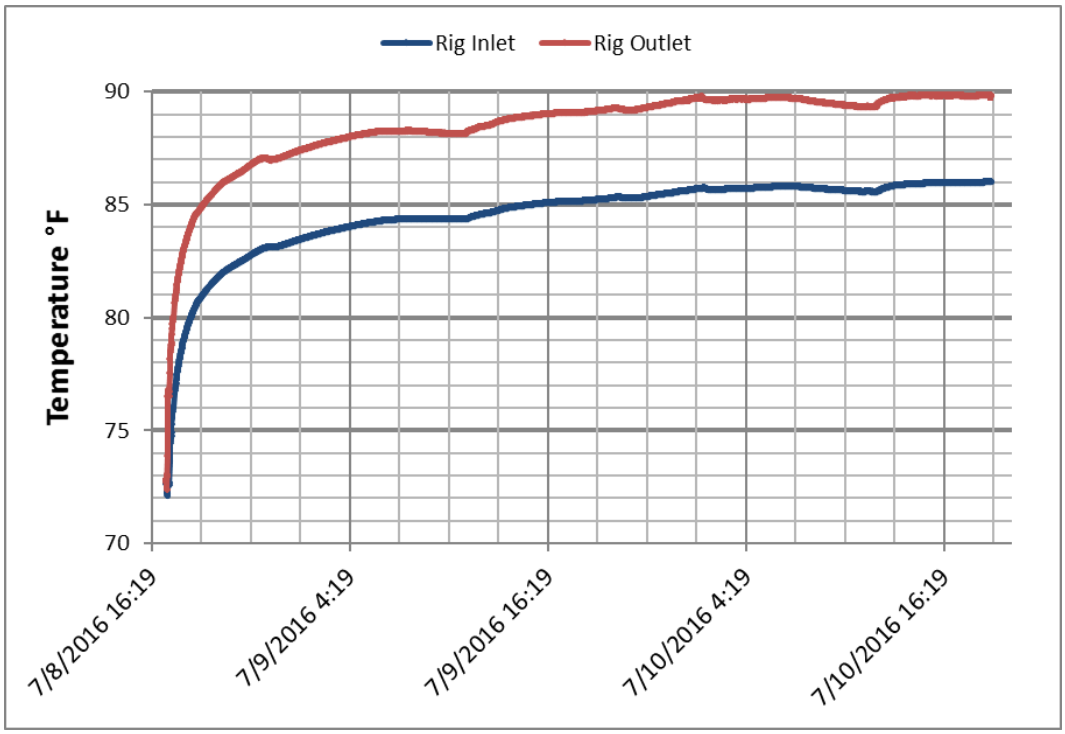

Figure 4-9: SPRT, 1st heat injection showing the change in temperature between the hot fluid exiting the rig outlet and the cooled fluid returning from the bore through the inlet of the rig.

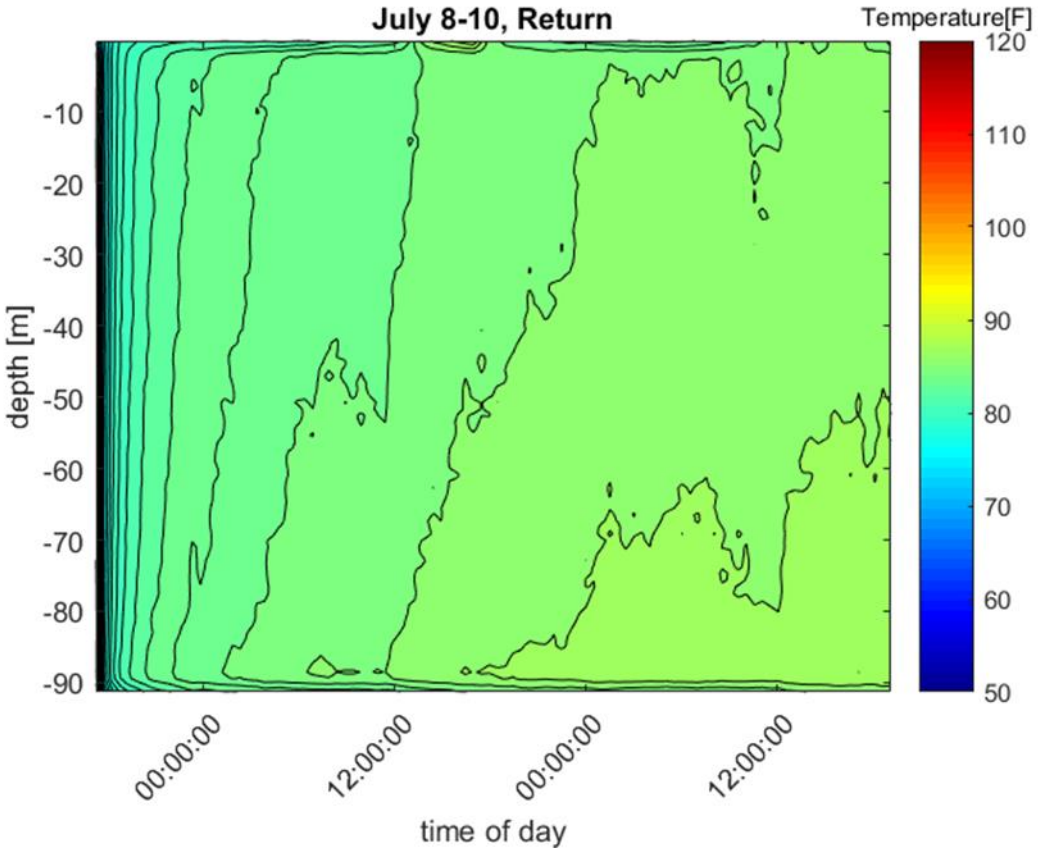

Figure 4-10: Fiber optic DTS temperature profiles from the return side of the U-tube during the 1st heat injection.

4.5.4 1st Thermal Decay

After the first heat injection period of 50 hours, the heat input and circulating pump were shut off to collect data on how quickly the ground dissipates the absorbed heat. This thermal decay is expected to occur at different rates along the depth of the U-tube depending on the properties of the ground that are present at that depth (Figure 4-11). Since the circulating pump is not active during this time, the temperature data provided by the SPRT's is not useful; it represents the temperature of the water in the rig above the surface which is influenced by the ambient as seen in Figure 4-12.

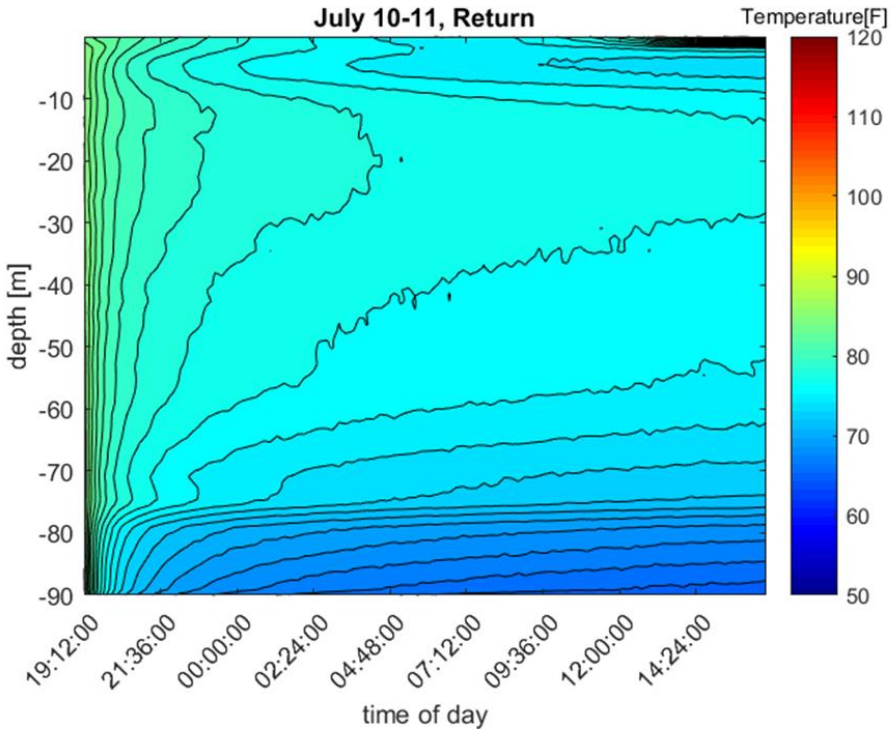

Figure 4-11: Fiber optic DTS, 1st thermal decay measurement

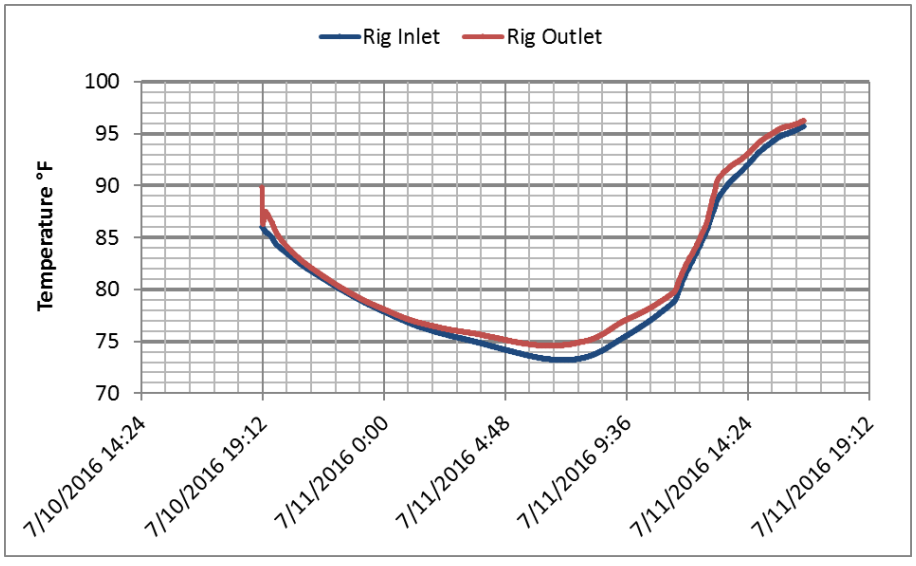

Figure 4-12: SPRT, 1st thermal decay. The plot shows the water sitting in the TRT rig which is above ground with the circulation pump off and therefore reflects the ambient temperature change throughout the day.

4.5.5 2nd Heat injection

The first heat injection produced a water-side temperature change that was comparatively low. The second heat injection occurred from 7/11/16 17:48 to 7/15/16 14:05 for a total of 92 hours. Prior to the start of the second heat injection, the circulating pump was run for an hour without heat input to get another pseudo-undisturbed ground temperature because the first heat input had changed the state of the ground (Figure 4-13 and Figure 4-14). As long as the pseudo-equilibrium temperature of the ground before the heat injection is known then the TRT can still give valid results; the initial storage temperature parameter in the TRNSYS model is simply updated to this value.

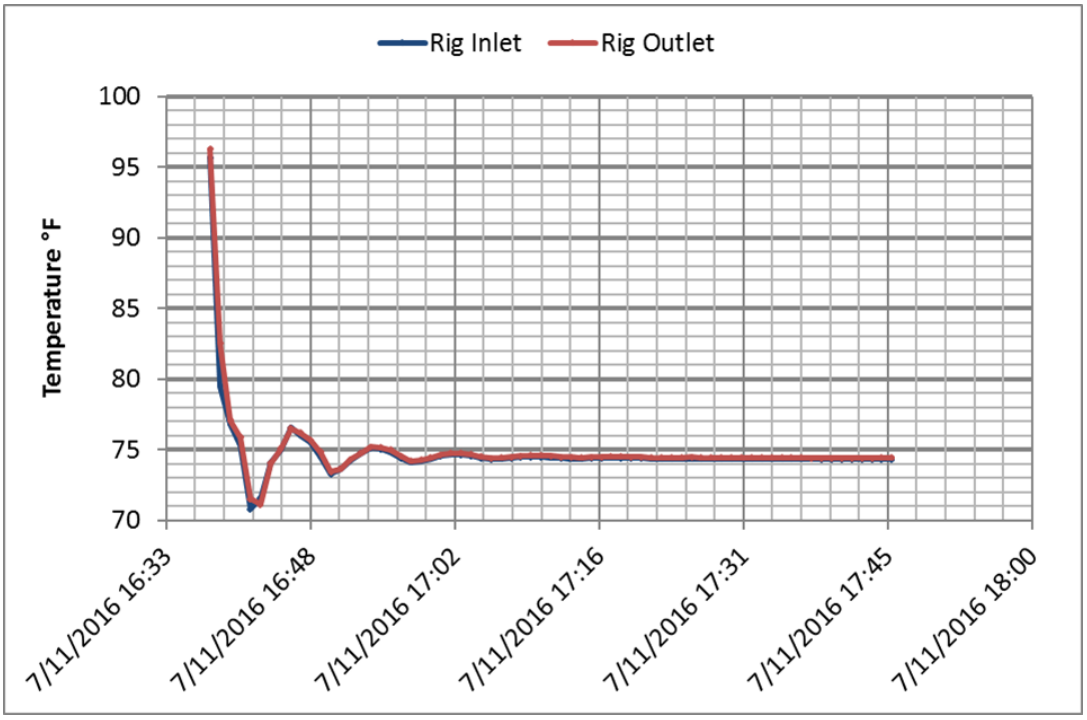

Figure 4-13: SPRT, 2nd Pseudo-undisturbed ground temperature measurement

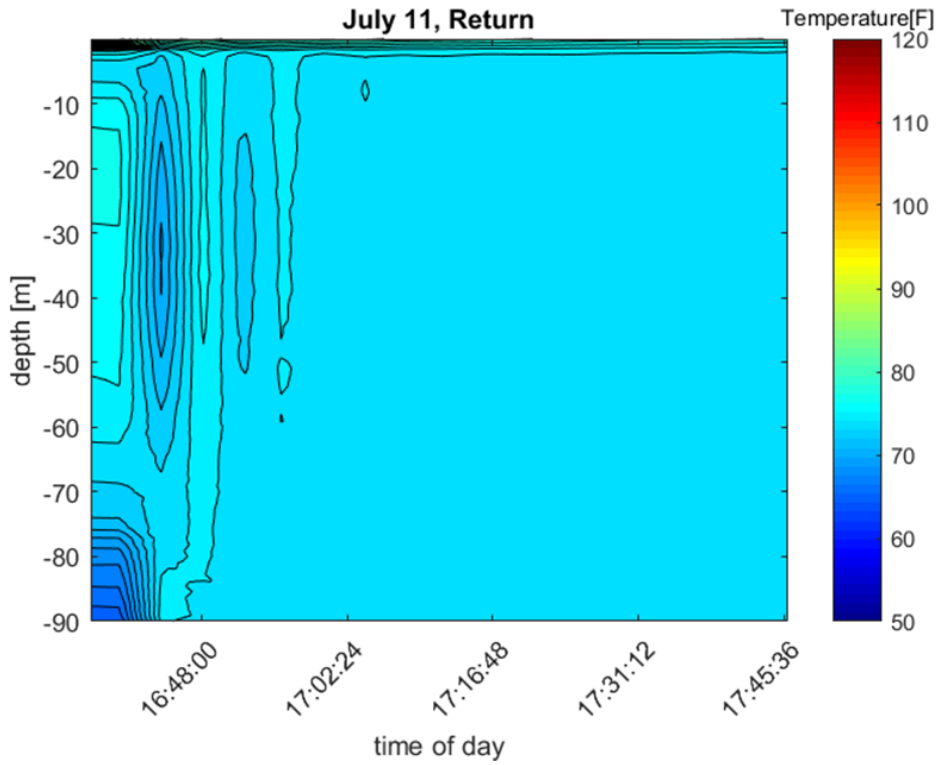

Figure 4-14: Fiber optic DTS, 2nd psuedo-undisturbed ground temperature measurement.

During the second heat injection the circuit breaker tripped for unknown reasons approximately 5 hours after the start which cut the power for two of the four heating elements; as a result the heat input was again reduced. After this was discovered, the breaker was reset and the heat injection resumed and proceeded normally for the rest of the heat injection. This effect is seen in the SPRT and fiber optic data plots in Figure 4-15 and Figure 4-16 as a sudden drop in temperature seen at about 7/11.2016 21:00.

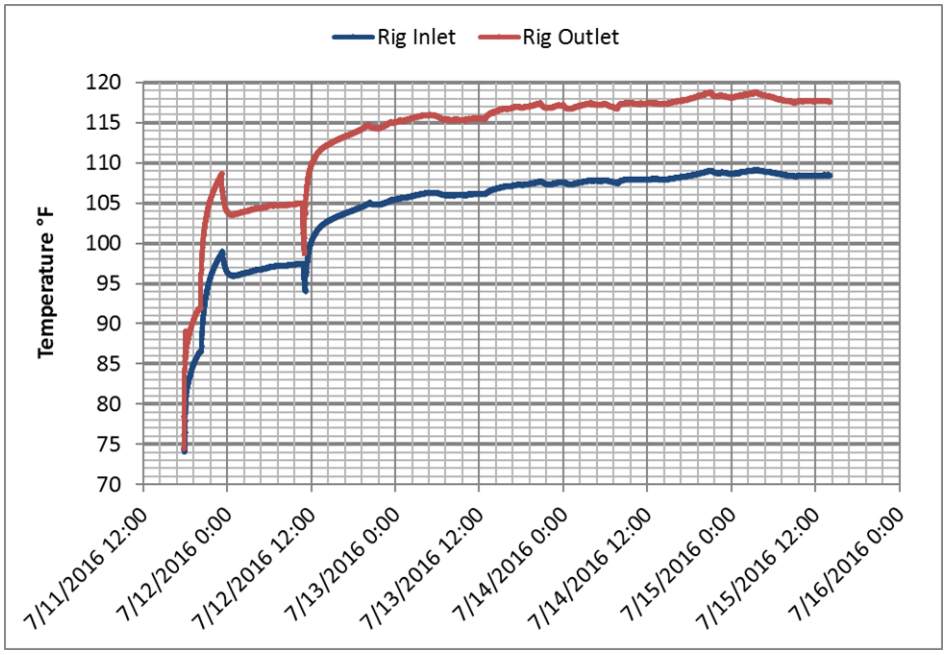

Figure 4-15: SPRT 2nd Heat Injection, note the anomaly in the otherwise similar trend to the 1st heat injection. This was caused by the circuit breaker shutting off two heating elements.

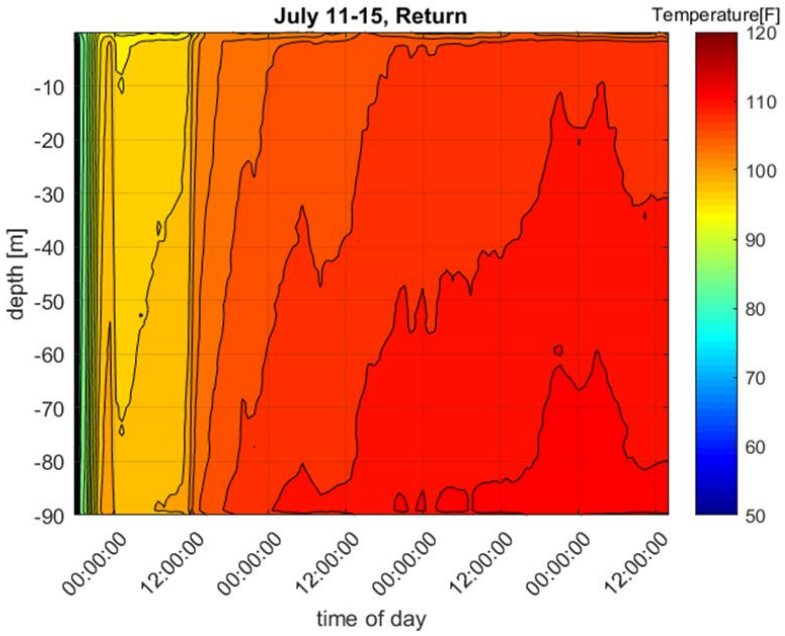

Figure 4-16: Fiber optic DTS, 2nd Heat Injection, note the yellow region during the first 12 hours. This was caused by the circuit breaker shutting off two heating elements, causing reduced heat input

4.5.6 2nd Thermal Decay

Again, after the heat injection period of 92 hours, the heat input and circulating pump were shut off to record data related to how the ground dissipates the heat input. This thermal decay is expected to occur at different rates along the depth of the u-tube depending on the properties of the ground that are present at that depth; the ground layers under the WID are summarized in Table 4-2.

Formation	Depth m (ft)	Porosity (%)	Thermal Conductivity W/m-K (Btu/hr-ft-°F)	Specific Heat Capacity kJ/kg-K (Btu/lb-°F)	Hydraulic Conductivity meters/day
Sand and Gravel	0	15	1.5 (0.9)	0.8	0.45
Tunnel City	20 (67)	5	2.6 (1.5)	0.9	0.3
Wonewoc	42.6 (140)	10	3.8 (2.2)	0.9	1.7
Eau Claire	70 (230)	0.1	2 (1.2)	0.7	0.0045
Mt. Simon	73 (240)	15	3 (1.7)	0.9	2.5
			Reference		
water			0.6 (0.3)	4.183 (1)	

Table 4-2: WID site ground thermal and hydraulic properties. (Parsen, et al. 2016)

For the thermal decay periods, the fiber-optic system provided some diagnostic insights because, with the circulating pump shut off, stratification of the ground surrounding the u-tubes could be detected. The fiber-optic data in Figure 4-11 and **Error! Reference s ource not found.** clearly show a region of increased apparent thermal conductivity at the

bottom 20 meters of the U-tube which can be deduced from the lower temperatures observed (darker blue).

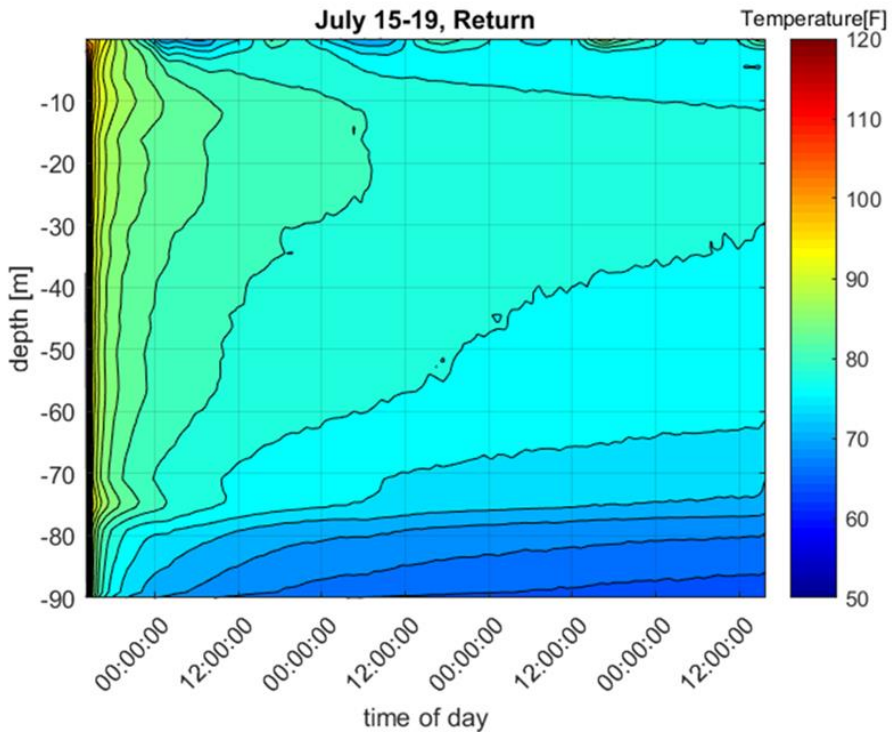

Figure 4-17: Fiber optic DTS, 2nd thermal decay.

This region coincides with the geologic region below the Eau Claire shale as shown in Figure 4-18 and indicated by Table 4-2 at 73 meters; this region also coincides with the location of the aquifer where the city of Madison draws most of its water. Recognizing that the geologic formation below the Eau Claire shale is very porous suggests that this region has increased water movement. (Krohelski, Bradbury, Hunt, & Swanson, 2000) This water movement enables advection that enhances heat removal from the geofield at the bottom 20 meters of each U-tube.

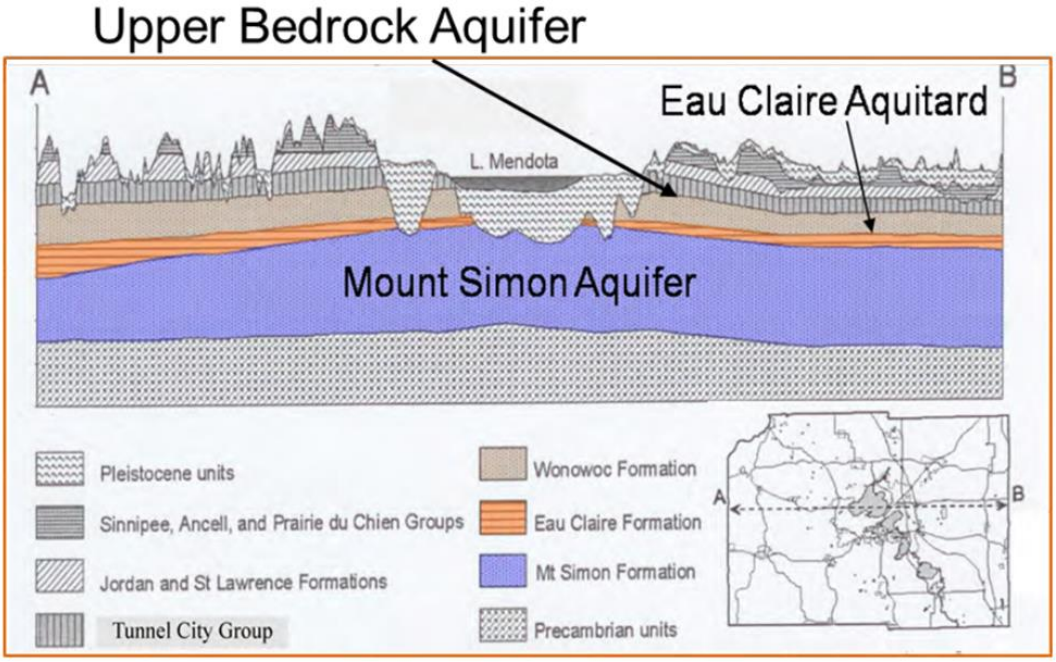

Figure 4-18: The Geological formation below Madison, WI. (Gotkowitz, McLaughlin, & Grande, 2002)

The opposite effect is also evident in the data from Figure 4-11 and Figure 4-17 at approximately 15 to 70 meters of depth where the abundance of slow moving groundwater provides little advection in conjunction with a high heat capacity due to the water. The 1st and 2nd thermal decay periods both display these trends of relatively rapid heat dissipation towards the bottom and persistently elevated temperatures seen across the large band in the middle of the formation.

4.5.7 3rd Undisturbed Ground Temperature

The pseudo-undisturbed ground temperature was measured for a third time to compare it with the previous two measurements. It can be observed from the temperature displayed in Figure 4-19 and Figure 4-20 after the initial mixing of the fluid.

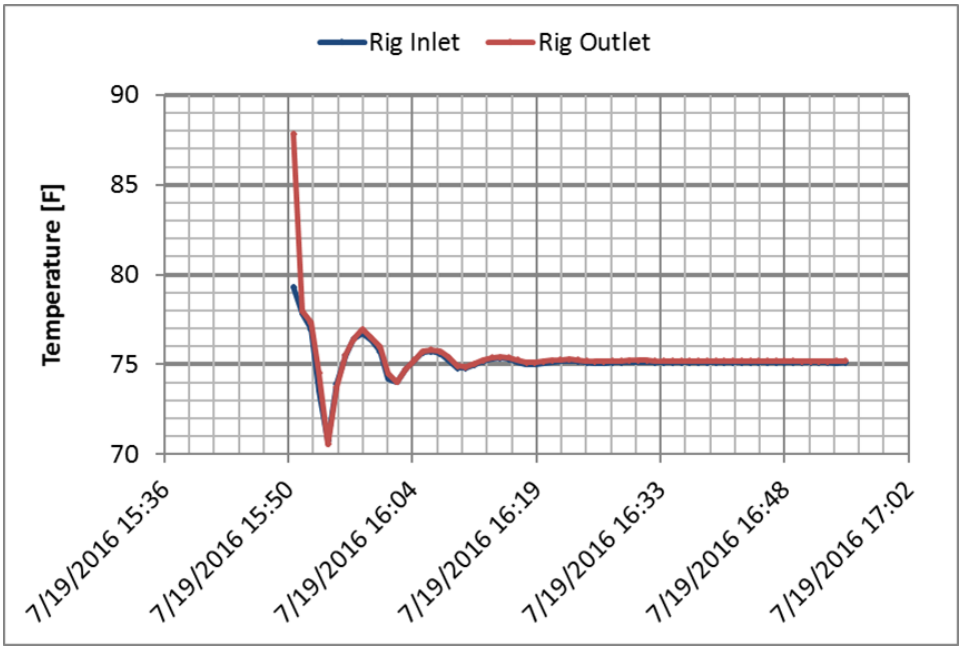

Figure 4-19: SPRT, 3rd pseudo-undisturbed ground temperature measurement.

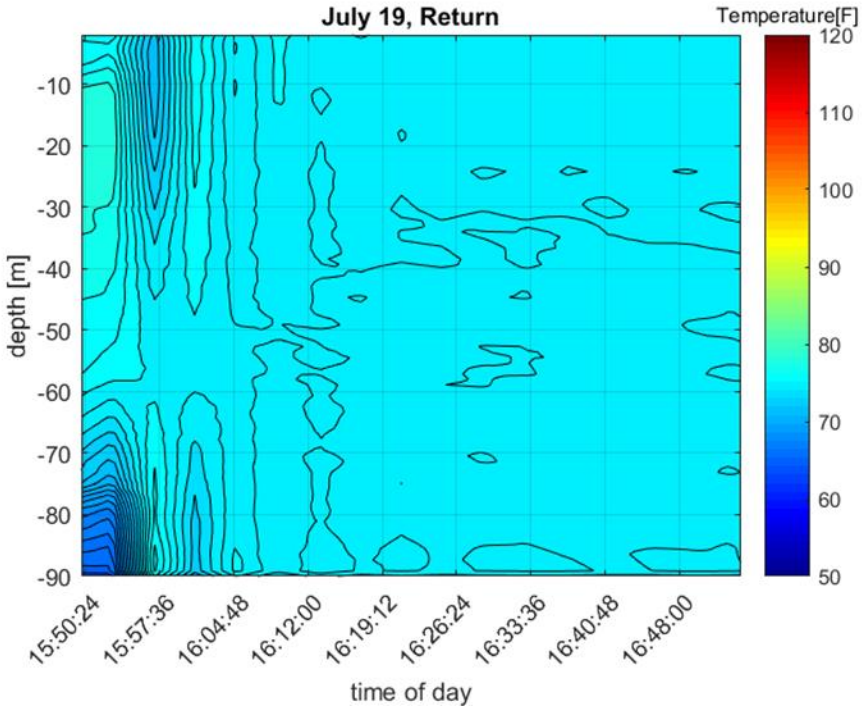

Figure 4-20: Fiber optic DTS, 3rd pseudo-undisturbed ground temperature measurement.

4.6 Quantitative Analysis

The stratification of the ground's thermal properties can be deduced qualitatively from the figures in the previous sections. The data from the SPRT's and fiber optic DTS system was also used to quantitatively analyze the data and infer values for the thermal conductivity of the two ground layers observed to have significantly different temperatures. The first layer was chosen to be from 10 to 70 meters in depth because of the relatively homogenous **elevated** temperatures within that region, as measured by the fiber optic DTS as seen in Figure 4-7. The second layer was chosen to be from 77 to 89 meters in depth because of the relatively homogenous **lower** temperatures within that region, again as measured by the fiber optic DTS. The top 10 meters were ignored because of the thermal interaction with the ambient that occurs at the very top of the u-tube and fiber. The bottom 2 meters were ignored because the lead ballast used to anchor the fiber affects the measurement for that section of fiber. The temperatures at the inlet/outlet of the TRT rig are measured by the SPRT probes and used to obtain the effective thermal conductivity of the entire formation as a traditional TRT would.

A subset of the quantified thermal conductivity values was then used to test whether there would be a difference in simulated long-term behavior of the GCHP system when the ground was treated homogenously versus separating it into two layers with different properties. The data used for this test were the 1^{st}, 2^{nd}, and entire depth, fiber optic DTS measured values. This information was input to a TRNSYS GCHP model discussed in Chapter 5 that simulates the performance of the entire geofield and the heat pump. Geofield behavior was quantified by determining how much time it took for the fluid temperature

entering the heat pump condenser to reach 50.5°C; the compressor's high temperature cutoff. The faster the cutoff temperature is reached the faster the field heats up therefore the poorer the performance. For both cases the heat pump was run with 6 out of 12 compressors on, so at 50% capacity. Using 1.48 Btu/hr-ft-°F for the entire ground, the heat pumps were able to operate continuously for 540 hours before reaching the cutoff temperature. When the ground was separated into the two layers specified in Table 4-3 and their respective thermal conductivities of 1.1 and 3.72 Btu/hr-ft-°F were used, the heat pumps could operate continuously for 420 hours. This is a difference of 120 hours or 5 days and at lower system capacities the difference becomes larger.

Although these data were all analyzed using the line source method only the SPRT data was also analyzed using the Crossed Contours parameter estimation technique (Leyde, 2016) which is discussed in Section 2.3. The results from Crossed Contours method analysis for the 1st and 2nd heat injection are shown in Figure 4-21 and Figure 4-22 respectively.

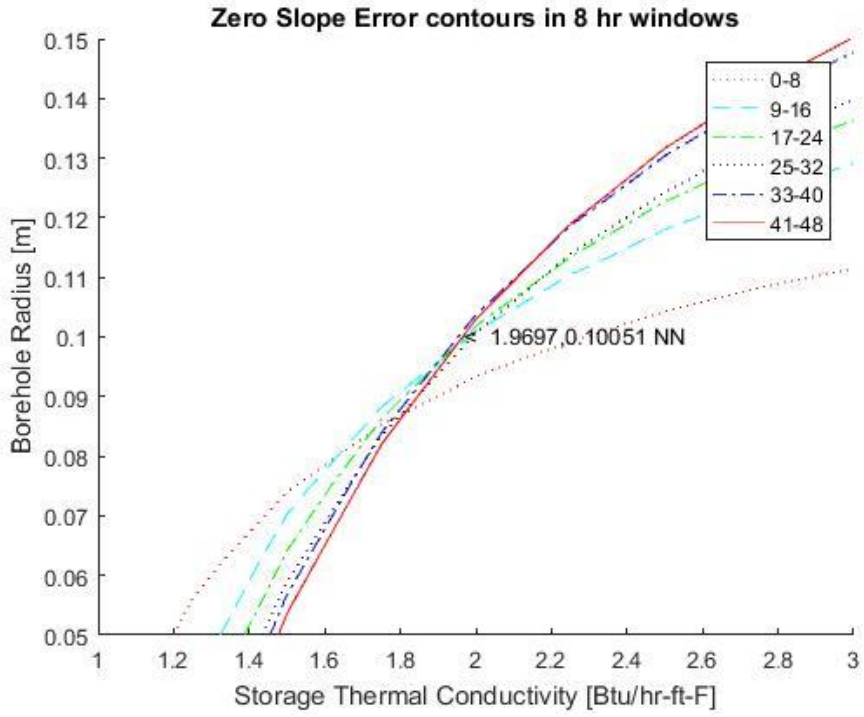

Figure 4-21: Result of the Crossed Contours method analysis of the 1st heat injection period showing the best intersection point that corresponds to the estimated thermal conductivity and borehole radius.

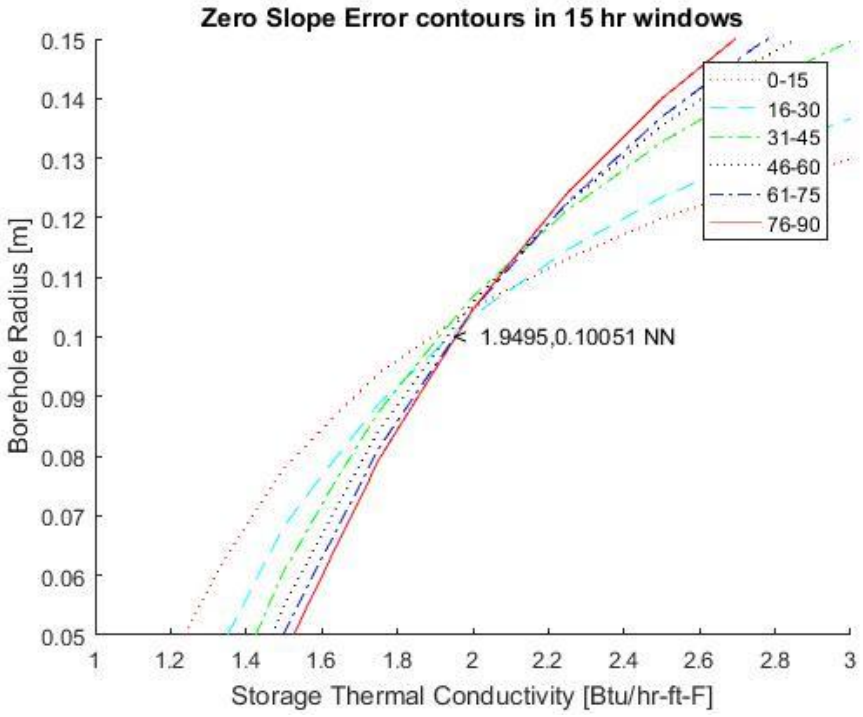

Figure 4-22: Result of the Crossed Contours method analysis of the 2nd heat injection period showing the best intersection point that corresponds to the estimated thermal conductivity and borehole radius.

Table 4-3 contains a summary of the thermal conductivity estimates from the various data and analysis performed. It shows that the thermal conductivity values vary significantly from the 1st to the 2nd heat injection for all cases, which should not happen if the TRT tests are providing an accurate or at least consistent estimate of the thermal conductivity. The only time the values are consistent between the 1st and 2nd heat injection is when the SPRT data is analyzed with the Crossed Contours parameter estimation technique. While it is true that material properties change with temperature, the thermal conductivity should not vary by as much as 90% of its initial value when the temperatures vary by at most 15°C. This effect has been investigated with multi-injection rate TRT's (Gustafsson & Westerlund, 2010). The

Crossed Contours method produces parameter estimates that are the best fit for the entire testing period.

Analysis Technique	Temperature Probe	Measured Region	Thermal Conductivity	
			1st Heat Injection, low heat	2nd Heat Injection, high heat
Line Source Method (LSM)	Fiber Optic DTS	First Layer (10-70m)	**1.91** [W/m-K] (1.10 [Btu/hr-ft-F])	**3.47** [W/m-K] (2.02 [Btu/hr-ft-F])
		Second Layer (77-89m)	**6.43** [W/m-K] (3.72 [Btu/hr-ft-F])	**7.37** [W/m-K] (3.37 [Btu/hr-ft-F])
		Entire Depth (10-89m)	**2.56** [W/m-K] (1.48 [Btu/hr-ft-F])	**4.01** [W/m-K] (1.78 [Btu/hr-ft-F])
	SPRT (thermistors)	Inlet/Outlet (0-89m)	**2.9** [W/m-K] (1.68 [Btu/hr-ft-F])	**5.83** [W/m-K] (3.37 [Btu/hr-ft-F])
CC method	SPRT (thermistors)	Inlet/Outlet (0-89m)	**3.41** [W/m-K] (1.97 [Btu/hr-ft-F])	**3.38** [W/m-K] (1.95 [Btu/hr-ft-F])
Other References				
Original TRT conducted during the WID's GCHP design phase. (GRTI, Inc., 2008)			**4.03** [W/m-K] (2.33 [Btu/hr-ft-F])	
Original TRT data analyzed with CC method parameter estimation (0-121m)			**3.62** [W/m-K] (2.09 [Btu/hr-ft-F])	
Sandstone[7]			**2.91** [W/m-K] (1.68 [Btu/hr-ft-F])	
Water			**0.59** [W/m-K] (0.34 [Btu/hr-ft-F])	

Table 4-3: Summary of quantitative analysis results.

[7] Sandstone and water properties obtained using property information from Engineering Equation Solver (EES) software at standard conditions.

4.7 Conclusions

The TRT provided very useful insights towards explaining the observed behavior of the bore field. It confirmed some theories and promoted new ones. The pseudo-undisturbed ground temperature measurements confirmed the altered state of the ground. The fiber optic DTS temperature profiles showed that above-normal ground temperatures have persisted despite minimal heat input to the ground over the past year-and-a-half.

The thermal decay tests using the fiber-optic data in Figure 4-11 and Figure 4-17 clearly show regions of different apparent thermal conductivity. Based on the geologic data gathered it can be concluded that the top 70 meters are defined by the presence of porous rock and abundant stagnant water with a low thermal conductivity combined with a high heat capacity that causes localized areas of persistently elevated temperatures. The bottom 25 meters lies below the Eau Claire shale and is a region of high ground water flows rate which increases the apparent thermal conductivity due to advection.

Data from the heat injection periods was used for the quantitative analysis. Two different analysis techniques were used along with different measurement techniques in different ground regions to produce the thermal conductivity estimates that are summarized in Table 4-3. These showed that the estimated thermal properties of the ground can vary through the measurement period so an analysis technique that accounts for this transient behavior should be used. The results also show that the ground cannot be treated as

homogenous with a single effective thermal conductivity when there is significant stratification of the ground.

Knowledge of this stratification would have a significant impact on the design of GCHP systems. In the case of the Wisconsin Institutes of Discovery, which is a cooling dominated building, the effect on the design would have taken the form of deeper wells. Subsequent chapters will discuss how a model of the entire heat pump was created and used with the parameters estimated from the new TRT to produce performance maps for the WID GCHP.

Chapter 5. Heat Pump Model

As discussed in previous sections, a significant operational issue associated with the WID's GCHP system is high geofield returning water temperatures that, in the limit, exceed the high temperature cutoff for the heat pump's compressors. The period of heat pump operation required to reach this condition varies depending on the amount and rate of thermal energy that was injected into the ground, in addition to how much time the ground was given to dissipate the energy naturally. Currently, the WID's GCHP is only used for emergency situations when access to the utility chilled water is interrupted. It is crucial to the data center housed within the WID that adequate cooling be provided continuously; therefore, knowing how long the cooling loads can be covered by the GCHP system is important and is one of the objectives of this research.

The multitude of diagnostic tests performed during this research project has provided new insight and data with which to build a predictive model of the geofield serving the WID's heat pump system. These models are used to generate performance maps of the GCHP based on different metrics like returning water temperatures, COP of the heat pump, and cooling capacity that guide the operation of the whole GCHP system.

5.1 Heat Pump Model

The heat pump model was implemented in TRNSYS and includes a model of the geofield as well (**Error! Reference source not found.**). The heat pump model within T RNSYS is a simple component that acts as black box that applies whatever equations are specified within it (Equations 5.1-5.4). In this application, it takes the temperature of the fluid

returning from the geofield model as well as the mass flow rate of that fluid as inputs. The actual operating capacity for the heat pumps is controlled by specifying how many of the 12 total compressors are active during the simulation. Based on these inputs, the model calculates the GCHP condenser leaving fluid temperature, COP, cooling capacity, and power consumption. The calculations are performed using curve fit model based on the actual heat pump manufacturer's performance data. A correction factor that accounts for the real performance of the heat pumps as-installed is included with the model. The heat pump performance equation and correction factor were developed by Knudson (2013) and used here with one major difference; Knudson prescribed the change in temperature across the condenser to calculate the leaving fluid temperatures but in the present model, the leaving condenser fluid temperature is calculated based on the mass flow rate of the fluid seen when the pumps were run at rated conditions.

$$\dot{Q}_{cool}[tons] = \left(548.539 - 1.2956 * T_{condenser,in}[°\mathrm{F}] - 0.0068226 * T_{condenser,in}[°\mathrm{F}]^2\right) * N_{compressors\ active} * 0.8 \quad (5.1)$$

$$COP = \left(12.0876 - 0.119419 * T_{condenser,in}[°\mathrm{F}] + 0.000302791 * T_{condenser,in}[°\mathrm{F}]^2\right) * 0.8 \quad (5.2)$$

$$Power[tons] = \frac{\dot{Q}_{cool}[tons]}{COP}, THR[tons] = \dot{Q}_{cool}[tons] + Power[tons] \tag{5.3}$$

$$T_{condenser,out}[K] = 3600 * \frac{THR[tons] * 3.5169}{\dot{m}_{water}\left[\frac{kg}{hr}\right] * c_{p,water}\left[\frac{kJ}{kg-K}\right]} + T_{condenser,in}[K] \tag{5.4}$$

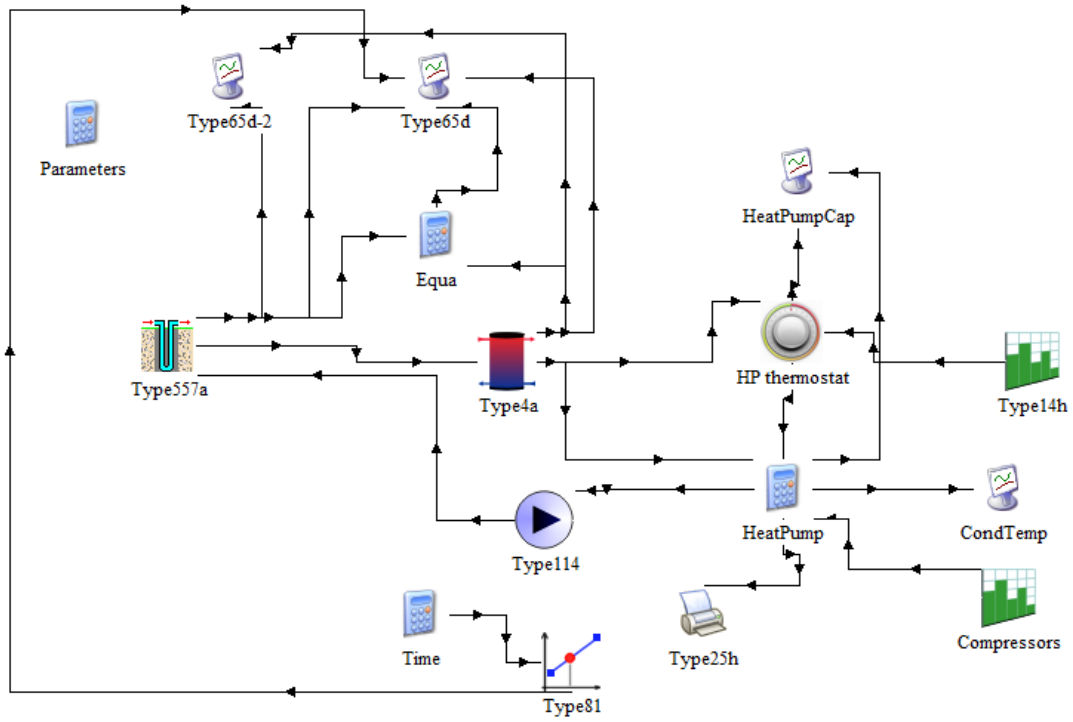

Figure 5-1: WID heat pump model as seen in the TRNSYS simulation studio. Showing how the different components connect to each other.

An important feature of the heat pump model the storage tank of water that simulated the thermal capacitance of the water within the entire geofield. It is a purely modeling

construct that is necessary if the heat pump model is to show the initial, rapid drop in temperature seen in the thermal decay tests discussed in sections 3.1, 3.7, and 4.5.

5.2 Model Validation

It is important to consider that the WID GCHP system has seen prior use so virgin/undisturbed ground conditions cannot be assumed. Since the system has been operated before, it was necessary to implement a preheat in the TRNSYS model in order to correctly simulate the GCHP. The preheat parameter in the TRNSYS geofield model component implements a sinusoidal variation of the specified preheat temperature to heat up the ground surrounding the storage volume. The temperature for the preheat was determined using the pseudo-undisturbed ground temperature because that is the actual condition of the local ground close to the bores. The preheat time period affects the temperature of the ground surrounding the local geofield and determines how far the thermal wave associated with the preheat has traveled. A set of hand logged data that was taken for a few months during 2013 (previously discussed in section 3.7 and shown in Figure 3-34) served as a basis to compare different preheat levels to the actual field data in order to determine if they were internally consistent. The resulting 1 year preheat at 72.6°F produced good agreement as seen in **Error! R eference source not found.**. The step-like shape of the temperature versus time profile associated with the model is caused by the intermittent operation of the circulating pump within the model, which is consistent with how the real, hand logged data were collected as discussed in section 3.7.

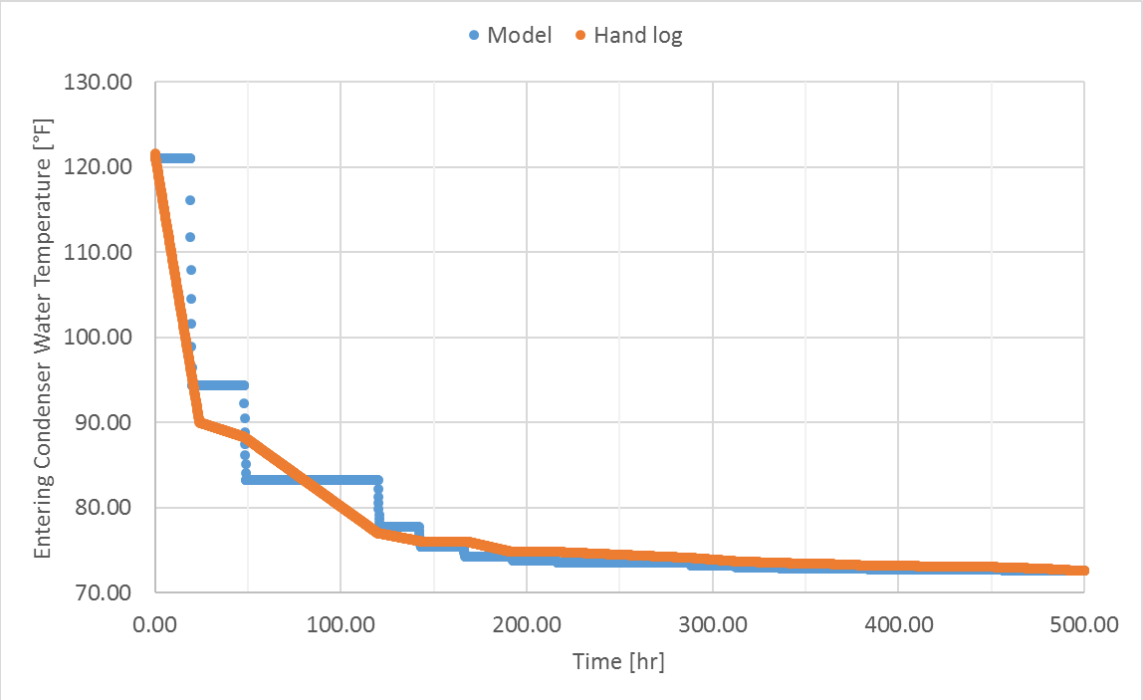

Figure 5-2: Entering condenser water temperature vs time in hours for the hand logged and modeled data used to validate the preheat setting.

5.3 Performance Maps

The GCHP system performance maps are intended to serve as a guideline for WID operations staff to better understand the limitations associated with continuous operation of the heat pump system in cooling mode while providing different levels of cooling capacity – given the characteristics of the WID geofield. These performance guidelines only apply to the cooling mode of the WID's GCHP system. The revised thermal conductivity and borehole radius estimates obtained from the new TRT were incorporated into the performance maps, specifically the thermal conductivities estimated using the Crossed Contours method which both averaged to 3.4 W/m-K (1.96 Btu/hr-ft-°F).

The heat pump “cutoff temperature” isotherms shown in the performance maps represents the assumed maximum condenser water temperature of 123°F which is based on the saturation temperature of the heat pump working fluid (R410a). When this temperature is reached, the heat pumps will automatically shut down on high compressor discharge pressure to prevent over pressuring the high-side of the units. The “design temperature” isotherms represent the values used in the design of the heat pumps according to the original (BOD , 2011).

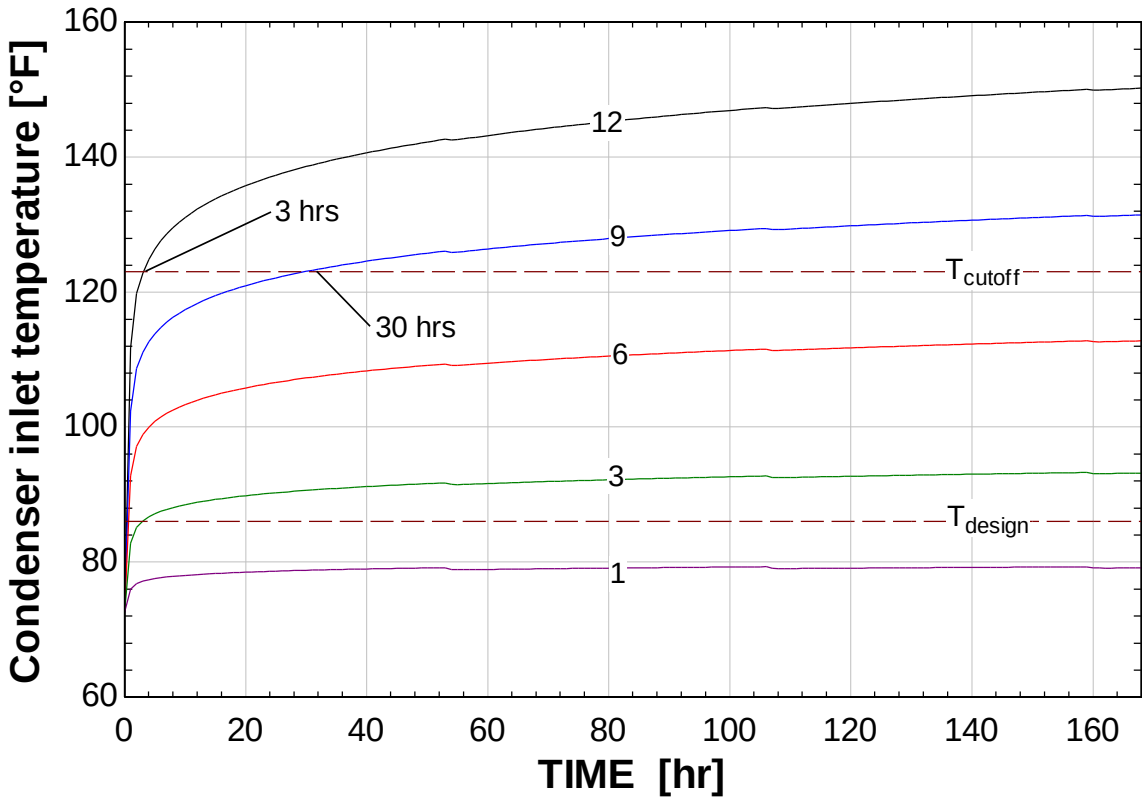

Figure 5-3: Entering condenser water temperature vs time in hours at various loads represented by the lines corresponding to the number of compressors active. This is for a 1-week time interval and 72.6 °F preheat. Isotherm lines for the safety cut-off and heat pump design temperatures are also plotted.

Figures 4-42 and 4-43 show how rapidly the entering condenser water temperature reaches the cutoff temperature when different numbers of heat pump compressors are operating. The period of runtime increases significantly as the number of operating compressors is reduced. With three compressors operating, the heat pump system can operate continuously for a full year or more without reaching the cutoff temperature. Longer operational periods come at the expense of diminished cooling capacity which also decreases rapidly as compressors are deactivated.

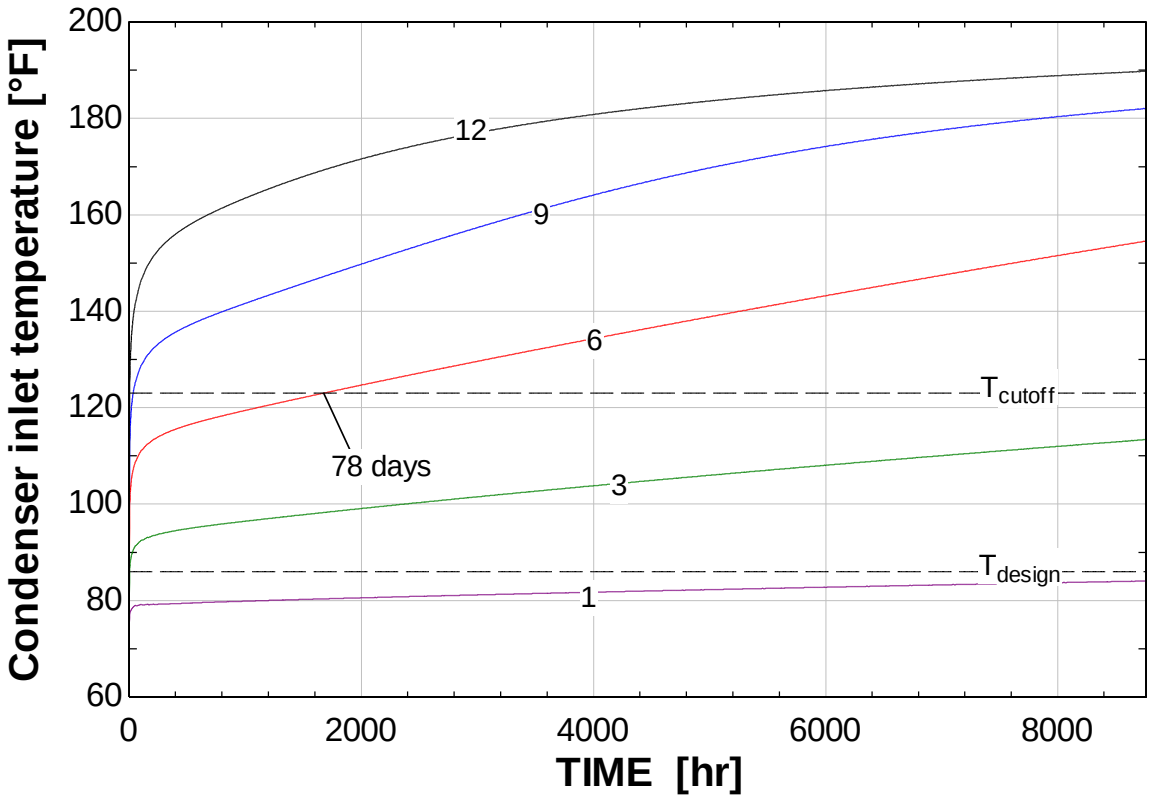

Figure 5-4: Entering condenser water temperature vs time in hours at various loads represented by the lines corresponding to the number of compressors active. This is for a 1-year time interval and 72.6 °F preheat. Isotherm lines for the safety cut-off and heat pump design temperatures are also plotted.

Depending on the performance metric of interest, there are alternative strategies to operate the GCHP system in cooling mode. For example, looking at the COP and maximum cooling capacity plots shown in Figure 5-5 and Figure 5-6, it becomes apparent that between 12 and 9 compressors approach the same cooling capacity while the COP of the 9 compressors operation remains higher than the 12 compressor operation.

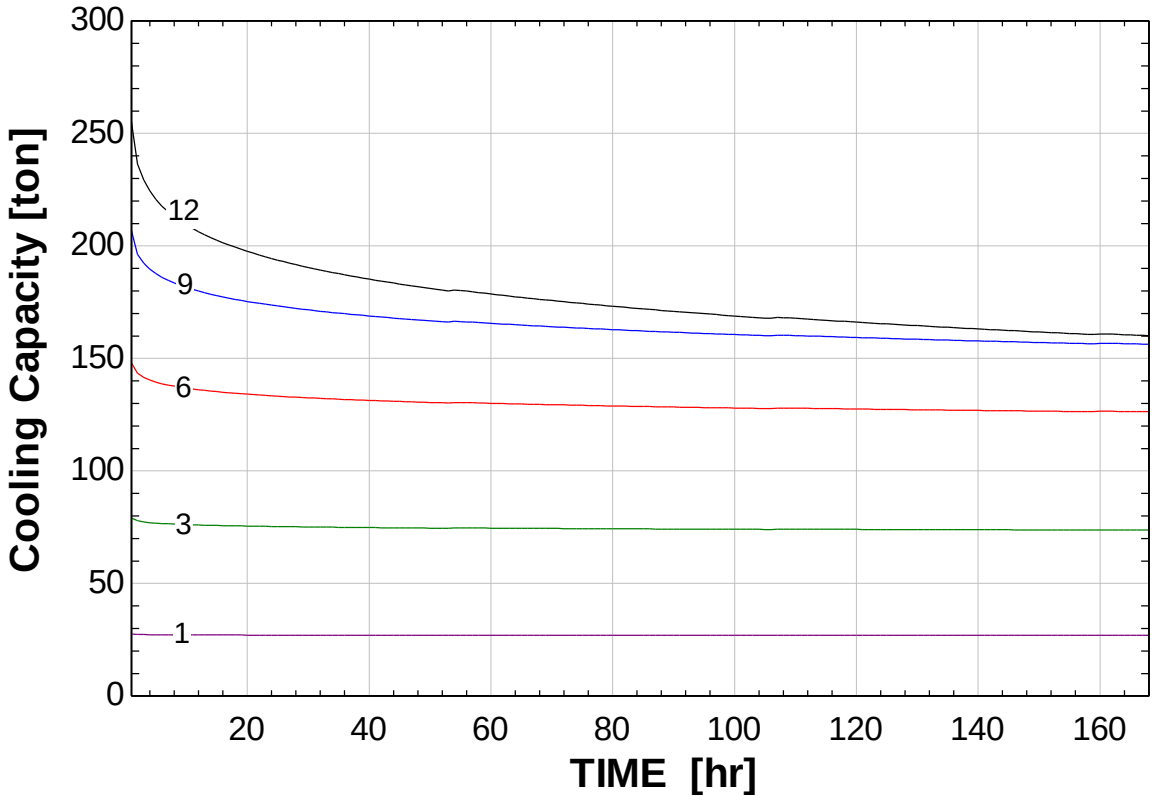

Figure 5-5: Maximum cooling power in tons vs time in hours at various loads represented by the lines corresponding to the number of compressors active. This is for a 1-week time interval and 72.6 °F preheat.

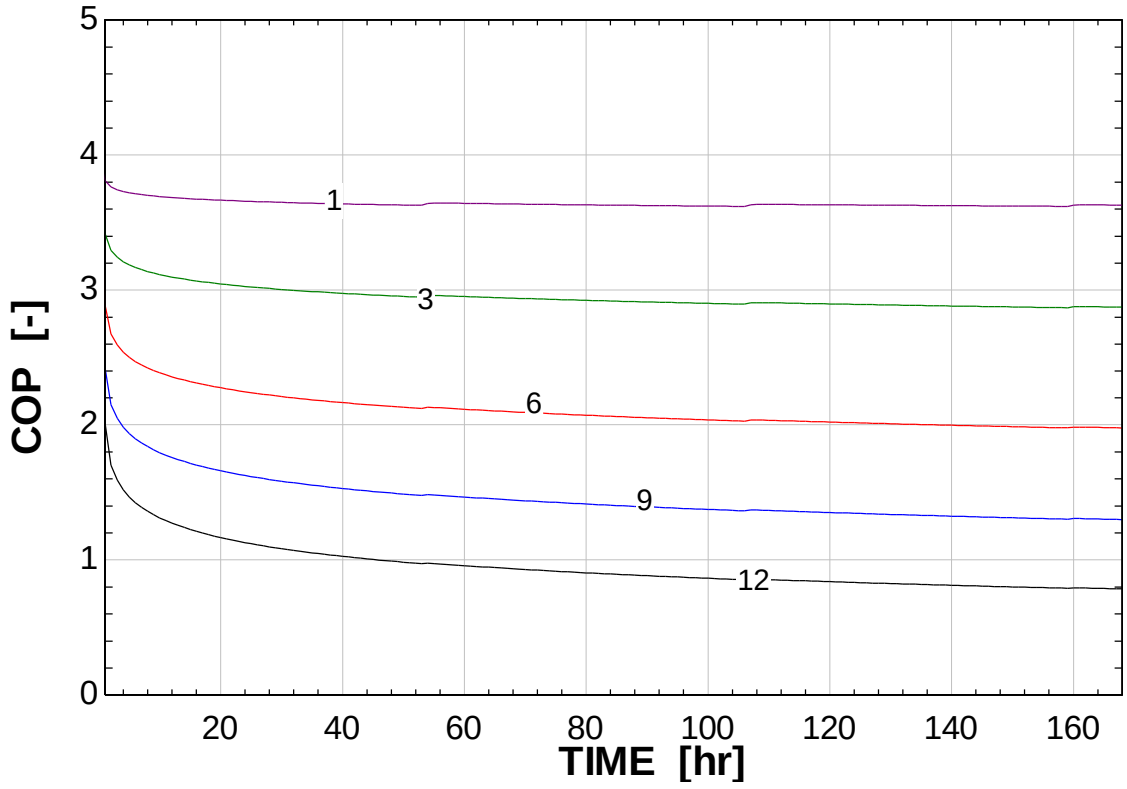

Figure 5-6: COP vs time in hours at various loads represented by the lines corresponding to the number of compressors active. This is for a 1-year time interval and 72.6 °F preheat.

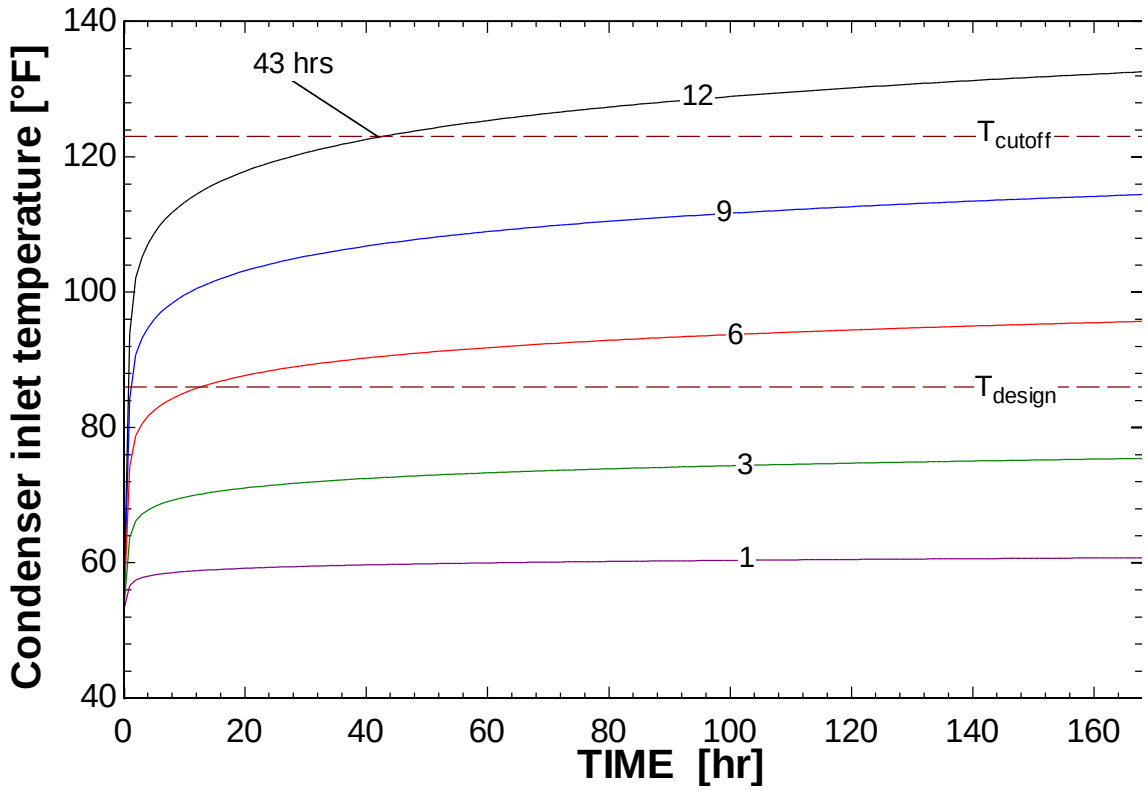

Figure 5-7: Entering condenser water temperature vs time in hours at various loads represented by the lines corresponding to the number of compressors active. This is for a 1-week time interval and virgin ground at 53°F with no preheat. Isotherm lines for the safety cut-off and heat pump design temperatures are also plotted.

A factor not included in these performance maps is the possibility of intermittent operation or cycling of the heat pumps. Successful operation of the heat pumps under cyclic duty will depend on the goal of the GCHP system (i.e., whether it is intended to be solely an emergency back up or whether it is intended to serve loads in the WID – albeit at a reduced capacity). What's definitive is that the GCHP system cannot operate continuously and indefinitely in cooling mode due to the limitations of the system rejecting heat into the ground; thereby, resulting in ground overheating.

Chapter 6. Summary of Conclusions and Sustainable Operation

6.1 Assessment of the Original Thermal Response Test

6.1.1 Line Source Method (LSM) Analysis

One of the first hypotheses proposed to explain the underperformance of the WID's geofield was an incorrect estimate of the ground thermal conductivity. The temperature data from the GRTI TRT was reanalyzed at first with the simplified LSM equation, which is what GRTI used, just to confirm the original estimate. The resultant thermal conductivity of 4.1 W/m-K (2.37 Btu/hr-ft-°F) is similar to the GRTI reported value of 4.03 W/m-K (2.33 Btu/hr-ft-°F).

The Line Source Method was also used to analyze a subset of the quantified thermal conductivity values from the new TRT to test whether there would be a difference in simulated long-term behavior of the GCHP system when the ground was treated homogenously versus separating it into two layers with different properties.

6.1.2 Crossed Contours Method Analysis

The GRTI TRT data was also reanalyzed using a borehole model made in TRNSYS coupled with the Crossed Contours parameter estimation technique. For the Crossed Contours analysis, the thermal conductivity and borehole radius were taken as the set of optimization parameters. This analysis gave an estimated thermal conductivity of 3.62 W/m-K (2.09 Btu/hr-ft-°F) and a borehole radius of 0.10 meters. The thermal conductivity by the CC method is 10% lower than the original GRTI TRT predicted, which is greater than the measurement uncertainty given by GRTI of ±5% but within the uncertainty of ±10%

recommended by Witte et al. for field testing the ground conductivity (Witte, et al. 2002). The reevaluation of the GRTI TRT is inconclusive since it neither concretely proves nor disproves that the ground thermal conductivity established during the design phase of the system was accurate.

6.2 Geofield Assessment and Field work

The results of the preliminary field work completed on the GCHP system proved inconclusive. There was no single definitive cause found that might explain the unusual behavior of the system, but various working hypotheses were proven false.

6.2.1 Pipe Fouling

While some fouling was observed when the pipes were cut and the system did test positive for bacteria, this was not enough to conclude that fouling has a significant effect on system performance. The borescope confirmed the presence of only a very thin film of dust on the walls of the U-tube. When the U-tubes were flushed out there was sediment present in the catch bucket and the water was quite murky but it was thought that this would have come from settling at the bottom of the tube and therefore, not affect the heat transfer. At the time, it was unknown what effect this sediment would have on the flow through the U-tube but during the hydronics testing there were no anomalies found.

6.2.2 Hydronics Testing

The hydronics testing resulted in two flow estimates: (1) 1,050 gpm based on pump curves and (2) 1,070 assuming 82 bores operated at the same average flow per bore (13 gpm) that are within 9% of the design flow rate of 984 gpm. There did not appear to be any flow

imbalance between the branches nor water-side fouling that would noticeably impact the performance of the field. However, the flat head vs. flow characteristic of the 4AC series pumps makes the geofield susceptible to significant decreases in system flow should water-side fouling occur in the future.

6.2.3 Temperature Profiles

The temperature profiles confirmed the persistent elevated temperatures but also revealed the surprisingly cool temperatures at the bottom 20 meters that are closer to the expected undisturbed ground temperature. This lead to a comparison with the geology of Madison which showed that the stratification of the temperatures matches the stratification of the geology. The lower temperatures present at that depth indicate an increased thermal conductivity. This increase is due to the relatively high movement of ground water caused by city water utility pumping within the Mt. Simon aquifer that is capped by the Eau Claire shale at about 70 meters of depth which restricts this effect to the bottom 20 meters of bore.

Meanwhile the region between 10 and 70 meters persists at an elevated temperature because it is characterized by an abundance of slow moving ground water which gives it both a large thermal capacitance and low thermal conductivity. These diagnostics have confirmed that ground with little or no water movement provides an effective thermal storage medium (Hellström, 1982).

6.3 New Thermal Response Test

Since the previous geofield assessment proved that there was nothing wrong with the system components, it was deduced that the behavior of the WID geofield is solely caused by

the geological properties of the ground. The diagnostic fieldwork also revealed stratification of the thermal properties of the ground which motivated the implementation of a new fiber optic distributed temperature sensing technique for conducting the test. The TRT provided very useful insights towards explaining the observed behavior of the bore field. It confirmed some theories and promoted new ones.

The pseudo-undisturbed ground temperature measurements confirmed the altered state of the ground. The profiles showed that above-normal ground temperatures have persisted despite minimal heat input to the ground over the past year-and-a-half.

The thermal decay tests using the fiber-optic data clearly show regions of high and low apparent thermal conductivity. Based on the geologic data gathered it can be concluded that the top 70 meters are defined by the presence of porous rock and abundant stagnant (perched) water with a low thermal conductivity combined with a high heat capacity that causes localized areas of persistently elevated temperatures. The bottom 25 meters on the other hand lies below the Eau Claire shale and is a region of high ground water flows rates which increase the apparent thermal conductivity due to advection.

Data from the heat injection periods from the in-situ TRT was used for the quantitative analysis. Two different analysis techniques were considered based on temperatures measured with different sensors at different ground regions to produce various thermal conductivities summarized in table 2. These showed that the estimated thermal properties of the ground can vary through the measurement period so an analysis technique that accounts for this transient behavior should be used.

The results also show that the ground cannot be treated as homogenous with a single effective thermal conductivity when there is significant stratification of the ground. A subset of the quantified thermal conductivity values was used to test whether there would be a difference in simulated long-term behavior of the GCHP system when the ground was treated homogenously versus separating it into two layers with different properties. For both cases the heat pump was run with 6 out of 12 compressors on, so at 50% capacity. Using 1.48 Btu/hr-ft-°F for the entire ground, the heat pumps were able to operate continuously for 540 hours before reaching the cutoff temperature. When the ground was separated into the two layers specified in Table 4-3 and their respective thermal conductivities of 1.1 and 3.72 Btu/hr-ft-°F were used, the heat pumps could operate continuously for 420 hours. This is a difference of 120 hours or 5 days and at lower system capacities the difference becomes larger.

Knowledge of the stratification of the thermal properties of the ground would have a significant impact on the design of GCHP systems. It would lead to a better estimate of the actual thermal conductivity of the ground rather than an effective conductivity that assumes a homogenous ground. The techniques used in this research could be used to find areas of increased thermal conductivity in the ground so they may be actively targeted during the design of the geofield. In the case of a cooling-dominated facility such as the WID, the design could have taken the form of wells that are closely packed since the thermal diffusivity is low and that are deep in order to take advantage of the improved heat transfer after 70 meters in depth

6.4 Sustainable Operation

Based on the extensive investigation into the behavior of the WID geofield and its subsystems, the GCHP system will be limited in its ability to sustainably operate at-capacity for extended periods of time unless the heat pump's heat rejection can be augmented. This can be achieved through external cooling such as a cooling tower, which would make it a hybrid system (Hackel, Nellis, & Klein, 2009), or cooled by the campus chilled water system through a heat exchanger. Another option would be to restore the heating mode of the GCHP system so that the field can be cooled by providing heat to the building.

GCHP systems are not suitable for cooling dominated applications which is why the WID GCHP was designed to be used for heating as well as cooling which balances the heat input to the ground in cooling mode with the heat extracted in heating mode. The ground can technically be assumed to be an infinite heat sink but not at timescales that would be useful. What ends up happening is that a rather small region immediately surrounding the U-tube heats up quickly while most of the ground in the geofield never experiences any warming. This was seen during the new TRT, when a temperature sensor was lowered into the south bore while the north bore had heat injected into it as part of the test. The sensor was left in the south bore for nearly a month and registered no change in temperature due to the heat injection to the adjacent bore.

The WID GCHP system, in its current condition with no capital investment for any of the significant modifications mentioned before, has two options for useful operation: as an emergency backup to the campus chilled water system or intermittent operation at a much reduced capacity. The operating procedures for each option are influenced by many factors

with the goal being to maintain the geofield returning water temperatures as close to design as possible. Being close to the design temperature provides the best COP but is very difficult to do and is more important for the intermittent operation than for use as an emergency backup. The rate of temperature saturation of the geofield will depend on the field's initial temperature and the number of heat pump modules operating. Performance maps have been prepared to facilitate WID operating staff in forecasting the extent of heat pump operation before reaching a condenser water threshold that puts the heat pumps at risk of shutting down due to high head pressure. These performance maps are provided in Section 5.3.

A continuation of this research should include the verification of the performance maps using the actual GCHP. Since these maps were generated using a mathematical model of the system they should be experimentally confirmed through real world operation of the heat pumps.

Finally, there are a few "firsts" associated with this project that are noteworthy. The installation of Permanent Wellhead Monitoring Stations (PWMS) on two of the bore holes is believed to be the first of its kind. These PWMS enabled the research team to conduct thermal response testing on bores that have been part of an active geofield – another believed to be first. These permanent access installations of the geofield provide the opportunity for much further research into the topic of GCHPs. The use of fiber-optic probes to obtain real-time temperature profiles on the supply and return side of the u-tube during a thermal response test is one of the first of its kind. This data offers the potential to generate more accurate ground thermal conductivity values – including the potential for anisotropic conductivity estimates to improve the ability of designers to forecast the field performance of

future systems. For the WID this might have meant fewer but deeper bores that could take advantage of the increased thermal conductivity caused by the advection of water below 70 meters

Chapter 7. Bibliography

Acuña, J., Mogensen, P., & Björn, P. (2009). Distributed Thermal Response Test on a U-Pipe Borehole Heat Exchanger. *11th International Conference on Thermal Energy Storage.* Stockholm: Academic Conferences Publishing.

ASHRAE. (2011). *HVAC Applications Handbook. IP Edition.*

Ballinger, Uihlein-Wilson, Affiliated Engineers Inc. (2011). *Wisconsin Institutes for Discovery Basis of Design.* WID Internal Document, Madison.

Banks, D. (2008). Chapter 12: Thermal Response Testing . In D. Banks , *An Introduction to Thermogeology Ground Source Heating and Cooling.* Oxford-Blackwell.

BOD . (2011). *WID Basis of Design.* WID Internal Document.

EnLink Geoenergy Services, Inc. (2010, December 3). *The Large Potential of Geothermal Heat Pump Systems*. Retrieved from Clean Technica: https://cleantechnica.com/2010/12/03/the-large-potential-of-geothermal-heat-pump-systems/

Gehlin, S. (2002). *Thermal Response Test, Method Development and Evaluation, Doctoral Thesis.* Sweden: Lulea University of Technology.

GeoPro, Inc. (2016, December 4). *Thermal Grout Lite*. Retrieved from geoproinc.com: https://geoproinc.com/products/thermalGroutLite.html

Gotkowitz, M. B., McLaughlin, P. I., & Grande, J. D. (2002). *Sources of naturally occuring chromium in bedrock aquifers underlying Madison, Wisconsin.* Madison: Wisconsin Geological and Natural History Survey.

GRTI, Inc. (2008). *Formation Thermal Conductivity Test and Data Analysis.* Geothermal Resource Technologies, Inc.

Gustafsson, A.-M., & Westerlund, L. (2010). Multi-injection rate thermal response test in groundwater filled borehole heat exchanger. *Renewable Energy, 35(5),* 1061-1070.

Hackel, S., Nellis, G., & Klein, S. (2009). Optimization of Cooling-Dominated Hybrid Ground-Coupled Heat Pump Systems. *ASHRAE Transactions 115(1).*

Hellström, G. (1982). *Model of duct storage system.* Sweden: University of Lund.

Kelly, J. (2009, January 6). *Deep Drilling Begins for Wisconsin Institutes for Discovery geothermal system.* Retrieved from University of Wisconsin-Madison News: http://news.wisc.edu/deep-drilling-begins-for-wisconsin-institutes-for-discovery-geothermal-system/

Knudson, R. (2013). *Energy Monitoring and Verification of Ground-Coupled Heat Pumps: Utilizing Live Building Control Data in the Wisconsin Institutes for Discovery.* MS Thesis, Madison.

Krohelski, J. T., Bradbury, K. R., Hunt, R. J., & Swanson, S. K. (2000). Numerical Simulation of Groundwater Flow in Dane County, Wisconsin. *Wisconsin Geological and Natural History Survey*.

Leyde, B. (2016). Determination of Vertical Borehole and Geological Formation Properties using the Crossed Contour Method. *Manuscript submitted for publication*.

Liuzzo-Scorpo, A., Nordell, B., & Gehlin, S. (2015). Influence of regional groundwater flow on ground temperature around heat extraction boreholes. *Geothermics*, 119-127.

McDaniel, A., Harper, M., Fratta, D., Tinjum, J. M., Choi, C. Y., & Hart, D. J. (2016). Dynamic Calibration of a Fiber-Optic Distributed Temperature Sensing Network at a District-Scale Geothermal Exchange Borefield. *Geo-Chicago*, 1-11.

Mogensen, P. (1983). Fluid to Duct Wall Heat Transfer in Duct System Heat Storages. *Int. Conf. On Subsurface Heat Storage in Theory and Practice* (pp. 652-657). Stockholm: Lulea University of Technology.

Parsen, M. J., Bradbury, K. R., Hunt, R. J., & Feinstein, D. T. (2016). *The 2016 Groundwater Flow Model for Dane County, Wisconsin.* Madison: Wisconsin Geological and Natural History Survey.

Pertzborn, A., Hackel, S., Nellis, G., & Klein, S. (2011). Experimental validation of a ground heat exchanger model in a hybrid ground source heat pump. *HVAC&R Research 17(6)*, 1101-1114.

Shonder, J. A., & Beck, J. V. (1999). Determining effective soil formation thermal properties from field data using a parameter estimation technique. *ASHRAE transactions, 105*, 458.

Synergy Boreholes and Systems ltd. (2016, November 22). *What is Geothermal?* Retrieved from Synergy boreholes : http://www.synergyboreholes.co.uk/geothermal_boreholes/index/what_is_geothermal/

Wisconsin Institutes for Discovery. (2016, 11 14). *Facility and History*. Retrieved from Wisconsin Institutes for Discovery: http://discovery.wisc.edu/home/discovery/facility/

Witte, H. J., Van Gelder, G. J., & Spitier, J. D. (2002). In situ measurement of ground thermal conductivity: a Dutch perspective. *ASHRAE Transactions 108.1*, (pp. 263-272).

Özdoğan-Dölçek, A. (2015). *Numerical Modeling of Heat Transport for Ground-Coupled Heat Pump (GCHP) Systems.* Doctoral dissertation, University of Wisconsin-Madison, Department of Civil and Environmental Engineering.

Appendix A – System Specification

GROUT SPEC

Grouting:

All bore holes shall be grouted completely with thermally enhanced grout in conformance with the IGSHPA standards specified in their publication, "Proper Grouting Procedures for Ground-Source Heat Pump System", and in conformance with all state and local requirements.

Settling of the grouting material will occur after the initial grouting, the contractor shall monitor each bore hole and continue adding grout as required.

The thermal conductivity of the grout shall be 1.0 btu/hr-ft-°F or greater. The grout shall have a maximum permeability rate of 6.9×10^{-8} cm/s, as determined by using the "Falling - Head Method" as recommended by the US Environmental Protection Agency to insure proper sealing.

Grouting compound shall be certified and listed by NSF to ANSI/NSF Standard 60, Drinking Water Treatment Chemicals - Health Effects.

The grout slurry shall consist of at least 40% solids by weight.

Lateral Piping:

All lateral piping shall be constructed of high density, polyethylene pipe, minimum SDR-11. All joints shall be made using the heat fusion joining method. Lateral pipes shall be purchased in such lengths and installed in such a manner as to minimize the number of fusion joints required.

All lateral piping shall be installed at a minimum depth of 72" below final grade.

Lateral piping supply and return lines or bundles shall be separated to minimize thermal interference between the two. The number of points where supply and return lines cross one another shall be minimized.

After connections to the vertical GLHE, each lateral shall be hydrostatically pressure tested. Testing shall be by water pressure at 100 psi for a minimum of 30 minutes. Exercise safety precautions during testing to guard against injury to personnel near lines being tested in case of pipe system component or joint failure under pressure. Results of all tests shall be recorded and supplied upon completion of the project.

Figure A- 1: DNR grout specification.

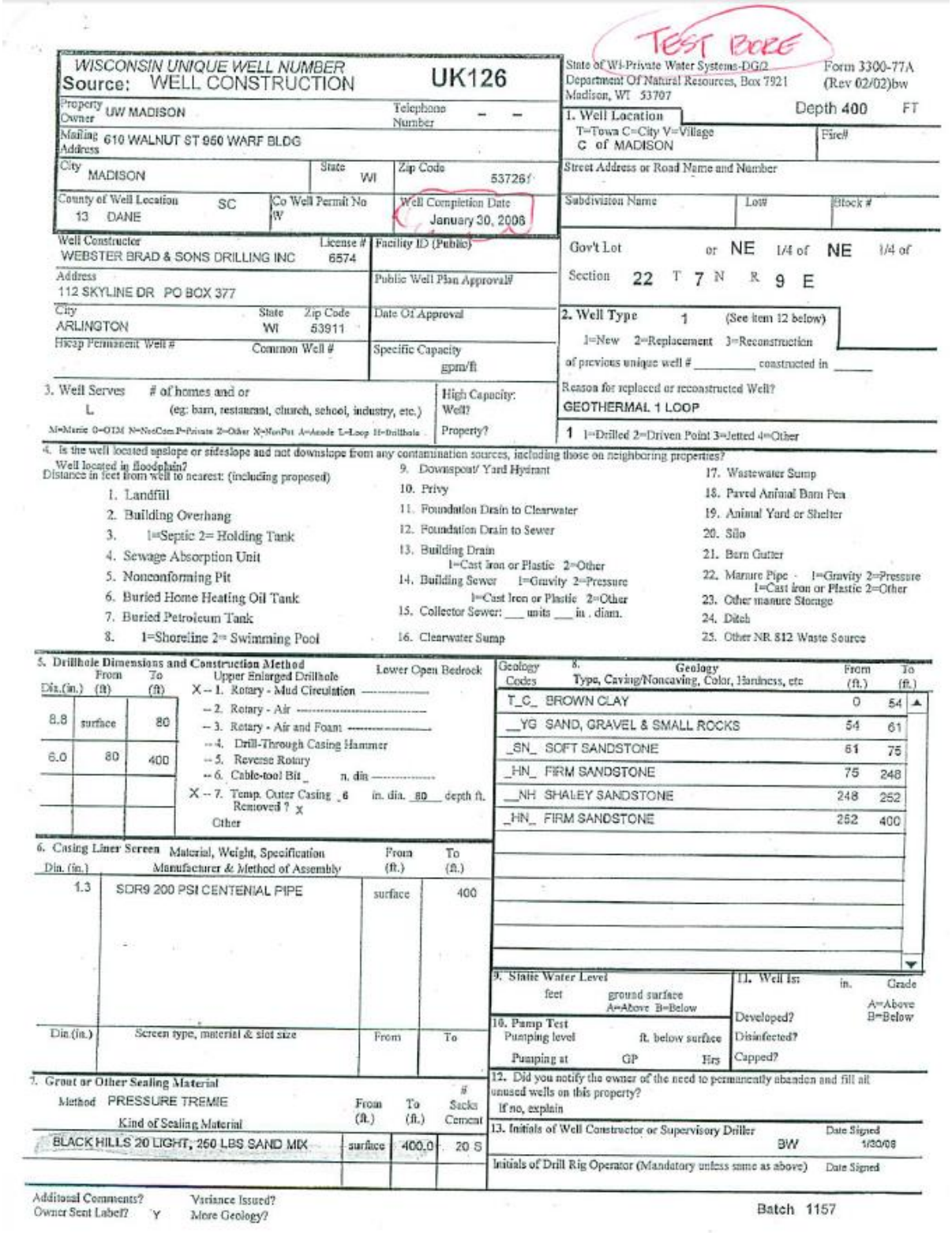

TEST BORE

WISCONSIN UNIQUE WELL NUMBER Source: WELL CONSTRUCTION — UK126

State of WI-Private Water Systems-DG/2, Department Of Natural Resources, Box 7921, Madison, WI 53707 — Form 3300-77A (Rev 02/02)bw

Property Owner: UW MADISON — Telephone Number: - -

Mailing Address: 610 WALNUT ST 950 WARF BLDG

City: MADISON — State: WI — Zip Code: 53726

County of Well Location: 13 DANE — Co Well Permit No: W — Well Completion Date: January 30, 2006

Depth 400 FT

1. Well Location — T=Town C=City V=Village: C of MADISON — Fire#

Street Address or Road Name and Number

Subdivision Name — Lot# — Block #

Well Constructor: WEBSTER BRAD & SONS DRILLING INC — License #: 6574 — Facility ID (Public)

Address: 112 SKYLINE DR PO BOX 377

City: ARLINGTON — State: WI — Zip Code: 53911

Public Well Plan Approval#

Date Of Approval

Hrcap Permanent Well # — Common Well #

Specific Capacity: gpm/ft

Gov't Lot — or NE 1/4 of NE 1/4 of

Section 22 T 7 N R 9 E

2. Well Type: 1 (See item 12 below) — 1=New 2=Replacement 3=Reconstruction

of previous unique well # _____ constructed in _____

Reason for replaced or reconstructed Well?: GEOTHERMAL 1 LOOP

3. Well Serves: L — # of homes and or (eg: barn, restaurant, church, school, industry, etc.) — M=Manic O=OTM N=NonCom P=Private 2=Other X=NonPot A=Anode L=Loop H=Drillhole

High Capacity: Well? Property?

1 1=Drilled 2=Driven Point 3=Jetted 4=Other

4. Is the well located upslope or sideslope and not downslope from any contamination sources, including those on neighboring properties?

Well located in floodplain?

Distance in feet from well to nearest: (including proposed)

1. Landfill
2. Building Overhang
3. 1=Septic 2= Holding Tank
4. Sewage Absorption Unit
5. Nonconforming Pit
6. Buried Home Heating Oil Tank
7. Buried Petroleum Tank
8. 1=Shoreline 2= Swimming Pool
9. Downspout/ Yard Hydrant
10. Privy
11. Foundation Drain to Clearwater
12. Foundation Drain to Sewer
13. Building Drain 1=Cast Iron or Plastic 2=Other
14. Building Sewer 1=Gravity 2=Pressure 1=Cast Iron or Plastic 2=Other
15. Collector Sewer: ___ units ___ in . diam.
16. Clearwater Sump
17. Wastewater Sump
18. Paved Animal Barn Pen
19. Animal Yard or Shelter
20. Silo
21. Barn Gutter
22. Manure Pipe 1=Gravity 2=Pressure 1=Cast Iron or Plastic 2=Other
23. Other manure Storage
24. Ditch
25. Other NR 812 Waste Source

5. Drillhole Dimensions and Construction Method — Lower Open Bedrock — Upper Enlarged Drillhole

Dia.(in.)	From (ft)	To (ft)
8.8	surface	80
6.0	80	400

X -- 1. Rotary - Mud Circulation
-- 2. Rotary - Air
-- 3. Rotary - Air and Foam
-- 4. Drill-Through Casing Hammer
-- 5. Reverse Rotary
-- 6. Cable-tool Bit _ n. dia
X -- 7. Temp. Outer Casing _6 in. dia. _80__ depth ft. Removed ? X
Other

Geology Codes	8. Geology Type, Caving/Noncaving, Color, Hardness, etc	From (ft.)	To (ft.)
T_C_	BROWN CLAY	0	54
__YG	SAND, GRAVEL & SMALL ROCKS	54	61
_SN_	SOFT SANDSTONE	61	75
_HN_	FIRM SANDSTONE	75	248
__NH	SHALEY SANDSTONE	248	252
_HN_	FIRM SANDSTONE	252	400

6. Casing Liner Screen — Material, Weight, Specification — Manufacturer & Method of Assembly

Dia. (in.)		From (ft.)	To (ft.)
1.3	SDR9 200 PSI CENTENIAL PIPE	surface	400

Dia.(in.)	Screen type, material & slot size	From	To

9. Static Water Level: feet — ground surface — A=Above B=Below

10. Pump Test: Pumping level ft. below surface — Pumping at GP Hrs

11. Well Is: in. Grade A=Above B=Below — Developed? — Disinfected? — Capped?

7. Grout or Other Sealing Material — Method: PRESSURE TREMIE — Kind of Sealing Material

	From (ft.)	To (ft.)	# Sacks Cement
BLACK HILLS 20 LIGHT, 250 LBS SAND MIX	surface	400.0	20 S

12. Did you notify the owner of the need to permanently abandon and fill all unused wells on this property?

If no, explain

13. Initials of Well Constructor or Supervisory Driller: BW — Date Signed: 1/30/06

Initials of Drill Rig Operator (Mandatory unless same as above) — Date Signed

Additional Comments? — Variance Issued?

Owner Sent Label? Y — More Geology?

Batch 1157

Figure A- 2: DNR drill log for test well 126.

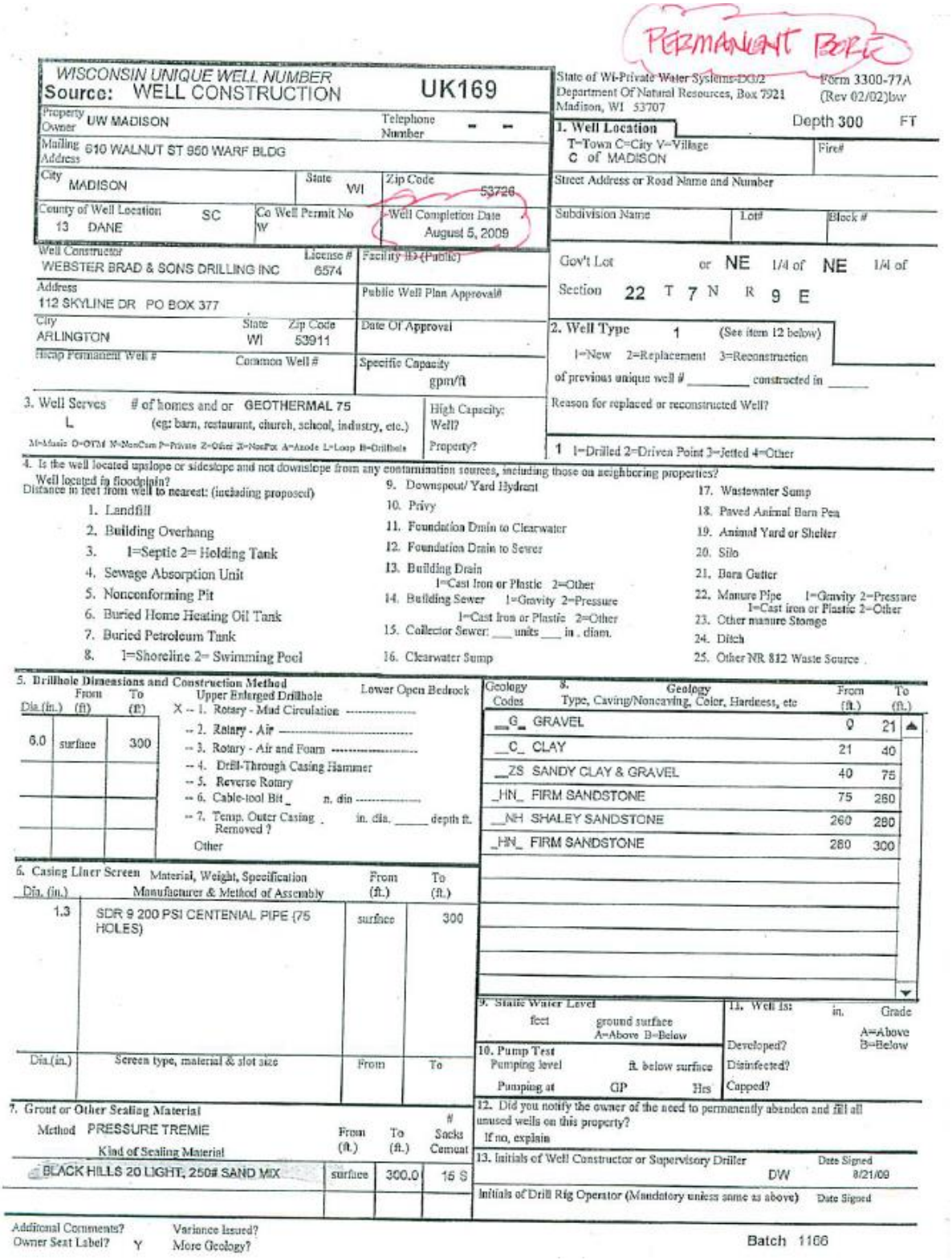

PERMANENT BORE

WISCONSIN UNIQUE WELL NUMBER
Source: WELL CONSTRUCTION UK169

State of WI-Private Water Systems-DG/2
Department Of Natural Resources, Box 7921
Madison, WI 53707

Form 3300-77A
(Rev 02/02)bw

Property Owner: UW MADISON
Telephone Number: - -
Depth 300 FT

Mailing Address: 610 WALNUT ST 950 WARF BLDG

City: MADISON
State: WI
Zip Code: 53726

County of Well Location: 13 DANE
Co Well Permit No: SC W
Well Completion Date: August 5, 2009

1. Well Location
T=Town C=City V=Village
C of MADISON
Fire#
Street Address or Road Name and Number
Subdivision Name
Lot#
Block #

Well Constructor: WEBSTER BRAD & SONS DRILLING INC
License #: 6574
Facility ID (Public)

Address: 112 SKYLINE DR PO BOX 377
Public Well Plan Approval#

City: ARLINGTON
State: WI
Zip Code: 53911
Date Of Approval

Gov't Lot or NE 1/4 of NE 1/4 of
Section 22 T 7 N R 9 E

Recip Permanent Well #
Common Well #
Specific Capacity: gpm/ft

2. Well Type 1 (See item 12 below)
1=New 2=Replacement 3=Reconstruction
of previous unique well # _____ constructed in _____
Reason for replaced or reconstructed Well?

3. Well Serves L # of homes and or GEOTHERMAL 75 (eg: barn, restaurant, church, school, industry, etc.)
M=Municipal O=Other N=NonCom P=Private Z=Other R=NonPot A=Anode L=Loop B=Drillhole
High Capacity: Well? Property?

1 1=Drilled 2=Driven Point 3=Jetted 4=Other

4. Is the well located upslope or sideslope and not downslope from any contamination sources, including those on neighboring properties?
Well located in floodplain?
Distance in feet from well to nearest: (including proposed)

1. Landfill
2. Building Overhang
3. 1=Septic 2= Holding Tank
4. Sewage Absorption Unit
5. Nonconforming Pit
6. Buried Home Heating Oil Tank
7. Buried Petroleum Tank
8. 1=Shoreline 2= Swimming Pool
9. Downspout/ Yard Hydrant
10. Privy
11. Foundation Drain to Clearwater
12. Foundation Drain to Sewer
13. Building Drain 1=Cast Iron or Plastic 2=Other
14. Building Sewer 1=Gravity 2=Pressure 1=Cast Iron or Plastic 2=Other
15. Collector Sewer: ___ units ___ in. diam.
16. Clearwater Sump
17. Wastewater Sump
18. Paved Animal Barn Pen
19. Animal Yard or Shelter
20. Silo
21. Barn Gutter
22. Manure Pipe 1=Gravity 2=Pressure 1=Cast Iron or Plastic 2=Other
23. Other manure Storage
24. Ditch
25. Other NR 812 Waste Source

5. Drillhole Dimensions and Construction Method
Lower Open Bedrock
Upper Enlarged Drillhole

Dia.(in.)	From (ft)	To (ft)
6.0	surface	300

X -- 1. Rotary - Mud Circulation
-- 2. Rotary - Air
-- 3. Rotary - Air and Foam
-- 4. Drill-Through Casing Hammer
-- 5. Reverse Rotary
-- 6. Cable-tool Bit _____ in. dia
-- 7. Temp. Outer Casing _____ in. dia. _____ depth ft. Removed ?
Other

Geology Codes	8. Geology Type, Caving/Noncaving, Color, Hardness, etc	From (ft.)	To (ft.)
_G_	GRAVEL	0	21
_C_	CLAY	21	40
_ZS	SANDY CLAY & GRAVEL	40	75
_HN_	FIRM SANDSTONE	75	260
_NH	SHALEY SANDSTONE	260	280
_HN_	FIRM SANDSTONE	280	300

6. Casing Liner Screen
Material, Weight, Specification
Manufacturer & Method of Assembly

Dia. (in.)		From (ft.)	To (ft.)
1.3	SDR 9 200 PSI CENTENIAL PIPE (75 HOLES)	surface	300

Dia.(in.)	Screen type, material & slot size	From	To

9. Static Water Level
feet ground surface
A=Above B=Below

11. Well is: in. Grade
A=Above B=Below
Developed?
Disinfected?
Capped?

10. Pump Test
Pumping level ft. below surface
Pumping at GP Hrs

12. Did you notify the owner of the need to permanently abandon and fill all unused wells on this property?
If no, explain

7. Grout or Other Sealing Material
Method PRESSURE TREMIE
Kind of Sealing Material

	From (ft.)	To (ft.)	# Sacks Cement
BLACK HILLS 20 LIGHT, 250# SAND MIX	surface	300.0	16 S

13. Initials of Well Constructor or Supervisory Driller: DW
Date Signed: 8/21/09
Initials of Drill Rig Operator (Mandatory unless same as above)
Date Signed

Additional Comments?
Owner Seat Label? Y
Variance Issued?
More Geology?

Batch 1166

Figure A- 3: DNR drill log for well 169.

GeoPro, Inc.
Corporate • 302 E. Warehouse St. • Elkton, SD 57026 • (877) 580-9348 • Fax (877) 580-9371
Sales • PO Box 150 • Bowie, TX 76230 • (940) 872-8097 • Fax (940) 872-3678

August 19, 2009

Webster & Son's Drilling Inc.
Attn: Brad Webster
112 Skyline Drive
Arlington, WI 53911
Phone: 608-635-7564
Fax: 608-635-8900

RE: Thermal Grout Thermal Conductivity Analysis Report

Thank you for participating in this "field quality control" program for the various Thermal Grout products. The objective of this analysis is to offer an unbiased verification of the thermal conductivity of the field mixed material. This analysis is intended to help ensure proper performance of the grouting material and that proper mixing procedures are consistently being followed throughout the project. It is recommended that, at a minimum, three separate analyses be performed on each commercial project.

Based on information supplied on the "Test Information Form" that accompanied the sample container, the tested specimen was collected on the following date from the following project:

Sample Received by Lab:	August 17, 2009
Sample Collection Date:	July 28, 2009, 2:00 p.m.
Project Name:	WID Building
City, State:	Madison, WI

GeoPro, Inc. uses a thermal needle method of analysis to determine thermal conductivity of fully hydrated grout specimens. Our analysis indicated that the thermal conductivity value of the specimen supplied from the project referenced above was as follows:

Thermal Conductivity: **.721** Btu/hr-ft-°F = 1.248 W/m-°K

If this value is lower than expected, please contact GeoPro, Inc. immediately at (605) 542-7391 to discuss possible reasons for a discrepancy and possible remedies.

We at GeoPro, Inc. believe that our combined efforts to provide this project with a high quality, high performance grouting material helps to build confidence in ground-source heat pump applications. We believe that increased confidence by all parties involved will help this industry achieve its objective of becoming a "main-stream" technology. Again, thank you for your participation in this program.

If you have any questions regarding this analysis, please contact me at (877) 580-9348 ext 106.

Sincerely,

Tyler Harbeck
GeoPro, Inc.

Figure A- 4: Grout sample testing results done before installation sample (1/6).

GeoPro, Inc.

Corporate • 302 E. Warehouse St. • Elkton, SD 57026 • (877) 580-9348 • Fax (877) 580-9371
Sales • PO Box 150 • Bowie, TX 76230 • (940) 872-8097 • Fax (940) 872-3678

September 2, 2009

Webster & Son's Drilling Inc.
Attn: Brad Webster
112 Skyline Drive
Arlington, WI 53911
Phone: 608-635-7564
Fax: 608-635-8900

RE: Thermal Grout Thermal Conductivity Analysis Report

Thank you for participating in this "field quality control" program for the various Thermal Grout products. The objective of this analysis is to offer an unbiased verification of the thermal conductivity of the field mixed material. This analysis is intended to help ensure proper performance of the grouting material and that proper mixing procedures are consistently being followed throughout the project. It is recommended that, at a minimum, three separate analyses be performed on each commercial project.

Based on information supplied on the "Test Information Form" that accompanied the sample container, the tested specimen was collected on the following date from the following project:

Sample Received by Lab:	August 28, 2009
Sample Collection Date:	Unknown
Project Name:	WID Building (Sample 3)
City, State:	Madison, WI

GeoPro, Inc. uses a thermal needle method of analysis to determine thermal conductivity of fully hydrated grout specimens. Our analysis indicated that the thermal conductivity value of the specimen supplied from the project referenced above was as follows:

Thermal Conductivity: **1.072** Btu/hr-ft-°F = 1.855 W/m-°K

If this value is lower than expected, please contact GeoPro, Inc. immediately at (605) 542-7391 to discuss possible reasons for a discrepancy and possible remedies.

We at GeoPro, Inc. believe that our combined efforts to provide this project with a high quality, high performance grouting material helps to build confidence in ground-source heat pump applications. We believe that increased confidence by all parties involved will help this industry achieve its objective of becoming a "main-stream" technology. Again, thank you for your participation in this program.

If you have any questions regarding this analysis, please contact me at (877) 580-9348 ext 106.

Sincerely,

Tyler Harbeck
GeoPro, Inc.

Figure A- 5: Grout sample testing results done before installation sample (2/6).

GeoPro, Inc.

Corporate • 302 E. Warehouse St. • Elkton, SD 57026 • (877) 580-9348 • Fax (877) 580-9371
Sales • PO Box 150 • Bowie, TX 76230 • (940) 872-8097 • Fax (940) 872-3678

September 2, 2009

Webster & Son's Drilling Inc.
Attn: Brad Webster
112 Skyline Drive
Arlington, WI 53911
Phone: 608-635-7564
Fax: 608-635-8900

RE: Thermal Grout Thermal Conductivity Analysis Report

Thank you for participating in this "field quality control" program for the various Thermal Grout products. The objective of this analysis is to offer an unbiased verification of the thermal conductivity of the field mixed material. This analysis is intended to help ensure proper performance of the grouting material and that proper mixing procedures are consistently being followed throughout the project. It is recommended that, at a minimum, three separate analyses be performed on each commercial project.

Based on information supplied on the "Test Information Form" that accompanied the sample container, the tested specimen was collected on the following date from the following project:

Sample Received by Lab:	August 28, 2009
Sample Collection Date:	Unknown
Project Name:	WID Building (Sample 2)
City, State:	Madison, WI

GeoPro, Inc. uses a thermal needle method of analysis to determine thermal conductivity of fully hydrated grout specimens. Our analysis indicated that the thermal conductivity value of the specimen supplied from the project referenced above was as follows:

Thermal Conductivity: **1.063** Btu/hr-ft-°F = 1.840 W/m-°K

If this value is lower than expected, please contact GeoPro, Inc. immediately at (605) 542-7391 to discuss possible reasons for a discrepancy and possible remedies.

We at GeoPro, Inc. believe that our combined efforts to provide this project with a high quality, high performance grouting material helps to build confidence in ground-source heat pump applications. We believe that increased confidence by all parties involved will help this industry achieve its objective of becoming a "main-stream" technology. Again, thank you for your participation in this program.

If you have any questions regarding this analysis, please contact me at (877) 580-9348 ext 106.

Sincerely,

Tyler Harbeck
GeoPro, Inc.

Figure A- 6: Grout sample testing results done before installation sample (3/6).

GeoPro, Inc.
Corporate • 302 E. Warehouse St. • Elkton, SD 57026 • (877) 580-9348 • Fax (877) 580-9371
Sales • PO Box 150 • Bowie, TX 76230 • (940) 872-8097 • Fax (940) 872-3678

September 2, 2009

Webster & Son's Drilling Inc.
Attn: Brad Webster
112 Skyline Drive
Arlington, WI 53911
Phone: 608-635-7564
Fax: 608-635-8900

RE: Thermal Grout Thermal Conductivity Analysis Report

Thank you for participating in this "field quality control" program for the various Thermal Grout products. The objective of this analysis is to offer an unbiased verification of the thermal conductivity of the field mixed material. This analysis is intended to help ensure proper performance of the grouting material and that proper mixing procedures are consistently being followed throughout the project. It is recommended that, at a minimum, three separate analyses be performed on each commercial project.

Based on information supplied on the "Test Information Form" that accompanied the sample container, the tested specimen was collected on the following date from the following project:

Sample Received by Lab:	August 28, 2009
Sample Collection Date:	Unknown
Project Name:	WID Building (Sample 1)
City, State:	Madison, WI

GeoPro, Inc. uses a thermal needle method of analysis to determine thermal conductivity of fully hydrated grout specimens. Our analysis indicated that the thermal conductivity value of the specimen supplied from the project referenced above was as follows:

Thermal Conductivity: **1.071** Btu/hr-ft-°F = 1.853 W/m-°K

If this value is lower than expected, please contact GeoPro, Inc. immediately at (605) 542-7391 to discuss possible reasons for a discrepancy and possible remedies.

We at GeoPro, Inc. believe that our combined efforts to provide this project with a high quality, high performance grouting material helps to build confidence in ground-source heat pump applications. We believe that increased confidence by all parties involved will help this industry achieve its objective of becoming a "main-stream" technology. Again, thank you for your participation in this program.

If you have any questions regarding this analysis, please contact me at (877) 580-9348 ext 106.

Sincerely,

Tyler Harbeck
GeoPro, Inc.

Figure A- 7: Grout sample testing results done before installation sample (4/6).

GeoPro, Inc.

Corporate • 302 E. Warehouse St. • Elkton, SD 57026 • (877) 580-9348 • Fax (877) 580-9371
Sales • PO Box 150 • Bowie, TX 76230 • (940) 872-8097 • Fax (940) 872-3678

August 19, 2009

Webster & Son's Drilling Inc.
Attn: Brad Webster
112 Skyline Drive
Arlington, WI 53911
Phone: 608-635-7564
Fax: 608-635-8900

RE: Thermal Grout Thermal Conductivity Analysis Report

Thank you for participating in this "field quality control" program for the various Thermal Grout products. The objective of this analysis is to offer an unbiased verification of the thermal conductivity of the field mixed material. This analysis is intended to help ensure proper performance of the grouting material and that proper mixing procedures are consistently being followed throughout the project. It is recommended that, at a minimum, three separate analyses be performed on each commercial project.

Based on information supplied on the "Test Information Form" that accompanied the sample container, the tested specimen was collected on the following date from the following project:

Sample Received by Lab:	August 17, 2009
Sample Collection Date:	July 30, 2009, 2:00 p.m.
Project Name:	WID Building
City, State:	Madison, WI

GeoPro, Inc. uses a thermal needle method of analysis to determine thermal conductivity of fully hydrated grout specimens. Our analysis indicated that the thermal conductivity value of the specimen supplied from the project referenced above was as follows:

Thermal Conductivity: **.802** Btu/hr-ft-°F = 1.387 W/m-°K

If this value is lower than expected, please contact GeoPro, Inc. immediately at (605) 542-7391 to discuss possible reasons for a discrepancy and possible remedies.

We at GeoPro, Inc. believe that our combined efforts to provide this project with a high quality, high performance grouting material helps to build confidence in ground-source heat pump applications. We believe that increased confidence by all parties involved will help this industry achieve its objective of becoming a "main-stream" technology. Again, thank you for your participation in this program.

If you have any questions regarding this analysis, please contact me at (877) 580-9348 ext 106.

Sincerely,

Tyler Harbeck
GeoPro, Inc.

Figure A- 8: Grout sample testing results done before installation sample (5/6).

GeoPro, Inc.
Corporate • 302 E. Warehouse St. • Elkton, SD 57026 • (877) 580-9348 • Fax (877) 580-9371
Sales • PO Box 150 • Bowie, TX 76230 • (940) 872-8097 • Fax (940) 872-3678

August 19, 2009

Webster & Son's Drilling Inc.
Attn: Brad Webster
112 Skyline Drive
Arlington, WI 53911
Phone: 608-635-7564
Fax: 608-635-8900

RE: Thermal Grout Thermal Conductivity Analysis Report

Thank you for participating in this "field quality control" program for the various Thermal Grout products. The objective of this analysis is to offer an unbiased verification of the thermal conductivity of the field mixed material. This analysis is intended to help ensure proper performance of the grouting material and that proper mixing procedures are consistently being followed throughout the project. It is recommended that, at a minimum, three separate analyses be performed on each commercial project.

Based on information supplied on the "Test Information Form" that accompanied the sample container, the tested specimen was collected on the following date from the following project:

Sample Received by Lab:	August 17, 2009
Sample Collection Date:	July 29, 2009, 2:00 p.m.
Project Name:	WID Building
City, State:	Madison, WI

GeoPro, Inc. uses a thermal needle method of analysis to determine thermal conductivity of fully hydrated grout specimens. Our analysis indicated that the thermal conductivity value of the specimen supplied from the project referenced above was as follows:

Thermal Conductivity:	.875	Btu/hr-ft-°F	=	1.514	W/m-°K

If this value is lower than expected, please contact GeoPro, Inc. immediately at (605) 542-7391 to discuss possible reasons for a discrepancy and possible remedies.

We at GeoPro, Inc. believe that our combined efforts to provide this project with a high quality, high performance grouting material helps to build confidence in ground-source heat pump applications. We believe that increased confidence by all parties involved will help this industry achieve its objective of becoming a "main-stream" technology. Again, thank you for your participation in this program.

If you have any questions regarding this analysis, please contact me at (877) 580-9348 ext 106.

Sincerely,

Tyler Harbeck
GeoPro, Inc.

Figure A- 9: Grout sample testing results done before installation sample (6/6).

Appendix B - Hydronics Testing

Test	Pump Freq. [hz]	Geofield Loop Isolation Valve Position				Measurements / Data Collected	Comments
		North	East	Far East	Campus Dr.		
1a	60	Open	Open	Open	Open	Loop flow – North, East, Far East, & Campus Drive Branch flow (North bore & South bore) – Circuit setter positions (supply & return) Circuit setter DP (supply-side) Circuit setter inlet pressure (return-side) Pumps – Speed (P-11 & P-12) Suction head (P-11 & P-12) Discharge head (P-11 & P-12)	<u>Expected flows:</u> System = 900 gpm North = 228 gpm East = 264 gpm Far East = 252 gpm Campus Dr =240 gpm
1b	40						
1c	20						
2a	60	Closed	Closed	Open	Closed	Loop flow – Far East Branch flow (North bore & South bore) – Circuit setter positions (supply & return) Circuit setter DP (supply-side) Circuit setter inlet pressure (return-side) Pumps – Speed (P-11 or P-12) Suction head (P-11 or P-12) Discharge head (P-11 or P-12)	Will need to run only one pump
2b	40						
2c	20						
3a	60	Closed	Open	Closed	Closed	Loop flow – East Pumps – Speed (P-11 or P-12) Suction head (P-11 or P-12) Discharge head (P-11 or P-12)	Run only one pump. Spot monitor the u-tube for any flow (due to loop isolation valve leakage)
3b	40						
3c	20						

Test	Pump Freq. [hz]	Geofield Loop Isolation Valve Position				Measurements / Data Collected	Comments
		North	East	Far East	Campus Dr.		
4a	60	Open	Closed	Closed	Closed	Loop flow – North Pumps – Speed (P-11 or P-12) Suction head (P-11 or P-12) Discharge head (P-11 or P-12)	Run only one pump Spot monitor the u-tube for any flow (due to loop isolation valve leakage)
4b	40						
4c	20						
5a	60	Closed	Closed	Closed	Open	Loop flow – Campus Drive Pumps – Speed (P-11 or P-12) Suction head (P-11 or P-12) Discharge head (P-11 or P-12)	Run only one pump Spot monitor the u-tube for any flow (due to loop isolation valve leakage)
5b	40						
5c	20						
6	60	Open	Open	Open	Open	Pump speed (P-11 & P-12) Pump suction head (P-11 & P-12) Pump discharge head (P-11 & P-12)	DEADHEAD ON BOTH PUMPS P-11 & P-12

Figure A- 10: Hydronics testing matrix

Appendix C - Permanent Access Monitoring Station Modes

Overview of Modes of Operation:

The following provides an overview of the modes of operation applicable to the North bore access ports and the South bore access ports that are configured within the Far East loop of the WID geofield.

Normal Operation (North and South bores)…….

- Allows normal operation of the Far East geofield branch including all 21 bores, with the research ports being isolated (inactive).
- Applies to both the North and South bores.
- After transitioning out of research port mode of operation, all residual water within the research port risers must be cleared to avoid freezing during wintertime.

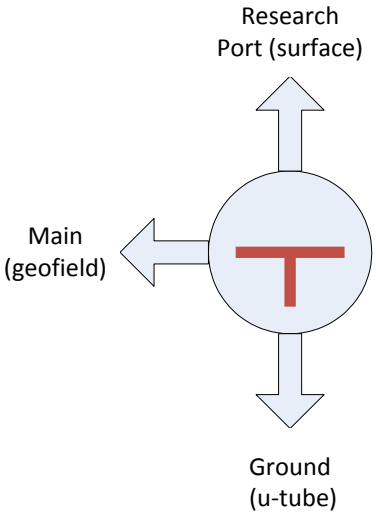

Research Mode – Field Isolated (North and South bores)……

- Isolates the respective bore from the rest of the geofield.
- Allows the Far East geofield to operate but with either one or two fewer bores active (i.e. 19 of 21 or 20 of 21 bores) depending on whether one or two bores are isolated.
- Applies to both North and South bores.

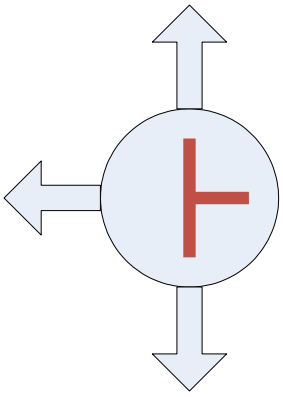

All Open (South bore-only)

……

- Allows operation of entire Far East branch of the geofield while keeping the South bore research port active.
- Appropriate caps must be installed on the research port risers for this mode of operation.
- **This mode of operation only applies to South well.**